Cooperative Diversity and Partner Selection in Wireless Networks

by

Mahinthan Veluppillai

A thesis
presented to the University of Waterloo
in fulfilment of the
thesis requirement for the degree of
Doctor of Philosophy
in
Electrical and Computer Engineering

Waterloo, Ontario, Canada, 2007

I hereby declare that I am the sole author of this thesis. This is a true copy of the thesis, including any required final revisions, as accepted by my examiners.

I understand that my thesis may be made electronically available to the public.

Abstract

Next generation wireless communication systems are expected to provide a variety of services including voice, data and video. The rapidly growing demand for these services needs high data rate wireless communication systems with reliability and high user capacity. Recently, it has been shown that reliability and achievable data rate of wireless communication systems increases dramatically by employing multiple transmit and receive antennas. Transmit diversity is a powerful technique for combating multipath fading in wireless communications. However, employing multiple antennas in a mobile terminal to achieve the transmit diversity in the uplink is not feasible due to the limited size of the mobile unit.

In order to overcome this problem, a new mode of transmit diversity called cooperative diversity (CD) based on user cooperation, was proposed very recently. By user cooperation, it is meant that the sender transmits to the destination and copies to other users, called partners, for relaying to the destination. The antennas of the sender and the partners together form a multiple antenna situation. CD systems are immuned not only against small scale channel fading but also against large scale channel fading. On the other hand, CD systems are more sensitive to interuser (between sender and partner) transmission errors and user mobility.

In this dissertation, we propose a bandwidth and power efficient CD system which could be accommodated with minimal modifications in the currently available direct or point-to-point communication systems. The proposed CD system is based on quadrature signaling (QS). With quadrature signaling, both sender's and partners' information symbols are transmitted simultaneously in his/her multiple access channels. It also reduces the synchronization as well as the interference problems that occur in the schemes reported in the literature.

The performance of the proposed QS-CD system is analyzed at different layers. First, we study the bit error probability (BEP) of the QS-CD system for both fixed and adaptive

relaying at the partner. It is shown from the BEP performance that the QS-CD system can achieve diversity order of two. Then, a cross-layer communication system is developed by combing the proposed QS-CD system at the physical layer and the truncated stop-and-wait automatic repeat request (ARQ) at the data link layer. The performance of the cross-layer system is analyzed and compared with existing schemes in the literature for performance metrics at the data link layer and upper layers, i.e., frame error rate, packet loss rate, average packet delay, throughput, etc. In addition, the studies show that the proposed QS-CD-ARQ system outperforms existing schemes when it has a good partner. In this respect, the proposed system is fully utilizing the communication channel and less complex in terms of implementation when compared with the existing systems.

Since the partner selection gives significant impact on the performance of the CD systems, partner selection algorithms (PSAs) are extensively analyzed for both static and mobile user network. In this case, each individual user would like to take advantage of cooperation by choosing a suitable partner. The objective of an individual user may conflict with the objective of the network. In this regard, we would like to introduce a PSA which tries to balance both users and network objectives by taking user mobility into consideration. The proposed PSA referred to as worst link first (WLF), to choose the best partner in cooperative communication systems. The WLF algorithm gives priority to the worst link user to choose its partner and to maximize the energy gain of the radio cell. It is easy to implement not only in centralized networks but also in distributed networks with or without the global knowledge of users in the network. The proposed WLF matching algorithm, being less complex than the optimal maximum weighted (MW) matching and the heuristic based Greedy matching algorithms, yields performance characteristics close to those of MW matching algorithm and better than the Greedy matching algorithm in both static and mobile user networks. Furthermore, the proposed matching algorithm provides around 10dB energy gain with optimal power allocation over a non-cooperative system which is equivalent to prolonging the cell phone battery recharge time by about ten times.

Acknowledgments

This dissertation is the result of four years of work whereby I have been supported and motivated by many people. It is a great time to express my gratitude for all of them. But, the words are inadequate to convey all my appreciation.

First of all, I would like to express my thanks to my supervisors Professor Jon W. Mark and Professor Xuemin (Sherman) Shen, for giving me this opportunity. They have been actively interested in my research work and have been available to advise me. Their guidance, dedication, patience and consistent support made my thesis work possible, and helped to reach several milestones in my academic career and to achieve many more in the future.

I would like to thank Professor Xinzhi Liu, Professor Murat Uysal and Professor Enhui Yang to serve in my doctoral thesis committee and for their insightful advices and comments that make me to improve the quality of this dissertation. I am very grateful to Professor Steven D. Blostein to be an external examiner. His constructive comments helps to refine the thesis as a valuable document.

It has been my great pleasure to work at the Centre for Wireless Communication (CWC), University of Waterloo. The support from Professor Weihua Zhuang and Professor Pin-Han Ho in research and scholarly activities was grateful at Broadband Communications Research (BBCR) group. I want to thank the present and past members of the BBCR lab including Dr. Jun Cai, Dr. Lin Cai, Dr. Mehrad Dianati, Dr. Xinhua Ling and Dr. Humphery Rutagemwa. Specially, I am very grateful for Dr. Lin Cai and Dr. Humphery Rutagemwa for the research collaboration, and sharing their knowledge and technical expertise. It is time to thank Mr. S. Niranjayan, PhD Student at University of Alberta, for general discussions in performance analysis of communication systems.

I acknowledge the Natural Sciences and Engineering Research Council (NSERC) for funding this research work. My sincere thanks to the University of Waterloo for the

scholarships and awards that includes International Doctoral Student Award and Doctoral Thesis Completion Award. In addition, my gratitude goes to the Department of Electrical and Computer Engineering for providing me numerous Teaching Assistantships. I would like to express my appreciation for the support and services of the administrative staffs, Wendy Gauthier, Wendy Boles, Karen Schooley, Lisa Hendel, Darlene Ryan and Elaine Garner.

I am very grateful to my Guru Kanagambigai for fascinating me in academic career. Moreover, I would like to thank my mother, brothers and sister for inspiring and encouraging me throughout my life. Especially, my heartfelt gratitude goes to my brother Matheesan for facilitating my arrival and settlement in Canada. Finally, my sincere thanks go to my beloved wife, Majantha and my son Maruthagan. Without my wife's support and prayers, this would not have been possible. At this moment, I pay my tribute to my late father and dedicated this thesis to him with my mother and wife.

Dedication

To my late father *Maruthappillai Veluppillai*,

my mother *Rajeswary Veluppillai* and

my beloved wife *Majantha Mahinthan*.

Contents

List of Figures

List of Tables

Chapter 1

Introduction

1.1 Research Motivation

Modern communication systems are an important part of our day to day life. Especially, wireless communication systems such as mobile phone, wireless local area network (WLAN), Bluetooth, etc., provide the freedom for users to roam and to communicate from anywhere at any time. The next generation broadband wireless communication systems are expected to provide wireless multimedia services such as high-speed Internet access, multimedia message services (MMS) and mobile computing. In this case, the wireless communication system designers face a number of challenges which include the limited availability of the radio frequency spectrum and a complex time-varying wireless channel environment. In addition, meeting the increasing demand for high data rates, better quality of service (QoS), fewer dropped calls, longer battery life and higher network/user capacity paves the way for innovative techniques that improve spectral efficiency and link reliability.

1.2 Problem Description

A signal transmitted through a wireless channel arrives at the destination along multiple paths. These paths arise from scattering, reflection and diffraction of the transmitted energy by the objects in the environment. The signals arriving along different paths are attenuated and interfere with each other. The signal attenuation and interference can be due to path loss, long term fading and short term fading. The path loss of a signal depends on both the propagation environment and the distance between the transmitter and the receiver. Long term fading results from the blocking effect of natural obstacles and buildings. Short term fading is due to the constructive and destructive nature of the multipath signals. In this case, time varying multipath signals give rise to effects in different dimensions such as time (delay spread), frequency (Doppler spread) and space (angle spread). Depending on the transmitted signal bandwidth, the fading channel can be viewed as frequency selective, time selective and space selective. The presence of channel impairments degrades the signal-to-interference-plus-noise-ratio (SINR) at the receiver. Sophisticated transmission/reception methods are needed to mitigate channel impairments.

Open loop power control can be used to combat path loss and long term fading effects to achieve reliable transmission. Sophisticated closed-loop power control can be used to combat short term fading [1]. However, the most appropriate way to combat short term fading is the exploitation of diversity with sophisticated signal processing. Diversity techniques are based on supplying several replicas of the same information bearing signal to the receiver over independently fading channels. There are several ways to provide the independently fading replicas of the information-bearing signal to the receiver. Temporal diversity, frequency diversity and spatial diversity are three main techniques that are widely used in wireless communication systems. For example, channel coding is used with appropriate interleaving method to provide temporal diversity. Frequency diversity normally introduces redundancy in the frequency domain by transmitting the same infor-

mation bearing signal over multiple carriers that are separated by the coherent bandwidth of the channel. By deploying multiple transmit and receive antennas, which are separated and/or polarized to create independent fading, spatial diversity can be achieved.

Recently, it has been shown that the achievable data rate of wireless communication systems increases dramatically by employing multiple transmit and receive antennas [2]-[5]. In these schemes, it is assumed that the complex-valued propagation coefficients between any pairs of transmit and receive antennas is statistically independent. Independent channel coefficients are obtained by placing transmit and receive antennas a few wavelengths (3λ -10λ) apart from each other. Because of the wide antenna separation, the traditional adaptive array concepts of beamforming and directivity cannot be applied to these systems. Depending on whether multiple antennas are used for transmission or reception, diversity is classified as transmit antenna diversity and receive antenna diversity. In receive antenna diversity schemes, multiple receive antennas are deployed at the receiver to receive multiple copies of the transmitted signal, which are then properly combined to mitigate the channel fading. In fact, receive antenna diversity schemes have been incorporated with the existing 2^{nd} generation mobile communication systems such as GSM and IS-136 to improve the mobile to base station transmission (uplink) [6]. Transmit antenna diversity is feasible in the downlink of a mobile communication system because multiple transmit antennas can be deployed at the base station to improve the downlink performance of the system. This is accommodated in the 3^{rd} generation mobile communication standards.

Due to the size and power limitations of the mobile unit, it is not feasible to deploy multiple antennas at the mobile unit. As a result, the mobile to base station transmission (uplink) has some bottleneck in the current mobile communication systems. This has motivated the rapidly growing research on transmit antenna diversity with user cooperation. In order to achieve transmit diversity in the uplink, other in-cell users antennas can be shared in a cooperative manner. This mode of gaining transmit diversity is called cooperative diversity (CD) [7–51]. Cooperative diversity schemes mitigate not only the

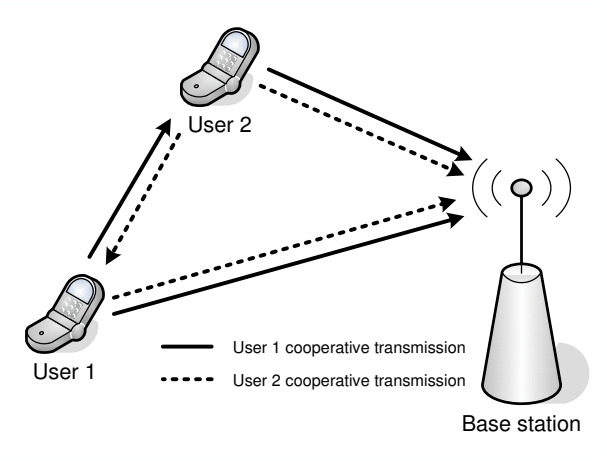

Figure 1.1: Cooperative diversity scheme for two users.

effects of short term fading but also the effects of long term fading, i.e., shadowing, by choosing the partner who does not experience shadowing.

In a cooperative diversity scheme, mobile users would share the time or frequency and other resources to relay the partner's information to the destination. Generally, most of the cooperative diversity schemes that are proposed in the literature have two phases in the transmission. For example, as shown in 1.1, two mobile users (called sender and partner) cooperate and transmit the information to the destination. In the first phase, the sender transmits its information to both the destination and the partner. In the second phase, the partner forwards the information to the destination. Finally, both received signals are combined at the destination. In this case, time is shared by the sender and partners to achieve cooperation.

Sharing resources reduces the effective transmission rate of a user. On the other hand, the user obtains diversity gain by cooperation. In this situation, we do not know whether direct or cooperative transmission is more beneficial. The performance is influenced by a number of factors that should be taken into account in the design of a cooperative diversity scheme. One of the important aspects that characterize the performance of the

cooperative diversity schemes is the quality of the interuser channel. If interuser channel is error free, the cooperative diversity scheme behaves like the conventional multiple input single output (MISO) scheme. In contrast, the performance of the cooperative diversity scheme is worse than that of direct transmission if the quality of interuser channel is worse than the source to destination channel. Therefore, selecting a best partner is important to get benefits from the cooperation. Due to mobility of the users, the partner selection algorithm should predict the movement of the users. The algorithm could be executed periodically by utilizing the predicted mobility information.

Other aspects such as the type of transmission scheme employed at the partner (amplify and forward, regenerate and forward), nature of the cooperative protocols (fixed, adaptive), channel coding, resource allocation, cooperative region, handoff between partners, etc., characterize the performance of a cooperative diversity scheme.

1.3 Main Contributions

The above mentioned considerations and constraints motivate us to propose a bandwidth and power efficient two-user based cooperative diversity scheme which could be accommodated with minimal modifications in the currently available direct or point-to-point communication systems. In addition, a partner selection algorithm is proposed to choose the appropriate cooperating partners in the centralized and distributed wireless communication networks with or without the global knowledge of users.

A quadrature signaling based cooperative diversity (QS-CD) scheme is proposed in which both user's and partner's information symbols are transmitted simultaneously in his/her multiple access channels. Simultaneous transmission helps to improve the performance of the scheme by dynamic resource allocation (power allocation, rate allocation, etc.) based on the qualities of the channels. In addition, the QS-CD system eliminates the additional synchronous transmission among the partners to receive the signal coherently

at the destination in the distributed space-time coded systems [10, 18] and reduces signaling complexity of the cooperative system. First, bit error performance of the QS-CD system is analyzed for fixed relaying at the partner. Second, the bit error performance of the QS-CD system is studied for adaptive relaying at the partner and it is generalized to M-QAM modulation. Third, based on the bit error performance study, the cooperative region within which cooperation can achieve a specified amount of energy gain over a non-cooperative diversity (NCD) system is determined.

Performance of a network deploying the proposed QS-CD system can be further enhanced by cross layer design between the physical, data link and network layers. A cross layer communication system by QS-CD and truncated stop-and-wait automatic repeat request (ARQ) is proposed in this thesis. The proposed QS-CD-ARQ system which is employing selection relaying at the relay is studied analytically by developing a Markov model to capture the behavior of the correlated fading (time selective) among the partners and partner-to-destination channels. This model helps us to study the effects of correlated packet losses. The performance metrics such as channel efficiency, packet loss rate, throughput, average packet delay and jitter are considered and the proposed system is compared with the existing schemes in the literature those are considering incremental relaying at the partner. The results show that the selection relaying outperforms incremental relaying schemes when it has a good partner. In addition, the proposed QS-CD-ARQ system is less complex in terms of implementation comparing with the system employing incremental relaying.

Furthermore, we are concerned with optimally matching active mobile users in a two-user-based cooperative diversity system to maximize the cooperative diversity energy gain in a radio cell. Matching theory and algorithms have been extensively investigated in the past for other applications, *e.g.,* scheduling, assignment. Both the state-of-the-art algorithms to obtain the optimal matching, and the approximation algorithms have been reported. The optimization problem for matching is formulated as a non-bipartite weighted-matching problem in a static network setting. The weighted-matching problem

can be solved using maximum weighted (MW) matching algorithm in polynomial time $O(n^3)$ where n is number active users in the network. To reduce the implementation and computational complexity, we develop a Worst-Link-First (WLF) matching algorithm by maximizing gain (MaxGain) of pair of user, which gives the user with the worse channel condition and the higher energy consumption rate a higher priority to choose its partner. The proposed WLF matching algorithm considers the fact that the nodes with worse channel condition generally get more benefits from the cooperation, which is not obvious in other applications. Furthermore, there are some characteristics which are unique in CD systems; thus, it is worth to re-investigate matching algorithms for this particular problem. The computational complexity of the proposed WLF-MaxGain algorithm is $O(n^2)$ while the achieved average energy gain is only slightly lower than that of the optimal maximum weighted-matching algorithm and similar to that of the Greedy matching algorithm (with computational complexity of $O(n^2 \log n)$) for a static-user network. We further investigate the optimal matching problem in mobile networks. By intelligently applying user mobility information in the matching algorithm, high cooperative diversity energy gain is achievable with moderate overhead. In mobile networks, the proposed WLF-MaxGain matching algorithm, being less complex than the MW and the Greedy matching algorithms, yields performance characteristics close to those of MW matching algorithm and better than the Greedy matching algorithm.

Finally, we show how to appropriately selecting partners for two-user cooperative diversity systems deploying an optimal power allocation strategy, considering not only for QS-CD system but also the other CD schemes in the literature. We first formulate and solve the power allocation problems of 2-user cooperation in cellular networks, considering both the *regenerate and forward* CD systems (including our proposed QS-CD system) and the *amplify and forward*. We also extend the optimal power allocation problems with the constraint that the relaying power at the partner be equal to the source's transmission power. We refer to this as the equal power constraint, which is desired for static wireless networks like sensor networks, in which nodes are equipped with the same

initial energy. The objective is to maximize the lifetime of the network; it is therefore necessary to minimize the energy consumption of the nodes with the maximum energy consumption rate. In this situation, equal power allocation (EPA) can maximize the lifetime of the pair. Second, by incorporating the optimum power allocation strategies proposed, we study the location of the optimal partner for a user. Then, the WLF matching algorithm is modified by minimizing maximum energy (MinMaxEnergy) spent by pair of cooperating users. The newly proposed WLF-MinMaxEnergy algorithm performs very close to the optimal MW matching algorithm. From the numerical results, we show that with optimal power allocation and the proposed matching algorithm, a $9 \sim 10$ dB cooperative diversity gain can be achieved, which is equivalent to prolonging the cell phone battery recharge time by about ten times.

1.4 Structure of the Thesis

The remainder of the thesis is organized as follows. A literature survey of cooperative communication systems and brief introduction to background subjects related to our work such as diversity combining techniques, automatic repeat request and matching algorithms are presented in Chapter 2.

In Chapter 3, the *fixed regenerate and forward* QS-CD system is proposed. First, we introduce the signal transmission and reception of the proposed system. Then, bit error probability is analyzed for both similar and dissimilar channels towards the destination. The effects of the interuser channel on the performance of the proposed system is studied in terms of diversity gain and coding gain. Finally, the cooperative region is derived for the proposed fixed QS-CD system that yields specified signal-to-noise-ratio (SNR) gain over a non-cooperative system (direct transmission scheme).

Chapter 4 presents the *adaptive regenerate and forward* QS-CD system in which the partner employs adaptive relaying. After the introduction of the transmission model, the

analytical derivation of bit error probability is given for the adaptive QS-CD system with QAM scheme. In addition, the analytical results are validated by simulation for 4-QAM and 16-QAM systems.

Effects of time correlated cooperative channels is studied in Chapter 5 by combining QS-CD system with ARQ at the data link layer. The proposed QS-CD-ARQ scheme based on selection relaying is analyzed using Markov modeling and validated via simulation. Moreover, the QS-CD-ARQ system is compared with the existing CD-ARQ schemes in the literature.

Existing matching algorithms such as MW, Greedy and random are presented along with the proposed WLF matching algorithm in Chapter 6. Then, the network employing CD systems is introduced and performance evaluation of the matching algorithms are given for a static network. Furthermore, how to group mobile users by considering user mobility information is studied in Chapter 6.

In Chapter 7, joint optimal power allocation and partner selection is introduced to maximize the energy saving in the wireless network. The joint scheme is generalized for most of the CD systems based on both *amplify and forward* and *regenerate and forward*. First, the power allocation problem is formulated and solved. Then, modified WLF algorithm is proposed by considering power allocation for better energy saving. Finally, the proposed joint system is evaluated numerically.

The contribution of this thesis is summarized in Chapter 8. In addition, the future research directions relevant to the works in this thesis are discussed. Final remarks of the thesis is given at the end of Chapter 8.

1.5 Bibliographic Notes

Most of the works reported in this dissertation can be found in peer reviewed research papers [74–83]. Chapter 3 appeared in [74, 75]. The work of Chapter 4 can be found in [76, 77]. Chapter 5 can be found in [78, 79]. Chapter 6 appeared in [80, 81]. The work of Chapter 7 is published in [82, 83].

Chapter 2

Literature Survey and Background

2.1 Introduction to Cooperative Diversity

Transmit diversity is a powerful technique for combating multipath fading in wireless communications. It is used in 3^{rd} generation mobile communication systems to increase the downlink data rate. However, employing multiple antennas in a mobile terminal to achieve transmit diversity is not feasible due to the limited size of the mobile unit. In order to overcome this problem, a new mode of gaining transmit diversity, called cooperative diversity, which uses the antennas of the other users in the same cell in a cooperative manner is proposed. A two-user cooperation scenario is depicted as shown in Fig. 1.1. The cooperative diversity systems are immuned not only against short term channel fading but also against long term channel fading. On the other hand, cooperative schemes are more sensitive to interuser transmission errors.

Based on the forwarding scheme employed by the partner, CD schemes can be divided into two categories: *amplify and forward* (relaying) and *regenerate and forward* (regenerative repeat). In *amplify and forward* schemes, the partner simply amplifies the signal received from the sender and retransmit it to the destination. To perform *am-*

plify and forward, the schemes require either complex transceiver for frequency division forwarding or large storage for time division forwarding. In the *regenerate and forward* schemes, which is also known as decode and forward, the partner demodulates, re-modulates and retransmits the received signal to the destination. *Regenerate and forward* schemes are more favorable for the mobile devices due to the implementation simplicity. CD schemes can be categorized into *fixed* and *adaptive*. In *fixed* CD schemes, the partner always forwards the information to the destination. In contrast, the partner of an *adaptive* CD scheme decides whether or not to forward the information based on either interuser channel quality or feedback from the destination or checking cyclic redundancy check (CRC) of the frame of bits. If the partner decides not to forward, then it may repeat transmitting its own information sent in the earlier time slot or remain silent. The *adaptive relaying* scheme can be categorized as *selection* and *incremental* [7]. For the selection relaying, the partner always forwards the information if he/she has error free information. On the other hand, incremental relaying forwards only when a request is made from the destination. Generally, both *amplify and forward* and *regenerate and forward* algorithms consist of two transmission phases as shown in Fig. 2.1 for multiple partner cooperation systems. In the first phase, transmission terminals transmit the information to their destinations and all potential partners. During the second phase, the partners transmit the information to the destination.

2.2 CD systems proposed in the literature

In this section, the CD systems proposed in the literature are categorized and discussed.

2.2.1 Cooperative Diversity with Orthogonal Transmission

In [7]- [9], a variety of low complexity cooperative diversity protocols are proposed based on repetition for frequency non-selective half duplex systems. These protocols employ

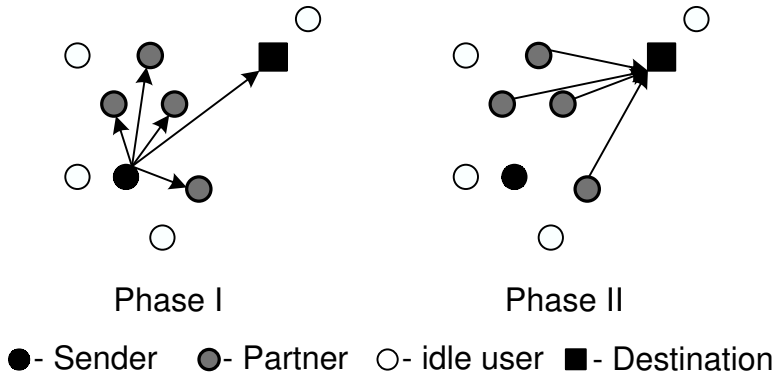

Figure 2.1: Two phase nature of cooperative diversity systems with multiple partners.

different types of processing at the partner, as well as different type of combining at the destination on terminals. That may be characterized as *fixed and adaptive* (selection and incremental) relaying. Here, channel allocation for different senders is made across the entire frequency band as shown in Fig. 2.2. Furthermore, subchannel allocation for different relays is made across the time span in each frequency subband, as shown in Fig. 2.3. Each subchannel contains a fraction $1/m^2$ of the total degree of freedom in the channel where m is the number of users in the NCD systems. Similar to non-cooperative transmission each sender and partner uses the fraction $1/m$ of the total degree of freedom in the channel to transmit to the destination.

The fixed *amplify and forward* scheme proposed in [7] can be viewed as repetition coding from two users, except that the partner amplifies its own receiver noise. The sender to partner channel fading coefficient is utilized at the partner to amplify the signal. Therefore, it is important to have accurate channel state information. The destination receiver can use maximum ratio combining to decode the information from two sub blocks of the received signal.

In fixed *regenerate and forward*, the partner can decode the information either by

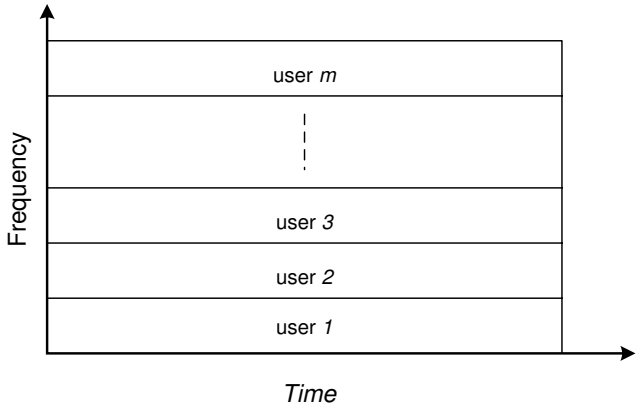

Figure 2.2: Channel allocation for m users in non-cooperative medium-access control.

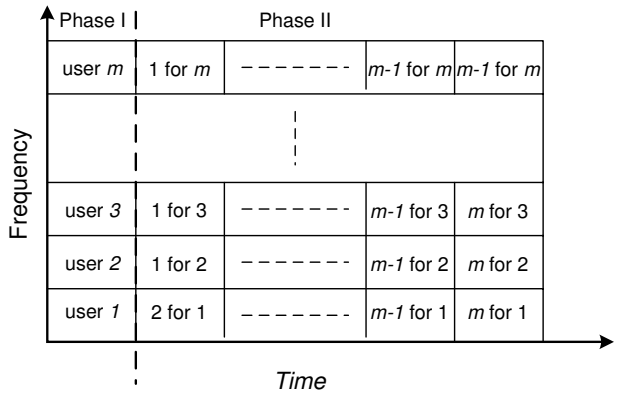

Figure 2.3: Subchannel allocation for m users in repetition based cooperative diversity medium-access control.

fully decoding the source message to estimate the source codeword or by estimating symbol by symbol. The regenerated signal is transmitted by the partner according to the repetition coding scheme. To combine the transmission from the sender and the partners, a suitably modified matched filter is employed at the destination. The selection relaying scheme functions based on the the channel quality between the sender and the partner (interuser). If the interuser channel quality falls below a certain threshold the sender simply continues its transmission to the destination in the form of repetition. If the interuser channel quality lies above the threshold, the partner forwards what it receives from the sender. The performance of selection *regenerate and forward* cooperative diversity scheme is analyzed for more than two terminals in [10]. It is shown in [10] that repetition protocol offer full spatial diversity for multiuser cooperation to achieve diversity gain.

However, full spatial diversity benefits of the repetition based cooperative diversity scheme come at a price of decreasing bandwidth efficiency with the number of cooperating users. The repetition-coded transmission of both fixed and selection relaying loses an additional 3dB from the two antenna transmit diversity bound at high SNR. To overcome the problem a hybrid ARQ based scheme, called incremental relaying, is proposed. Here, the partner forwards what it receives from the sender if the feedback from the destination indicates that the direct transmission from the sender to the destination alone was not successful. This scheme has been shown as information theoretically efficient. But, It has lots of implementation and complexity issues such as partner should aware about ARQ, resource allocation to the partner transmission for short duration (one frame duration), etc.

Both *Fixed amplify and forward*, and *incremental amplify and forward* achieve diversity order of two. The performance of the fixed *regenerate and forward* scheme is mainly dependant on the interuser channel quality. By contrast, *incremental amplify and forward* overcomes these additional losses by relaying the information only when necessary. *Incremental amplify and forward* is useful in developing higher layer network

protocols that select between direct transmission and cooperative diversity. Such algorithms and their performance represent an interesting area of future research and a key ingredient for fully incorporating cooperative diversity into wireless networks. There are costs associated with the proposed cooperative protocols. Cooperation with half-duplex operation requires twice the bandwidth of direct transmission for a given rate, and leads to larger effective SNR losses for increasing spectral efficiency.

A *selection regenerate and forward* scheme for cooperative diversity networks is proposed in [11–13]. The influence of the data rate, path loss and network geometry on the cooperative scheme is studied in [11] with the assumption that interuser channel quality is always good. In this scheme, the channel is divided into two subchannels in the time domain which demands a bandwidth twice as large compared to the NCD scheme. In addition, the scheme wastes radio resources when the interuser channel incurs error.

In [14], a CD system based on regenerate and forward and superposition modulation at the partner is proposed. At the partner, the sender's and the partners' information are modulated using superposition modulation proposed. The destination decodes the information using a maximum a posteriori probability (MAP) detector. This CD system outperforms the classical *regenerate-and-forward* cooperation schemes by 1-2 dB at the expense of a more complex receiver.

So far, all the systems mentioned above assume that perfect channel state information (CSI) is available at the respective receivers or can be estimated. In slow-fading scenarios, CSI can be estimated from training sequences. However, CSI may not be accurately obtainable if the fading coefficients vary quickly. Since the coherence time decreases in a fast fading situation, estimation of CSI substantially reduces the data transmission rate due to pilot tones insertion. In this passage, the CD systems that can perform without CSI are presented. CD systems based on differential modulation are proposed and analyzed in [15] and [16] for *regenerate and forward* and *amplify and forward*, respectively. The system proposed in [15] can decode the information at the partner and the destina-

tion without CSI. For *amplify and forward*, the system proposed in [16] can handle the differentially modulated transmission from the sender to the destination. This scheme can be classified as a fixed CD system. Non coherent modulation and demodulation method is proposed for both *regenerate and forward* and *amplify and forward* in [17]. The proposed system considering binary frequency shift keying (BFSK) modulation and compare the results with coherent modulation systems.

2.2.2 Cooperative Diversity based on Space-Time Coding

In [7–9] and reference there in, full spatial diversity benefits of these repetition based cooperative diversity algorithms come at a price of decreasing bandwidth efficiency with the number of cooperative terminals. An alternative approach to improve bandwidth efficiency of the algorithms is proposed in [10, 18] based on space-time codes (STC) called distributed space-time coding (DSTC). In this case, partners utilize a suitable STC in the second phase. Therefore all the partners can transmit simultaneously on the same subchannels as shown in Fig 2.4. Similar to the non-cooperative scheme, repetition based cooperative diversity scheme utilizes 1/m of the total degree of freedom in phase II. In contrast, each partner employing DSTC transmits in $1/2$ the total degree of freedom in the channel. By requiring more computational complexity in the terminals, DSTC can achieve full diversity without any feedback. An outage analysis is given in [10] on a random coding argument.

In [19], an extension of the DSTC of [10, 18] to K amplifying relays is presented. An exact average symbol error rate performance of this system is derived for phase shift keying (PSK) transmissions over Rayleigh-fading channels. The proposed system in [19] can achieve diversity order of $K + 1$. In addition, asymptotic study of a cooperative scheme operating in *amplify-and-forward* for a large number of relays is presented in [20]. A channel dependent optimal code design rule is derived by utilizing the pairwise error probability (PEP) derivation. A DSTC systems based super orthogonal space-time

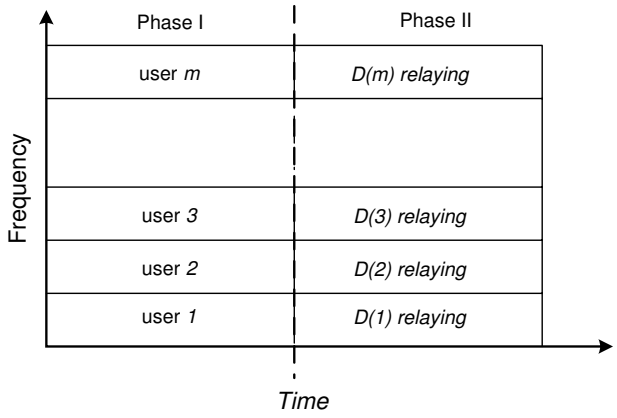

Figure 2.4: Channel allocation for m users in distributed space-time coded cooperative diversity medium-access control.

trellis code is proposed in [21], in which the performance is investigated through the derivation of PEP. A differential DSTC scheme is presented in [22] which can decode the STC at the receivers without the knowledge of CSI, with a few dB penalty in SNR gain. Similar study is done for both *regenerate and forward* and *amplify and forward* in [23].

But in practice, the number of users participating in the cooperative event is unknown. In cooperative operation, the signals transmitted from some of the antennas may disappear due to deep fading. To overcome this problem, the columns of the code matrix should be orthogonal to each other. Space-time block code based on orthogonal design is a better candidate for this scenario. The DSTC system has a major disadvantage in synchronous reception in *Phase II* at the destination due to the different propagation delays among the partners to destination links.

In [24] and [25] asynchronous DSTC systems are presented for trellis and block coding, respectively. Based on the code proposed in [24], various generalizations of optimal rate-diversity tradeoff codes proposed in [52] are constructed for a distributed

environment in [26]. However, the proposed asynchronous systems can work without synchronous reception at the destination, with the penalty of the loss in energy gain by few dB over synchronous systems.

Most of the works reported earlier consider the flat fading channel. But, three distributed space-time block coded (DSTBC) methods, such as distributed time reversal, distributed single carrier and distributed orthogonal frequency division multiplexing (OFDM), are introduced for frequency selective channels in [27]. The proposed methods are investigated for Alamounti's space-time block code (STBC) [53] and shown that the proposed schemes can achieve the diversity order of $L + 1$ where L is the channel memory.

2.2.3 Cooperative Diversity for CDMA Sytems

A new form of cooperative strategy employed by two users based on a combination of block Markov encoding and backward decoding is proposed in [31]- [33]. The information-theoretic capacity, outage, and coverage analysis in [31] illustrates the potential benefits of cooperation. It is also shown that the cooperation is beneficial for both users in terms of increasing the achievable rates and decreasing the probability of outage. Alternatively, cooperation can also be used to increase the cell size of a cellular system. Based on the signal structure used for the information-theoretic analysis, a possible code-division multiple-access (CDMA) implementation is proposed in [31] and it is extended for high-rate CDMA systems using multiple spreading codes in [32]. In addition, the potential uses of cooperation in cellular and wireless ad hoc networks are discussed.

The benefits of cooperation and practical issues within the CDMA framework are further analyzed in [32]. The CDMA cooperative structure suggested in [31] is investigated in terms of probability of error for both optimal receiver and low complexity sub-optimal receiver. It is also shown that cooperative diversity not only offers improvement in throughput but also increases the coverage of a cell. Benefits of cooperation, when a mobile using multiple CDMA code for high rate systems, is also studied. Finally, it is

shown that cooperation is superior to no cooperation at the expense of complexity even though the mobile does not have channel phase information.

The authors of [31]- [33] indicate that their scheme is not necessarily optimal, which paves the way for an optimal cooperative diversity scheme. The sub optimum receiver given in [31]- [33] also has some limitations in performance and practical implementations. In addition, the scheme wastes transmit power of both users when interuser channel exhibits errors.

2.2.4 Cooperation based on Channel Coding

A different framework based on channel coding, called coded cooperation, is proposed in [34–38]. The key ideas of the scheme are cooperation through partitioning a user's codeword and avoiding error propagation through error correction by the partner. Instead of repeating the symbols, the codeword of each user is partitioned into two sets; one partition is transmitted by the sender and the other by the partner through partial or complete decoding. Generally, various forward error correcting block or convolutional code can be used in conjunction with either puncturing or product codes for cooperation. More specifically, rate compatible punctured convolutional (RCPC) code is selected in [34]- [36]. In [34] and [35], a simulation study of the proposed scheme is given. In addition, analytical derivation of pairwise error probability of the scheme is given and compared with the simulation results in [36]. In [37], rate compatible punctured turbo (RCPT) code is considered instead of RCPC.

Another coding technique called distributed turbo coding is proposed for cooperative diversity system with quasi-static relay channel in [39] and [40]. The source broadcast a recursive systematic convolutional code to both the partner and the destination. The partner decodes, interleaves and re-encodes the message and forwards it to the destination. The destination detects the data by introducing both direct and regenerated messages into an iterative decoder. In addition, the information theoretic limit on outage probability of

the distributed turbo codes is analyzed.

The performance of the coded cooperation schemes is bounded by the tradeoff between coding gain and diversity gain. Furthermore, channel coding, which is used in this scheme, is designed for non-cooperative diversity systems. A development of channel coding which accounts for the effects of all the channels associated with cooperative transmission is fruitful to optimize the performance of a coded cooperation system.

2.2.5 Information Theoretic Study on Cooperative Diversity

In this section, we summarize the information theoretic analysis on cooperative diversity given in the literature. This includes diversity-multiplexing tradeoff bounds and average symbol error probability (SEP) and outage probability analysis.

Generally, a multiple input and multiple output (MIMO) system provides both diversity gain and multiplexing gain. But, there is a fundamental tradeoff between how much of each type of gain any MIMO system can get. The diversity and multiplexing tradeoff, which is actually the tradeoff between the BEP and the data rate of a system, is studied in [54]. It is further extended to MIMO multiple access channels in [55]. Similar analysis is done in [41] for cooperative diversity schemes such as amplify and forward, regenerate and forward and DSTC. Achievable diversity-multiplexing tradeoff for half duplex cooperative systems is studied in [42] and [43].

Based on the parameterization quantifying given in [56], the average SEP and outage probability are analyzed for multi-branch multi-hop non-regenerative cooperative diversity systems in [44]. The method presented in [56] enables the derivations of average SEP for high SNR by looking at the probability density function (PDF) of the SNR around zero. The error probability analysis given in [44] reveals that the error gain of multi-hop systems stems from reduced path loss, while that of multi-branch systems comes from both the reduced path loss and the diversity.

2.3 Background

In this section, a brief introduction of background related to our work such as diversity combining techniques, automatic repeat request and matching algorithms is presented.

2.3.1 Diversity Combining Techniques

Diversity combing is a technique that combines multi-branch signals to one enhanced signal. Generally, it can be classified as selection combing (SC), equal gain combining (EGC) and maximum ratio combining (MRC) [58]. The SC selects the best signal among all the branches. It is very simple to implement and gives worse performance by ignoring other branches. The EGC gives equal weights for all the branches by considering the phase of the received signal and sum all of them as one signal. Since it gives the same weight to both weak signal branches as well strong signal branches, the weak signal may destroy the information carried by the strong signal. EGC is better than SC. The MRC gives the optimal performance by weighting each branch proportional to the signal amplitude [59] and summing them. That means the branches with strong signal are further amplified while weak signals are attenuated. The MRC needs accurate signal amplitude and phase information for proportional weighting. However, the performance of the MRC scheme is far better than those of the other two.

2.3.2 Automatic Repeat Request

Automatic repeat request is an error control mechanism used in data communication systems [60]. The destination sends a feedback to the sender by positive acknowledgement (ACK) or negative acknowledgement (NAK) for each data frame. The destination checks each data frame using CRC for error. If the received frame is in error, the destination sends a NAK and the sender re-transmits the data frame. Otherwise, the destination

sends an ACK and the sender transmits a new data frame. In addition to feedback, the sender has a timeout mechanism. If the sender does not receive the feedback within the specified time after transmission of the data frame, timeout occurs and the sender re-transmit the date frame. The re-transmission process continues until the data frame is successfully received or re-transmission exceed the maximum number of re-tries. If the number of re-transmissions is bounded by the maximum number of re-tries, such ARQ system is called a truncated-ARQ systems.

Depending on the mechanism employed, the ARQ schemes can be stop-and-wait ARQ, go-back-N ARQ, selective repeat ARQ, etc. The stop-and-wait ARQ is simple compared with others and it transmits one frame at a time and waits for feedback or time-out before sending the next frame or retransmit the same frame. In other ARQ schemes, the sending process continues to send a number of frames specified by a window size even without receiving an ACK packet from the destination.

2.3.3 Matching Algorithms

Graph theory defines the matching as a set of edges without common vertices. Let $\mathcal{G} = \{\mathcal{V}, \mathcal{E}\}$ be a graph, where $\mathcal{V}$ is a set of vertices and $\mathcal{E} \subseteq \mathcal{V} \times \mathcal{V}$ is a set of edges between vertices. A subset $\mathcal{S}$ of $\mathcal{E}$ is called a *matching* subset if there are no two edges in $\mathcal{S}$ sharing the same vertex. If a vertex is incident to an edge in the $\mathcal{S}$, the vertex is matched. Otherwise, the vertex is unmatched.

Generally, matching can be categorized as bipartite and non-bipartite matching. A bipartite matching is done between two disjoint sets of vertices in a graph such that no edge has both end-points in the same set. On the other hand, the matching can be done any of two vertices in a graph called non-bipartite matching. In this thesis, we are concerned with non-bipartite matching algorithms.

If each edge has an associated value w in a non-bipartite graph, it is called weighted non-bipartite graph. Maximizing the weight is equivalent to maximizing $w(\mathcal{S}) = \sum_{e_{i,j} \in \mathcal{S}} w(e_{i,j})$

among all possible matchings, which is a non-bipartite weighted-matching problem. The maximum weighted matching algorithm developed in [61] can yield the optimal solution for the non-bipartite weighted-matching problem in polynomial time, $O(n^3)$. In addition, the heuristic based Greedy matching algorithm [62] gives sub-optimal performance with the complexity of $O(n^2 \log n)$.

Chapter 3

Fixed Cooperative Diversity System

Orthogonal signaling helps to easily distinguish the signals at the receiver. The inner product of two orthogonal signals is zero. This orthogonal property of the signals can be achieved in numerous ways for the communication system, i.e., quadrature signaling (in-phase and quadrature components of quadrature amplitude or phase shift keying modulation), frequency shift keying , orthogonal frequency division multiplexing, Walsh spreading codes, etc.

In this chapter, a bandwidth and energy efficient CD system based on quadrature signaling is proposed for a two-user cooperation over flat fading channels. Quadrature signaling is achieved by transmitting in the in-phase and quadrature components of a PSK/QAM modulation scheme. The proposed scheme is a *fixed regenerate and forward* type; this means the relay always regenerates the symbol and forwards it to the destination. The power and bandwidth of the proposed cooperative scheme are equal to those of a non-cooperative scheme. Both symbol-by-symbol detection and a absence of CRC checking in the partner's device offer implementation simplicity and reduce the processing delay. In addition, processing delay at the partner's mobile and propagation delay difference between the direct and the partner transmissions are taken into account at the base station (BS) receiver. Furthermore, the proposed scheme is simpler to implement

than the CD systems reported in the literature, since the proposed scheme only needs the additional hardware to receive the uplink signal of the partner. It also can be easily switched between cooperative and non-cooperative modes based on the interuser signal-to-noise ratio (ISNR). Our contributions in this chapter can be summarized as follows:

- Derivation of bit error performance of the proposed scheme for both similar[1] and dissimilar channels towards the BS.
- Derivation and presentation of diversity gain that can be achieved by the CD scheme under various interuser and user to BS channel conditions.
- Derivation of the cooperative region for both specified CD gain and specified bit error performance over direct transmission.

The rest of the chapter is organized as follows. The transmission model and the signal reception procedure at the partner and at the destination are described in Section 3.1. Bit error probability (BEP) of the system is analyzed in Section 3.2. Section 3.3 studies the diversity gain and coding gain of the proposed system. The region of the partner for cooperation, called cooperative region, is derived in Section 3.4. The chapter is summarized in section 3.5.

3.1 Transmission Model

Consider a cooperative wireless communication system in which each mobile user cooperates with another mobile user (the partner) to transmit information in the uplink as shown in Fig. 1.1. In each cooperative mobile device, both own and partner's information are simultaneously transmitted using quadrature signaling[2].

[1] By similar channel, it is meant that the signal-to-noise ratios of both sender and partner are equal at the destination (BS).

[2] With quadrature signaling, a user transmits the partner's signal as well as its own. Thus the roles of sender and partner are interchangeable.

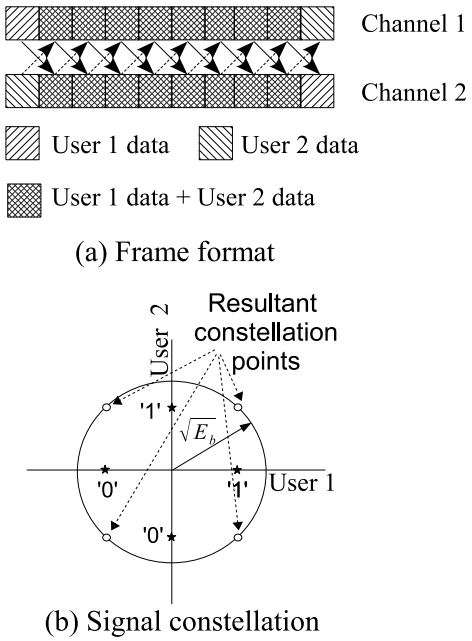

Figure 3.1: Transmission frame format and the signal constellation of the proposed modulation scheme.

3.1.1 Signal Transmission

The transmission frame format and the signal constellation of the QPSK modulation scheme are shown in Fig. 3.1. Fig. 3.1(a) shows a frame of information symbols transmitted by *user 1* in *channel 1* and *user 2* in *channel 2*. In the first symbol interval, each user transmits its own information only. In successive symbol intervals, each user transmits not only its own information but also the partner's information received in the previous symbol interval. But, in the last symbol interval of the frame, each user transmits the partner's information only. In our proposed scheme, *user 1* and *user 2* use the in-phase and the quadrature components of a QPSK modulated signal, respectively. This means that each user equivalently employs BPSK modulation. The signal constellation is illustrated in Fig. 3.1(b).

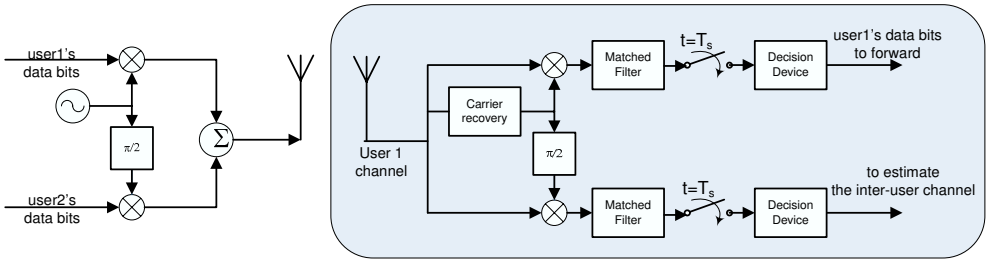

Figure 3.2: Transceiver structure of the mobile terminal.

The standard QPSK transceiver is modified as shown in Fig. 3.2 to accommodate the proposed scheme. As mentioned above, both *user 1*'s and *user 2*'s data bits are fed to the in-phase and quadrature branches of the transmitter, respectively. In the uplink receiver of *channel 1*, the in-phase and quadrature components are demodulated separately to forward the detected *user 1*'s data bits to the base station. In addition, we assume that the channel fading coefficients are available at the respective receivers to demodulate the symbol using matched filtering.

3.1.2 Signal Reception

The receiver structure at the BS is shown in Fig. 3.3. The signals are received from both users' channels and combined using a maximum ratio combiner. To decode the information of *user 1*, the received signal from channel 1 is delayed by one symbol interval and combined with the received signal from channel 2 in the MRC. Similarly, to decode the information of *user 2*, the received signal from channel 2 is delayed by one symbol interval and combined with the received signal from channel 1. The output of the MRC is sent to a decision device which converts it to a binary data.

The baseband equivalent received signals from *user 1* and *user 2* at the BS is de-

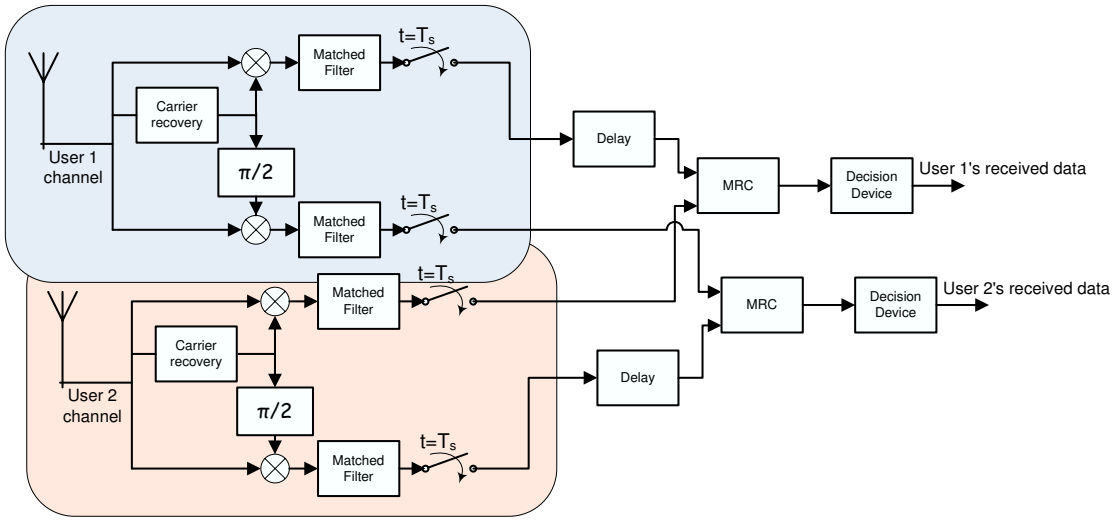

Figure 3.3: Receiver of the base station

noted as $r_{1,B}(t)$ and $r_{2,B}(t)$, respectively. Similarly, *user 2*'s uplink signal received by *user 1* and *user 1*'s uplink signal received by *user 2* are denoted as $r_{2,1}(t)$ and $r_{1,2}(t)$, respectively. From the system model, $r_{1,B}(t)$, $r_{2,B}(t)$, $r_{2,1}(t)$ and $r_{1,2}(t)$ can be written as,

$$\begin{aligned} r_{1,B}(t) &= h_{1,B}(t)s_1(t) + \eta_{1,B}(t) \\ r_{2,B}(t) &= h_{2,B}(t)s_2(t) + \eta_{2,B}(t) \\ r_{2,1}(t) &= h_{2,1}(t)s_2(t) + \eta_{2,1}(t) \\ r_{1,2}(t) &= h_{1,2}(t)s_1(t) + \eta_{1,2}(t) \end{aligned} \tag{3.1}$$

where the channel fading coefficient between user i and the BS is denoted by $h_{i,B}(t)$ and the channel fading coefficient from user i to user j is denoted by $h_{i,j}(t)$. When the interuser channel is symmetric, $h_{1,2}(t) = h_{2,1}(t)$. The channels are modeled as Rayleigh flat fading channels. $\eta_{1,B}(t)$, $\eta_{2,B}(t)$, $\eta_{1,2}(t)$ and $\eta_{2,1}(t)$ are additive noise at the respective receivers and modeled as zero mean circularly symmetric, complex Gaussian distributed with variance $N_0/2$. $s_1(t)$ and $s_2(t)$ are transmitted signals from *user 1* and

user 2, respectively, and are chosen from the QPSK signal constellation shown in Fig. 3.1(b). Therefore, $s_1(t)$ and $s_2(t)$ can be written as follows:

$$\begin{aligned} s_1(t) &= \sqrt{E_b/2}(b_1(t) + j\bar{b}_2(t - T_s)) \\ s_2(t) &= \sqrt{E_b/2}(\bar{b}_1(t - T_s) + jb_2(t)) \end{aligned} \tag{3.2}$$

where $b_1(t)$ and $b_2(t)$ are BPSK information symbols of *user 1* and *user 2*, respectively, and $\bar{b}_i(.)$, $i = 1, 2$, are the corresponding reproduced symbols at the partners. T_s denotes the symbol duration and E_b is the bit energy of non-cooperative transmission.

Using maximum likelihood (ML) detection at *user 1* to detect *user 2*'s data we have

$$\check{b}_2 = \Im\{h^*_{2,1}(t)r_{2,1}(t)\}. \tag{3.3}$$

where the superscript * denotes conjugate of a complex number and conjugate transpose of a matrix. Similarly, detecting *user 1*'s data at *user 2* yields

$$\check{b}_1 = \Re\{h^*_{1,2}(t)r_{1,2}(t)\}. \tag{3.4}$$

The decision rule is,

$$\bar{b}_i = \begin{cases} 1 & \text{if } \check{b}_i > 0 \\ -1 & \text{otherwise} \end{cases}. \tag{3.5}$$

In the above, the symbols $\Re\{Z\}$ and $\Im\{Z\}$ denote the real and the imaginary parts of the complex number Z, respectively. At the BS, the signals received from both user channels are combined using MRC and decoded. The results are

$$\begin{aligned} \tilde{b}_1 &= \Re\{h^*_{1,B}(t - T_s)r_{1,B}(t - T_s) + h^*_{2,B}(t)r_{2,B}(t)\} \text{ and} \\ \tilde{b}_2 &= \Im\{h^*_{2,B}(t - T_s)r_{2,B}(t - T_s) + h^*_{1,B}(t)r_{1,B}(t)\}. \end{aligned} \tag{3.6}$$

Choose

$$\hat{b}_i = \begin{cases} 1 & \text{if } \tilde{b}_i > 0 \\ -1 & \text{otherwise} \end{cases}. \tag{3.7}$$

3.1.3 Non Cooperative Diversity System

When user cooperation is not beneficial, the system can be switched to non cooperative diversity (NCD) system. In this chapter, NCD system are referred to the conventional direct communication system between user-to-destination. In such a circumstance, NCD system uses standard BPSK modulation with bit energy E_b.

3.2 Analysis of Bit Error Probability

Without loss of generality, consider the data transmission of *user 1*. Assume quasi static flat Rayleigh fading, i.e., $h_{1,B}(t) = h_{1,B}(t - T_s) = h_{1,B}$, $h_{2,B}(t) = h_{2,B}(t - T_s) = h_{2,B}$, $h_{1,2}(t) = h_{1,2}$ and $h_{2,1}(t) = h_{2,1}$. Define $\mathbf{H} = \begin{bmatrix} h_{1,B} & h_{2,B} \end{bmatrix}^T$ where $[\cdot]^T$ denotes matrix transpose and

$$\mathbf{r} = \begin{bmatrix} r_{1,B}(t - T_s) \\ r_{2,B}(t) \end{bmatrix} = \begin{bmatrix} h_{1,B} \\ \Theta h_{2,B} \end{bmatrix} b_1 + \begin{bmatrix} \eta_{1,B}(t - T_s) \\ \eta_{2,B}(t) \end{bmatrix} \tag{3.8}$$

where Θ is an indicator of decoding error of b_1 at *user 2* i.e., $\Theta = -1$ with probability $P_{1,2}$ and $\Theta = 1$ with probability $1 - P_{1,2}$, where $P_{1,2}$ is the interuser average bit error probability. The decision rule at the MRC receiver can be written as [3]

$$\hat{b}_1 = sign\{\Re(\mathbf{H}^* \mathbf{r})\} = sign\{\Re((|h_{1,B}|^2 + \Theta\,|h_{2,B}|^2) b_1 + \eta)\} \tag{3.9}$$

[3] We assume that the channel fading coefficients $h_{1,B}$ and $h_{1,B}$ are perfectly known at the receiver.

where η is the additive noise with zero mean and variance $(|h_{1,B}|^2 + |h_{2,B}|^2)N_0/2$ and the instantaneous error probability for equiprobable bits is given by

$$\begin{aligned}
P_e^c &= P\left(\hat{b} = 1 | b_1 = -1\right) \\
&= P\left(\eta > (|h_{1,B}|^2 + \Theta\,|h_{2,B}|^2)\sqrt{E_b/2}\right) \\
&= (1 - P_{1,2})P\left(\eta > (|h_{1,B}|^2 + |h_{2,B}|^2)\sqrt{E_b/2}\right) + P_{1,2}P\left(\eta > (|h_{1,B}|^2 - |h_{2,B}|^2)\sqrt{E_b/2}\right) \\
&= (1 - P_{1,2})Q\left(\frac{(|h_{1,B}|^2 + |h_{2,B}|^2)\sqrt{E_b/2}}{\sqrt{(|h_{1,B}|^2 + |h_{2,B}|^2)N_0/2}}\right) + P_{1,2}Q\left(\frac{(|h_{1,B}|^2 - |h_{2,B}|^2)\sqrt{E_b/2}}{\sqrt{(|h_{1,B}|^2 + |h_{2,B}|^2)N_0/2}}\right) \\
&= (1 - P_{1,2})P_{MRC}^c + P_{1,2}P_{dMRC}^c,
\end{aligned} \tag{3.10}$$

where $P_{MRC}^c = Q\left(\frac{(|h_{1,B}|^2+|h_{2,B}|^2)\sqrt{E_b/2}}{\sqrt{(|h_{1,B}|^2+|h_{2,B}|^2)N_0/2}}\right)$, $P_{dMRC}^c = Q\left(\frac{(|h_{1,B}|^2-|h_{2,B}|^2)\sqrt{E_b/2}}{\sqrt{(|h_{1,B}|^2+|h_{2,B}|^2)N_0/2}}\right)$ and the superscript c denotes instantaneous value .

3.2.1 Derivation of P_{MRC}

Let P_{MRC} denote the average BEP of the MRC. In this subsection, we reformulate the derivation of the BEP of multi branch MRC given in [63] for the BEP of the two branch MRC. Let $\gamma_i = \frac{E_b}{N_0}|h_{i,B}|^2$ be the received bit energy-to-noise spectral density ratio and $\bar{\gamma}_i$ be the average bit energy-to-noise spectral density ratio from the i^{th} channel. Note that energy-to-noise spectral density ratio is equivalent to signal-to-noise ratio (SNR). For notational convenience, we will refer to γ as the SNR throughout the thesis.

3.2.1.1 Dissimilar Channel towards BS

The γ_i has a chi-squared distribution with two degrees of freedom. The PDF of γ_i can be written as

$$p_{\gamma_i}(\gamma_i) = \frac{1}{\bar{\gamma}_i}\exp^{-\gamma_i/\bar{\gamma}_i} \tag{3.11}$$

Let $\mathbf{E}\{|h_{i,B}|^2\} = \sigma_{i,B}^2$, then $\bar{\gamma}_i = \sigma_{i,B}^2(E_b/N_0)$. The characteristic function of γ_i can be written as

$$\phi_{\gamma_i}(j\omega) = \frac{1}{1 - j\omega\bar{\gamma}_i}. \tag{3.12}$$

Since $\gamma = \gamma_1 + \gamma_2$, the characteristic function of γ is

$$\phi_{\gamma}(j\omega) = \frac{1}{(1 - j\omega\bar{\gamma}_1)(1 - j\omega\bar{\gamma}_2)}. \tag{3.13}$$

Inverse Fourier transforming the characteristic function in (3.13) yields the probability density function of γ, which can be written as

$$p(\gamma) = \left(\frac{\bar{\gamma}_1}{\bar{\gamma}_2 - \bar{\gamma}_1}\right)\frac{1}{\bar{\gamma}_1}\exp^{-\gamma/\bar{\gamma}_1} + \left(\frac{\bar{\gamma}_2}{\bar{\gamma}_1 - \bar{\gamma}_2}\right)\frac{1}{\bar{\gamma}_2}\exp^{-\gamma/\bar{\gamma}_2}, \quad \gamma \geq 0. \tag{3.14}$$

By rewriting the P_{MRC}^c in terms of γ_1 and γ_2, we have

$$P_{MRC}^c = Q\left(\sqrt{\gamma_1 + \gamma_2}\right) \quad = Q\left(\sqrt{\gamma}\right). \tag{3.15}$$

By averaging the instantaneous error probability (3.15) over the pdf given in (3.14), we have

$$\begin{aligned} P_{MRC} &= \int_0^{\infty} Q\left(\sqrt{\gamma}\right) p(\gamma) d(\gamma) \\ &= \frac{1}{2}\left[\frac{\bar{\gamma}_1}{\bar{\gamma}_1 - \bar{\gamma}_2}\left(1 - \sqrt{\frac{\bar{\gamma}_1}{2 + \bar{\gamma}_1}}\right) + \frac{\bar{\gamma}_2}{\bar{\gamma}_2 - \bar{\gamma}_1}\left(1 - \sqrt{\frac{\bar{\gamma}_2}{2 + \bar{\gamma}_2}}\right)\right]. \end{aligned} \tag{3.16}$$

3.2.1.2 Similar Channel towards BS

In this case, both channels have equal bit energy-to-noise spectral density ratio at the BS, so that $\bar{\gamma}_1 = \bar{\gamma}_2$. From (3.13), the characteristic function of γ becomes

$$\phi_{\gamma}(j\omega) = \frac{1}{(1 - j\omega\bar{\gamma}_1)^2}. \tag{3.17}$$

Inverse Fourier transforming the characteristic function in (3.17) yields the probability density function of γ,

$$p(\gamma) = \frac{1}{\bar{\gamma}_1^2}\gamma\exp^{-\gamma/\bar{\gamma}_1} \quad \gamma \geq 0. \tag{3.18}$$

By averaging the instantaneous error probability (3.15) over the pdf given in (3.18), we have

$$\begin{aligned} P_{MRC} &= \int_0^\infty Q\left(\sqrt{\gamma}\right) p(\gamma) d(\gamma) \\ &= \left(2 + \sqrt{\frac{\bar{\gamma}_1}{2+\bar{\gamma}_1}}\right) \left[\frac{1}{2}\left(1 - \sqrt{\frac{\bar{\gamma}_1}{2+\bar{\gamma}_1}}\right)\right]^2 . \end{aligned} \tag{3.19}$$

3.2.2 Derivation of Lower Bound of P_{dMRC} (P^L_{dMRC})

When the interuser channel incurs bit error, the MRC operation is equivalent to subtracting one signal from the other, and we refer to this operation as differential MRC (dMRC).

$$\begin{aligned} P^c_{dMRC} &= Q\left(\frac{(|h_{1,B}|^2 - |h_{2,B}|^2)\sqrt{E_b/2}}{\sqrt{(|h_{1,B}|^2 + |h_{2,B}|^2)N_0/2}}\right) \\ &> Q\left(\sqrt{\frac{|(|h_{1,B}|^2 - |h_{2,B}|^2)|E_b}{N_0}}\right) \\ &= Q\left(\sqrt{|\gamma_1 - \gamma_2|}\right) \end{aligned} \tag{3.20}$$

Therefore γ can be written as

$$\gamma = \begin{cases} \gamma_1 - \gamma_2 & \text{if } \gamma_1 \geq \gamma_2 \\ \gamma_2 - \gamma_1 & \text{otherwise} \end{cases} . \tag{3.21}$$

By considering the property of γ given in (3.21), P^L_{dMRC} can be expressed as

$$P^L_{dMRC} = P(\gamma_1 \geq \gamma_2)P(e|\gamma_1 \geq \gamma_2) + P(\gamma_1 < \gamma_2)P(e|\gamma_1 < \gamma_2). \tag{3.22}$$

3.2.2.1 Derivation of $P(\gamma_1 \geq \gamma_2)$ and $P(\gamma_1 < \gamma_2)$

On the basis that γ_1 and γ_2 are independent, the joint pdf is given by

$$p_{\gamma_1,\gamma_2}(\gamma_1, \gamma_2) = \frac{1}{\bar{\gamma}_1 \bar{\gamma}_2} \exp^{-\gamma_1/\bar{\gamma}_1} \exp^{-\gamma_2/\bar{\gamma}_2} . \tag{3.23}$$

Therefore,

$$\begin{aligned} P(\gamma_1 \geq \gamma_2) &= \int_0^{\infty} \int_0^{\gamma_1} \frac{1}{\bar{\gamma}_1 \bar{\gamma}_2} \exp^{-\gamma_1/\bar{\gamma}_1} \exp^{-\gamma_2/\bar{\gamma}_2} d(\gamma) \\ &= \frac{\bar{\gamma}_1}{\bar{\gamma}_1 + \bar{\gamma}_2}. \end{aligned} \tag{3.24}$$

Similarly,

$$P(\gamma_2 > \gamma_1) = \frac{\bar{\gamma}_2}{\bar{\gamma}_1 + \bar{\gamma}_2}. \tag{3.25}$$

3.2.2.2 Derivation of $P(e|\gamma_1 \geq \gamma_2)$ and $P(e|\gamma_1 < \gamma_2)$

By considering the case $\gamma = \gamma_1 - \gamma_2 \geq 0$, the characteristic function of γ becomes

$$\begin{aligned} \phi_{\gamma}(j\omega) &= \frac{1}{(1 - j\omega\bar{\gamma}_1)(1 + j\omega\bar{\gamma}_2)} \\ &= \left(\frac{\bar{\gamma}_1}{\bar{\gamma}_2 + \bar{\gamma}_1}\right) \frac{1}{(1 - j\omega\bar{\gamma}_1)} + \left(\frac{\bar{\gamma}_2}{\bar{\gamma}_2 + \bar{\gamma}_1}\right) \frac{1}{(1 + j\omega\bar{\gamma}_2)} \end{aligned} \tag{3.26}$$

Inverse Fourier transforming the characteristic function in (3.26) yields the pdf of γ:

$$p(\gamma) = \left(\frac{1}{\bar{\gamma}_1 + \bar{\gamma}_2}\right) \left(\exp^{-\gamma/\bar{\gamma}_1} + \exp^{-\gamma/\bar{\gamma}_2}\right), \quad \gamma \geq 0. \tag{3.27}$$

By averaging the instantaneous BEP (3.20) over the pdf given in (3.27),

$$\begin{aligned} P(e|\gamma_1 \geq \gamma_2) &= \int_0^{\infty} Q\left(\sqrt{\gamma}\right) p(\gamma) d(\gamma) \\ &= \frac{1}{2}\left[\frac{\bar{\gamma}_1}{\bar{\gamma}_1 + \bar{\gamma}_2}\left(1 - \sqrt{\frac{\bar{\gamma}_1}{2 + \bar{\gamma}_1}}\right) + \frac{\bar{\gamma}_2}{\bar{\gamma}_1 + \bar{\gamma}_2}\left(1 - \sqrt{\frac{\bar{\gamma}_2}{2 + \bar{\gamma}_2}}\right)\right]. \end{aligned} \tag{3.28}$$

Similarly, we can show that for the case $\gamma = \gamma_2 - \gamma_1 > 0$,

$$P(e|\gamma_1 < \gamma_2) = 1 - P(e|\gamma_1 \geq \gamma_2). \tag{3.29}$$

Using (3.24), (3.25), (3.28) and (3.29) in (3.22), we have

$$P_{dMRC}^{L} = \left(\frac{\bar{\gamma}_2}{\bar{\gamma}_1 + \bar{\gamma}_2}\right) + \left(\frac{\bar{\gamma}_1 - \bar{\gamma}_2}{\bar{\gamma}_1 + \bar{\gamma}_2}\right) \frac{1}{2}\left[\frac{\bar{\gamma}_1}{\bar{\gamma}_1 + \bar{\gamma}_2}\left(1 - \sqrt{\frac{\bar{\gamma}_1}{2 + \bar{\gamma}_1}}\right) + \frac{\bar{\gamma}_2}{\bar{\gamma}_1 + \bar{\gamma}_2}\left(1 - \sqrt{\frac{\bar{\gamma}_2}{2 + \bar{\gamma}_2}}\right)\right]. \tag{3.30}$$

Letting $\bar{\gamma}_1 = \bar{\gamma}_2$ in (3.30) for the case of similar channels towards the BS,

$$P_{dMRC}^{L} = \left(\frac{\bar{\gamma}_2}{\bar{\gamma}_1 + \bar{\gamma}_2}\right) = 0.5 \tag{3.31}$$

3.2.3 The Bit Error Probability of Interuser Channel

The average BEP of interuser channel is given by [63],

$$P_{1,2} = \frac{1}{2}\left(1 - \sqrt{\frac{\bar{\gamma}_{1,2}}{2+\bar{\gamma}_{1,2}}}\right) \tag{3.32}$$

where $\bar{\gamma}_{1,2} = \frac{E_b}{N_0} E\{|h_{1,2}|^2\} = \sigma_{1,2}^2 \frac{E_b}{N_0}$.

3.2.4 Lower Bound of the BEP of the Proposed Scheme

Substituting the derived average BEP terms instead of the instantaneous BEP terms in (3.10), the lower bound of the average BEP of the proposed scheme can be written as

$$P_e^L = (1 - P_{1,2})P_{MRC} + P_{1,2}P_{dMRC}^L. \tag{3.33}$$

3.2.5 Differential Signal-to-noise Ratio (dSNR)

Because of the proximity, we expect the interuser channel between *user* i and *user* j to be of better quality than the i^{th} channel (between *user* i and BS) and define the differential signal-to-noise ratio as

$$dSNR_i[dB] = \bar{\gamma}_{i,j}[dB] - \bar{\gamma}_i[dB]. \tag{3.34}$$

3.2.6 Numerical Results

In this subsection, we present the performance of the proposed cooperative diversity scheme. The BEP of the proposed scheme has been evaluated analytically and via simulation. In our simulation, a frame, consisting of 128 information symbols (effectively it needs 129 symbol durations to transmit in cooperation), is transmitted through a Rayleigh flat fading channel. The noise is assumed as a zero mean complex Gaussian process with

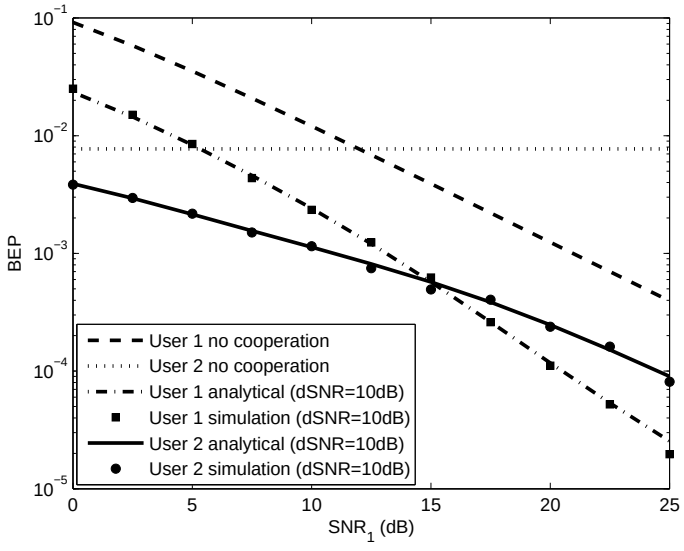

Figure 3.4: Bit error performance of both users when SNR of user 2 is fixed at 12dB for differential SNR gain of 10 dB.

variance $N_0/2$. The channel is also considered as slow fading that remains constant over the interval of a frame. We assume that the fading channel coefficients is available at the respective receivers for decoding the received signal. In practice, the fading channel coefficients has to be estimated with associated estimation error.

The BEPs as a function of *user 1*'s SNR of the proposed cooperative diversity scheme for dissimilar channels are plotted in Fig. 3.4 and Fig. 3.5. Here, $\bar{\gamma}_2$ is fixed at 12dB and $\bar{\gamma}_1$ varies from 0 to 25 dB. Inspection of these figures show that the analytical results for lower bound coincide with the simulation results. This is because the difference between P_{dMRC} and P^L_{dMRC} is not significant in the calculation of the overall BEP. In Fig. 3.4, the simulation and analytical results of the proposed scheme are compared with the non-cooperative scheme for both users at a differential SNR gain of 10dB. For the non-cooperative diversity scheme, we consider direct transmission of standard BPSK modulated signals with the same symbol energy as the proposed cooperative diversity scheme. Further, the results show that the BEP of both users is enhanced significantly

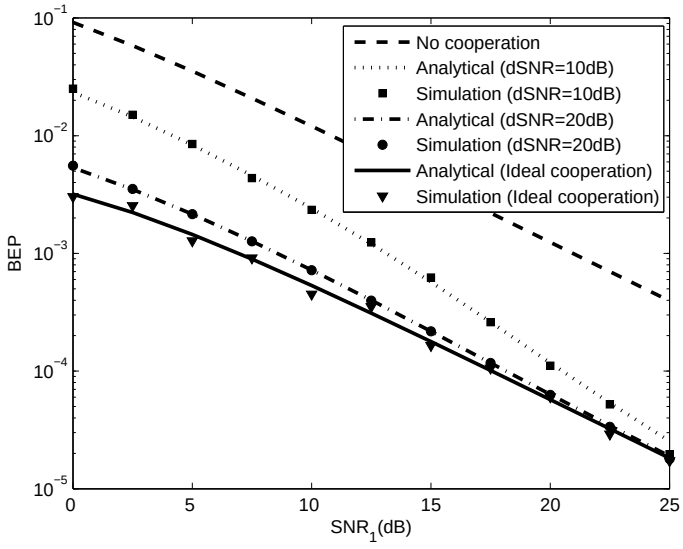

Figure 3.5: Bit error performance of user 1 when SNR of user 2 is fixed at 12dB for differential SNR gains of 10 and 20dB.

by the proposed scheme. It means that cooperation enhances not only the performance of the user far away from the BS but also the user near to the BS. In addition, the BEP improves with the interuser channel quality, as shown in Fig. 3.5 for *user 1*. Thus, the BEP performance of the proposed scheme improves as the dSNR gain increases. For ideal cooperation, the performance of the proposed scheme is the same as that of the conventional MRC scheme with one transmit and two receive antennas.

In Fig. 3.6, the BEP of the proposed scheme for various dSNR is compared with those of non-cooperative diversity scheme, Alamouti's space-time block coding (STBC) scheme [53] and ideal cooperation (assuming that the partner's information is perfectly decoded) scheme, when $\bar{\gamma}_1 = \bar{\gamma}_2$. The proposed scheme achieves diversity order of two when ideal cooperation takes place, and similar performance can be achieved when dSNR is 20dB or better. It gives a 3dB gain over the non-cooperative diversity scheme when dSNR is 3dB. In addition, Fig. 3.6 shows that the performance of the proposed scheme is similar to that of the non-cooperative diversity scheme when dSNR = 0dB. It

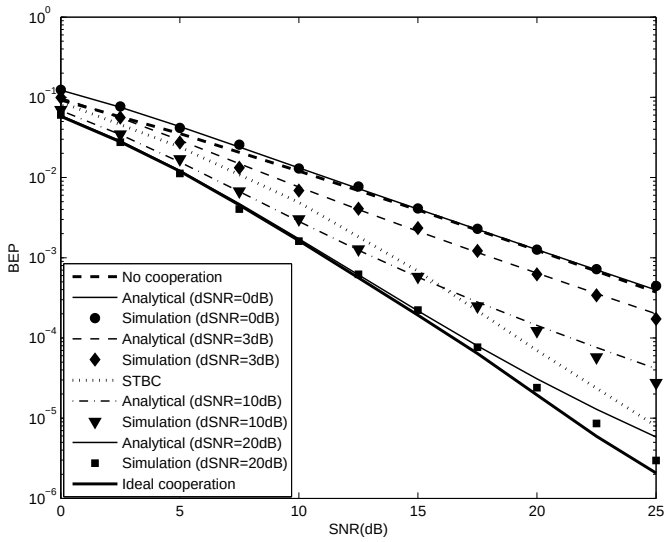

Figure 3.6: Bit error performance of user 1 compared with Alamouti scheme for similar channels towards the BS for various interuser channel conditions.

is also noted that cooperation is not beneficial when the interuser channel is worse than the channel between the user and the BS. In this similar channel case, the performance of the proposed scheme can be compared with Alamounti's STC scheme with two transmit and one receive antenna employing standard BPSK modulation. Because orthogonal transmit diversity degrades performance by 3dB from the optimal transmit/receive diversity scheme like MRC, the proposed scheme outperforms Alamouti's scheme, [53] at high interuser SNR, e.g., the dSNR = 20dB case.

In summary, we show that the derived analytical lower bound of the BEP follows the simulated BEP ($P_e \approx P_e^L$). In addition, the results indicate that the diversity gain achieved by the proposed scheme increases with the interuser channel quality.

3.3 Diversity Gain and Coding Gain

In the previous section, we studied the effects of the interuser channel on the performance of the proposed scheme in which the diversity gain achieved by the system increases with the interuser channel quality. An alternative way to characterize the performance is to plot the diversity gain and coding gain[4] for specified channel conditions. This will help us to know the range of interuser channel quality of interest for a better cooperation.

3.3.1 Derivation of P_e at High SNR

By considering high SNR for both interuser and user-to-BS transmissions ($\bar{\gamma}_1 \gg 1$, $\bar{\gamma}_2 \gg 1$,$\bar{\gamma}_{1,2} \gg 1$), (3.16) can be approximated by

$$P_{MRC} \approx \frac{3}{4\bar{\gamma}_1\bar{\gamma}_2} \tag{3.35}$$

and (3.30) by

$$P_{dMRC}^{L} \approx \frac{\bar{\gamma}_2}{\bar{\gamma}_1+\bar{\gamma}_2} + \frac{\bar{\gamma}_1-\bar{\gamma}_2}{(\bar{\gamma}_1+\bar{\gamma}_2)^2}. \tag{3.36}$$

Further, the interuser BEP given by (3.32) reduces to

$$P_{1,2} \approx \frac{1}{2\bar{\gamma}_{1,2}}. \tag{3.37}$$

Based on the high SNR approximations (3.35), (3.36) and (3.37), the BEP of the proposed scheme given by (3.33) can be written as

$$\begin{aligned} P_e^L &\approx \frac{1}{2\bar{\gamma}_{1,2}}\frac{\bar{\gamma}_2}{\bar{\gamma}_1+\bar{\gamma}_2} + \frac{3}{4\bar{\gamma}_1\bar{\gamma}_2} + \frac{1}{2\bar{\gamma}_{1,2}}\frac{\bar{\gamma}_1-\bar{\gamma}_2}{(\bar{\gamma}_1+\bar{\gamma}_2)^2} - \frac{1}{2\bar{\gamma}_{1,2}}\frac{3}{4\bar{\gamma}_1\bar{\gamma}_2} \\ &\approx P_e. \end{aligned} \tag{3.38}$$

The asymptotic behavior of the BEP versus $\bar{\gamma}_1$ curve is dominated by the first term of (3.38) even though the remaining terms provide higher order diversity. The average bit

[4]The term coding gain is used here to represent any system gain, e.g., modulation, not necessarily channel coding.

error probability of the proposed system is of the form given in [56] and [64] and can be approximated by

$$P_e \approx (G_c \bar{\gamma}_1)^{-G_d}, \tag{3.39}$$

where G_d is the variable diversity gain and G_c is the coding gain. A similar study is given in [45] for non-regenerative cooperative diversity systems. From (3.38), G_d can be written as

$$G_d = \begin{cases} k & \bar{\gamma}_{1,2} < \bar{\gamma}_1^2 \\ 2 & \bar{\gamma}_{1,2} \geq \bar{\gamma}_1^2 \end{cases}, \tag{3.40}$$

and G_c as

$$G_c = \begin{cases} \left[\frac{l}{2(1+l)} + \frac{3}{4l\bar{\gamma}_1^{2-k}} + \frac{1-l}{2(1+l)^2\bar{\gamma}_1} - \frac{3}{8l\bar{\gamma}_1^2} \right]^{-\frac{1}{k}} & \bar{\gamma}_{1,2} < \bar{\gamma}_1^2 \\ \left[\frac{3}{4l} + \frac{l}{2(1+l)\bar{\gamma}_1^{k-2}} + \frac{1-l}{2(1+l)^2\bar{\gamma}_1^{k-1}} - \frac{3}{8l\bar{\gamma}_1^k} \right]^{-\frac{1}{2}} & \bar{\gamma}_{1,2} \geq \bar{\gamma}_1^2 \end{cases} \tag{3.41}$$

where $k = \log_{\bar{\gamma}_1} \bar{\gamma}_{1,2}$ and $l = \frac{\bar{\gamma}_2}{\bar{\gamma}_1}$.

When $\bar{\gamma_1} = \bar{\gamma_2}$, the proposed scheme exhibits similar channel characteristics towards the BS. The BEP is approximately given by

$$P_e \approx \frac{1}{4\bar{\gamma}_{1,2}} + \frac{3}{4\bar{\gamma}_1^2} - \frac{3}{8\bar{\gamma}_{1,2}\bar{\gamma}_1^2}. \tag{3.42}$$

The coding gain, G_c, reduces to

$$G_c = \begin{cases} \left[\frac{1}{4} + \frac{3}{4\bar{\gamma}_1^{2-k}} - \frac{3}{8\bar{\gamma}_1^2} \right]^{-\frac{1}{k}} & \bar{\gamma}_{1,2} < \bar{\gamma}_1^2 \\ \left[\frac{3}{4} + \frac{1}{4\bar{\gamma}_1^{k-2}} - \frac{3}{8\bar{\gamma}_1^k} \right]^{-\frac{1}{2}} & \bar{\gamma}_{1,2} \geq \bar{\gamma}_1^2 \end{cases} \tag{3.43}$$

3.3.2 Numerical Results

The achieved diversity gain and coding gain are plotted in Fig. 3.7 as a function of k, with l as a parameter. The diversity gain increases linearly with k until $k = 2$. After that, it remains constant at two. On the other hand, the coding gain decreases with k

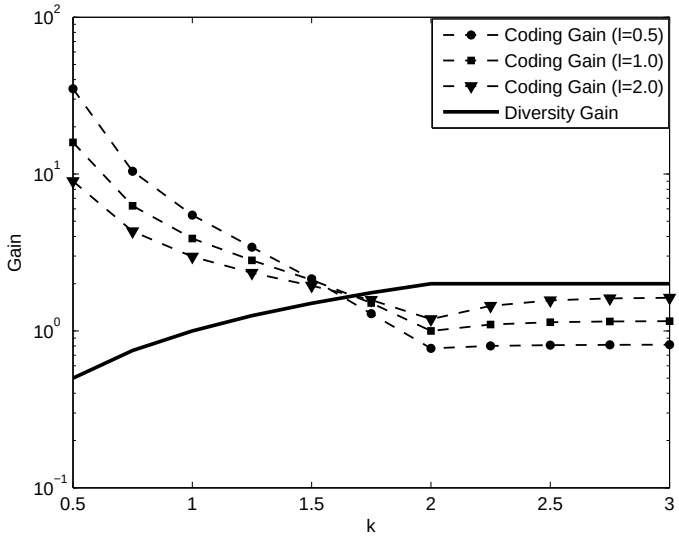

Figure 3.7: Coding gain and diversity gain achieved by the scheme at high SNR for various interuser and user 2 to BS channel conditions.

until $k = 2$. Afterward, it increases slightly and saturates to the coding gain of the MRC scheme. From Fig. 3.7, we observe that the performance improvement is not significant when $k > 2$. This is more clearly shown in the Fig. 3.8 where the BEP performance is plotted as a function of k for various values of l. The performance of the proposed cooperative diversity system is worse than that of the direct transmission when $k < 1$. From these observations, we conclude that k should be in the range between 1 and 2 for a beneficial cooperation. Due to the interuser channel errors, a system with $l > 1$ performs better at higher values of k (approximately greater than 1.6) and a system with $l < 1$ performs better at lower values of k. In conclusion, for cooperation to be worthwhile, the quality of the interuser channel should be better than that of the user to BS channel.

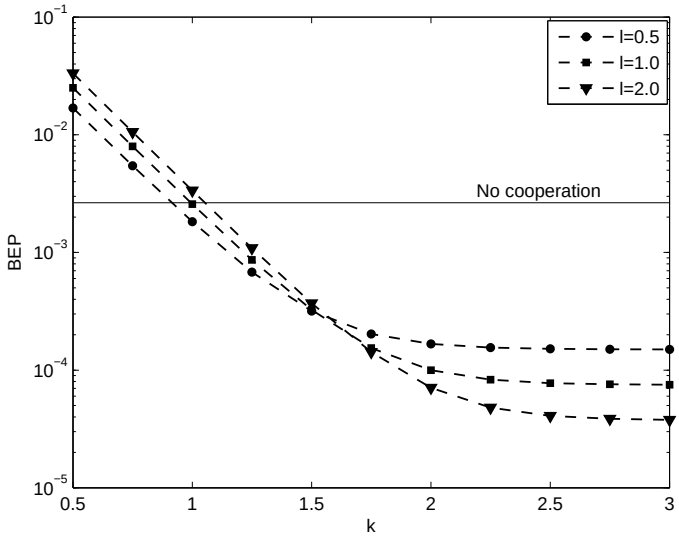

Figure 3.8: BEP of the proposed scheme at high SNR for various interuser and user 2 to BS channel conditions.

3.4 Cooperative Region

To achieve a specified diversity gain or BEP, it is necessary to know the geographical region within which the partner has to be located in order to cooperate. In this section, we derive a cooperative region of the proposed cooperative diversity scheme that yields specified SNR gain over a non-cooperative scheme (direct transmission scheme).

3.4.1 Analytical Derivation

The path losses are dependent on the distance between the transmitter and the receiver as well as on the propagation environment. There are many path loss models reported in the literature and several of these are given in [58]. We consider the log-distance path loss model in our analysis:

$$\sigma_{i,j}^2 \propto d_{i,j}^{-\alpha}, \tag{3.44}$$

where $d_{i,j}$ is the distance between i and j and α is the path loss exponent [58]. Since $\bar{\gamma}_i = \sigma_{i,B}^2 (E_b/N_0)$, from (3.44),

$$\bar{\gamma}_i = \left(\frac{d_0}{d_{i,B}}\right)^{\alpha} \bar{\gamma}_0 \tag{3.45}$$

where $\bar{\gamma}_0 = (E_b/N_0)E|h_0|^2$ is the average SNR at the reference distance d_0 and h_0 is a fading coefficient with unity variance, i.e., $\sigma_0^2 = 1$. Without loss of generality, considering *user 1* located at the reference point, (3.45) can be written as

$$\bar{\gamma}_2 = \left(\frac{d_{1,B}}{d_{2,B}}\right)^{\alpha} \bar{\gamma}_1. \tag{3.46}$$

Similarly,

$$\bar{\gamma}_{1,2} = \left(\frac{d_{1,B}}{d_{1,2}}\right)^{\alpha} \bar{\gamma}_1. \tag{3.47}$$

Substituting (3.46) and (3.47) in (3.38) yields

$$\begin{aligned} P_e \approx \frac{1}{4}\left(1+\sqrt{\frac{\bar{\gamma}_1}{R_{1,2}^{\alpha}+\bar{\gamma}_1}}\right)\left[\left(\frac{R_{2,B}^{\alpha}}{R_{2,B}^{\alpha}-1}\right)\left(1-\sqrt{\frac{\bar{\gamma}_1}{2+\bar{\gamma}_1}}\right)+\left(\frac{1}{1-R_{2,B}^{\alpha}}\right)\right. \\ \left.\left(1-\sqrt{\frac{\bar{\gamma}_1}{2R_{2,B}^{\alpha}+\bar{\gamma}_1}}\right)\right]+\frac{1}{2}\left(1-\sqrt{\frac{\bar{\gamma}_1}{R_{1,2}^{\alpha}+\bar{\gamma}_1}}\right)\left[\left(\frac{1}{R_{2,B}^{\alpha}+1}\right)\right. \\ \left.+\frac{1}{2}\left(\frac{R_{2,B}^{\alpha}-1}{R_{2,B}^{\alpha}+1}\right)\left(\frac{R_{2,B}^{\alpha}}{R_{2,B}^{\alpha}+1}\right)\left(1-\sqrt{\frac{\bar{\gamma}_1}{2+\bar{\gamma}_1}}\right)\right]+\frac{1}{4}\left(1-\sqrt{\frac{\bar{\gamma}_1}{R_{1,2}^{\alpha}+\bar{\gamma}_1}}\right) \\ \left(\frac{R_{2,B}^{\alpha}-1}{R_{2,B}^{\alpha}+1}\right)\left(\frac{1}{1+R_{2,B}^{\alpha}}\right)\left(1-\sqrt{\frac{\bar{\gamma}_1}{2R_{2,B}^{\alpha}+\bar{\gamma}_1}}\right) \end{aligned} \tag{3.48}$$

where $R_{2,B} = \frac{d_{2,B}}{d_{1,B}}$ and $R_{1,2} = \frac{d_{1,2}}{d_{1,B}}$ are normalized distances.

For a given BEP, define the cooperative diversity energy gain, G_{cd}, as

$$G_{cd} = \frac{\bar{\gamma}_i^{nc}}{\bar{\gamma}_i} \tag{3.49}$$

where $\bar{\gamma}_i^{nc}$ is the average SNR of the non-cooperative diversity scheme to achieve the same bit error probability as the cooperative diversity scheme.

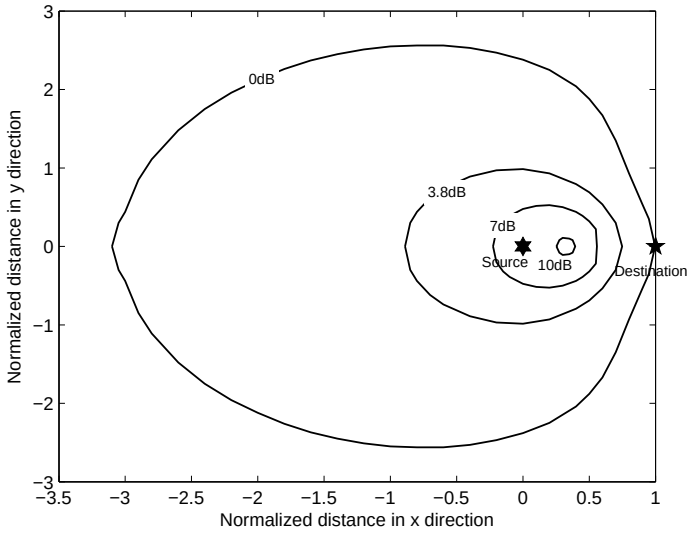

Figure 3.9: Cooperative region of the proposed scheme for various SNR gain over direct transmission when $P_e = 10^{-2}$ and $\alpha = 3$ (urban area).

3.4.2 Numerical Results

The geographical area within which the partner has to be located in order to have a successful cooperation is called the cooperative region. The cooperative region should be known to all users as well as to the BS. To plot the cooperative region, we fix the location of the source and destination at a unit distance apart ($d_{1,B} = 1$). Furthermore, the Cartesian coordinates of the source, destination and the partner are represented by (0,0), (1,0) and (x, y), respectively. Therefore, to achieve the given G_{cd}, the contour of the partner is bounded by

$$R_{2,B} = \sqrt{(x-1)^2 + y^2} \tag{3.50}$$

and

$$R_{1,2} = \sqrt{x^2 + y^2}. \tag{3.51}$$

Substituting (3.49), (3.50) and (3.51) in (3.48) yields a function of contour in terms of x and y with P_e, $\bar{\gamma}_i^{nc}$,G_{cd} and α as parameters.

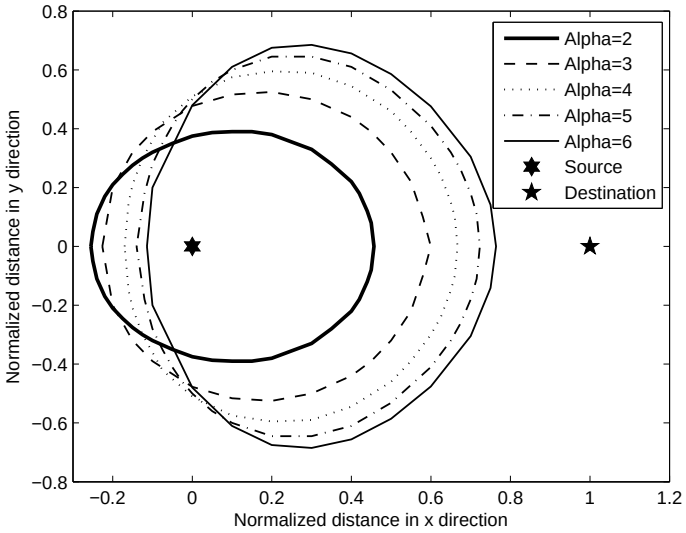

Figure 3.10: Cooperative region of the proposed scheme for various path loss coefficient α when $P_e = 10^{-2}$ and $G_{cd} = 7dB$.

In Fig. 3.9, cooperative regions are drawn for various SNR gains over non-cooperative transmission to achieve a $P_e = 10^{-2}$ when $\alpha = 3$. The cooperative region shrinks when the SNR gain increases and is located nearer to user 1 (*sender*) rather than the BS (*destination*). This is due to the fact that the interuser channel should be better than the channel between the user and the BS. In addition, similar cooperative regions for various path loss exponents, α, are compared in Fig. 3.10, where $P_e = 10^{-2}$ and $G_{cd} = 7dB$. The cooperative region expands in both the x and y directions and moves towards the destination when α increases. Since the cooperative region increases with α, the maximum achievable G_{cd} by the scheme also increases. These results will help us to design an algorithm to choose a cooperative partner and to manage the cooperation handoff with the interaction of higher layer protocols.

3.5 Summary

A bandwidth and power efficient *fixed regenerate and forward* cooperative diversity scheme is proposed based on quadrature signaling. The proposed scheme is simple and can easily be switched between the cooperative and the non-cooperative modes of operation. The diversity gain achieved and the bit error performance of the proposed cooperative diversity scheme can be improved as the interuser channel signal strength increases. In addition, the range of interuser signal strength of interest is also identified for a better cooperation. Finally, a cooperative region is derived for a specified BEP and SNR gain over the NCD scheme.

In fixed CD systems, the partner forwards the information without any error checking. This may lead to error propagation and reduces the overall system performance. To overcome this problem, we propose a CD system based on adaptive relaying at the partner in the next chapter.

Chapter 4

Adaptive Cooperative Diversity System

In contrast to fixed-relaying-based CD systems, adaptive relaying at the partner can provide more diversity gain without the constraint that the interuser channel should be better than the source-to-destination channel at the expense of increased device and signaling complexity. In this chapter, we consider an *adaptive regenerate and forward* QS-CD system which employs cyclic redundancy checksum (CRC) in the partner's device to check the correctness of the received frame before making a decision whether or not to regenerate and forward[1]. The asymptotic behavior of the bit error probability of the proposed scheme is derived for QAM modulation as a function of the received SNR at the relay and at the destination. The tightness of the derived analytical upper bound of BEP is validated using simulation.

The major contributions of this chapter are (i) the proposal of adaptive relaying of the sender signal by the cooperating partner in a quadrature signaling based regenerate and forward CD systems, and (ii) the derivation of an analytical upper bound of the BEP that

[1]With error detection only, the partner forwards only when no error is detected. If channel coding were used at the transmitter, then forward error correction to implement adaptive regenerate and forward would be more efficient than the simple CRC. In our case, we do not use channel coding, so error detection using CRC is employed and assumed that CRC perfectly detects the bit error.

shows its degree of tightness. The proposed CD system has the following advantages in implementations.

- Minimal modification over existing point-to-point systems (adaptive modulation system)
- Interuser channel can be estimated using the previously transmitted frame(s) when it is relayed to destination by the partner.
- The partner is not aware of the end-to-end link level ARQ scheme, which is studied in detail in the next chapter.

The rest of the chapter is organized as follows. Section 4.1 describes the transmission model under consideration. Section 4.2 analyzes the performance of the proposed CD system and numrical results are given in Section 4.3. Finally, the chapter is summarized in section 4.4.

4.1 Transmission Model

We consider an M-QAM signaling cooperative diversity scheme in which a mobile user (the sender) cooperates with another mobile user (the partner) to transmit signals in the uplink of an infrastructure based network. Similar to the fixed CD system in Chapter 3, in each cooperative mobile device, both its own and its partner's signals are simultaneously transmitted using quadrature signaling. Instead of QPSK modulation, we are concerned with the transmissions of M-QAM signals in this chapter. The base station and each of the mobile devices has a single antenna, so, the cooperative diversity scheme emulates a "two-input one-output" (2I1O) situation. The signals transmitted by the sender and relayed by the partner are combined at the BS receiver using maximal ratio combining.

The transmission frame format of the M-QAM modulation scheme is shown in Fig. 4.1(a), with the signal constellation of 4PAM/16-QAM modulation shown in 4.1(b). In

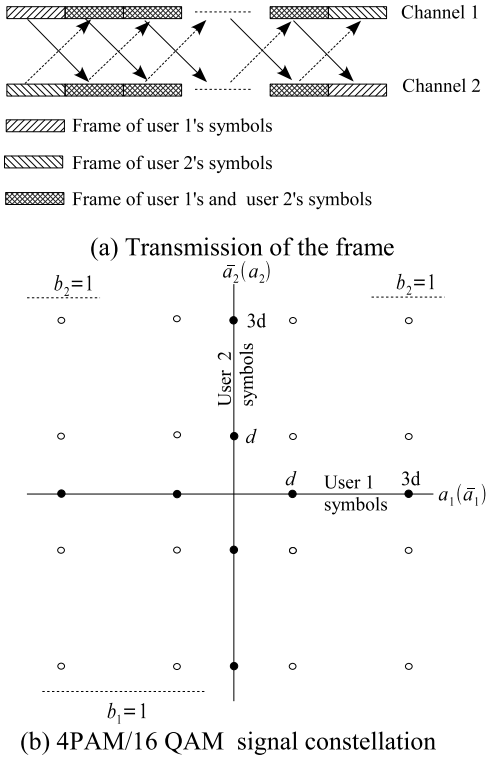

Figure 4.1: (a) Frame transmission format and (b) signal constellation of 4-PAM/16-QAM using quadrature signaling

quadrature signaling, we assign the in-phase channel to *user 1* and the quadrature channel to *user 2*. Fig. 4.1(a) shows frames of information symbols transmitted by *user 1* in multiple access *channel 1* and by *user 2* in multiple access *channel 2*. In the first frame interval of a cooperative session, each user transmits its own information only. In successive frame intervals, each user transmits not only its own information but also the regenerated version of the partner's information received in the previous frame interval. But, in the last frame interval of the cooperation session, each user transmits the regenerated version of the partner's information only. Since *user 1* and *user 2* use the in-phase and the quadrature components of the M-QAM modulation, respectively, each user equivalently employs I-PAM modulation, where $I = \sqrt{M}$. In the uplink receiver of

both users, the in-phase and quadrature components are demodulated separately and the detected and regenerated partner's frame is forwarded to the BS if the frame is detected error free.

Throughout the chapter, we assume that the interuser and the user-to-BS channels exhibit flat Rayleigh fading, and that the two channels are independent of each other, static over a frame interval, and change independently from frame to frame. We suppose that, each frame is comprised of N_S symbols. In addition, it is assumed that channel state information (channel fading coefficient) is available at the respective receivers to demodulate the signals and proper synchronization has been established.

At the BS, the signals received from both users are combined using MRC as shown in Fig. 3.3. To decode the information of *user 1*, the received signal from *channel 1* is delayed by one frame interval and combined with the received signal from *channel 2* at the MRC. Similarly, to decode the information of *user 2*, the received signal from *channel 2* is delayed by one frame interval and combined with the received signal from *channel 1*. The output of the MRC is sent to a decision device which converts it to a binary format.

Let the baseband equivalent received signals from *user i*, $i = 1, 2$, at the BS be denoted as $r_{i,B}(t)$. Similarly, *user i*'s uplink signal received by *user j*, $j = 1, 2$ and $i \neq j$, is denoted as $r_{i,j}(t)$. From the transmission model, $r_{i,B}(t)$ and $r_{i,j}(t)$ can be written as:

$$\begin{aligned} r_{i,B}(t) &= h_{i,B}(t)s_i(t) + \eta_{i,B}(t) \\ r_{i,j}(t) &= h_{i,j}(t)s_i(t) + \eta_{i,j}(t), \end{aligned} \tag{4.1}$$

where the channel fading coefficient between user i and the BS is denoted by $h_{i,B}(t)$ and that from user i to user j by $h_{i,j}(t)$. When the interuser channel is symmetric, $h_{i,j}(t) = h_{j,i}(t)$. The processes $\eta_{i,B}(t)$ and $\eta_{i,j}(t)$ are additive noise at the respective receivers and modelled as zero mean circularly symmetric, complex Gaussian distributed with variance $N_0/2$ per dimension, where N_0 is the one-sided power spectral density of white Gaussian noise. $s_i(t)$, chosen from the M-QAM signal constellation in a similar

manner that shown in Fig. 4.1(b), is the transmitted signal from *user i*. Therefore, $s_1(t)$ and $s_2(t)$ can be written as $s_1(t) = \sqrt{log_2 M \cdot E_b/2}(a_1(t) + j\bar{a}_2(t - T_f))$ and $s_2(t) = \sqrt{log_2 M \cdot E_b/2}(\bar{a}_1(t - T_f) + ja_2(t))$, where $a_i(t)$ is the I-PAM information symbol of *user i* and $\bar{a}_i(.)$ is the corresponding reproduced symbol at the partner. T_f is the frame duration and E_b is the energy spent for a bit using NCD transmission. To have a power consumption equal to that of an NCD system, the CD system equally shares the power in transmitting the user's and the partner's information bits at each mobile device.

If each user relays the partner's information, the signals received at the BS from both user channels are combined using MRC and decoded using the ML rule [63]. The decoded symbols are given by

$$\begin{aligned}\tilde{a}_1 = \arg\min_{\bar{a}_1 \epsilon S_I} \Big\{ & \Re\{h^*_{1,B}(t - T_f) r_{1,B}(t - T_f) + h^*_{2,B}(t) r_{2,B}(t)\} \\ & - (|h_{1,B}(t - T_f)|^2 + |h_{2,B}(t)|^2)\bar{a}_1 \Big\} \\ \tilde{a}_2 = \arg\min_{\bar{a}_1 \epsilon S_I} \Big\{ & \Im\{h^*_{2,B}(t - T_f) r_{2,B}(t - T_f) + h^*_{1,B}(t) r_{1,B}(t)\} \\ & - (|h_{1,B}(t)|^2 + |h_{2,B}(t - T_f)|^2)\bar{a}_2 \Big\},\end{aligned} \tag{4.2}$$

where the notations $\Re\{Z\}$ and $\Im\{Z\}$ denote the real and the imaginary parts of the complex number Z, respectively. S_I is the set of I-PAM information symbols.

4.2 Performance Analysis

The performance measures of the CD system described in Section 4.1 are the interuser frame error probability, P_{FEP}, the BEP at the output of the MRC, P_{MRC}, when the partner helps, and the BEP of the MRC output, P_{NH}, when the partner does not help. In addition, we also present the BEP of the NCD (conventional I-PAM) system from [57]. Finally, analytical and simulation results are presented to demonstrate the tightness of the analytical upper bound and to study the performance characteristics of the proposed CD system.

Since the roles of sender and partner in quadrature signaling are interchangeable, in the derivations to follow we consider *user 1* as the sender and *user 2* as the partner.

4.2.1 Average Interuser frame error probability (P_{FEP})

We consider pairwise error probability of a frame transmitted by the sender and received by the partner where each frame consists of N_S symbols. A pairwise error occurs if there is a symbol error in a frame. Using the approach proposed in [57], the PEP between the transmitted frame X and the received frame $\hat{X}$, conditional on the channel fading coefficient, $H = [h_{1,2}(1)h_{1,2}(2)....h_{1,2}(N_S)]^T$, of I-PAM transmission is given by

$$\begin{aligned} & P(X \longrightarrow \hat{X}|H) \\ = \; & \frac{1}{I\log_2 I}\sum_{m=1}^{\log_2 I}\sum_{i=0}^{(1-2^{-m})I-1}\lambda(I,m,i) \\ \times \; & Q\left((2i+1)\sqrt{\frac{3\log_2 I.E_b}{4(I^2-1)N_0}\sum_{n=1}^{N_S}\left|h_{1,2}(n)\left(x(n)|_m-\hat{x}(n)|_m\right)\right|^2}\right) \end{aligned} \quad (4.3)$$

where $x(n)|_m$ and $\hat{x}(n)|_m$ are respectively the transmitted and received m^{th} bit of the n^{th} I-PAM modulated symbols of a frame. The parameter $\lambda(I,m,i) = (-1)^{\lfloor\frac{i.2^{m-1}}{I}\rfloor}(2^{m-1} - \lfloor\frac{i.2^{m-1}}{I}+\frac{1}{2}\rfloor)$, where the symbol $\lfloor\cdot\rfloor$ denotes the integer greater than or equal to its argument. For a quasi-static fading channel, $h_{1,2}(n) = h_{1,2}$. Let $\bar{\gamma}_{1,2} = \frac{E_b}{N_0}\mathrm{E}\{|h_{1,2}|^2\}$ be the interuser signal-to-noise ratio where E{.} is the expectation operator. The PEP can be derived by averaging the conditional PEP over $h_{1,2}$ [65]:

$$\begin{aligned} P(X \longrightarrow \hat{X}) \; = \; & \frac{1}{I\log_2 I}\sum_{m=1}^{\log_2 I}\sum_{i=0}^{(1-2^{-m})I-1}\lambda(I,m,i) \\ \times \; & \left(1-\sqrt{\frac{3\log_2 I.(2i+1)^2 N_{e|m}\bar{\gamma}_{1,2}}{2(I^2-1)+3\log_2 I.(2i+1)^2 N_{e|m}\bar{\gamma}_{1,2}}}\right) \end{aligned} \quad (4.4)$$

where $N_{e|m}$ is the number of symbol errors in a frame due to error in the m^{th} bit of the symbol. Therefore, the frame error probability (FEP), P_{FEP}, can be written as

$$\begin{aligned} P_{FEP} &\leq \sum_{X} P(X) \sum_{X \neq \hat{X}} P(X \longrightarrow \hat{X}) \\ &= \frac{1}{I \log_2 I} \sum_{m=1}^{\log_2 I} \sum_{i=0}^{(1-2^{-m})I-1} \lambda(I, m, i) \\ &\quad \times \sum_{N_{e|m}=1}^{N_S} \left(1 - \sqrt{\frac{3 \log_2 I.(2i+1)^2 N_{e|m} \bar{\gamma}_{1,2}}{2(I^2-1) + 3 \log_2 I.(2i+1)^2 N_{e|m} \bar{\gamma}_{1,2}}} \right). \end{aligned} \tag{4.5}$$

For the case of 2-PAM modulation, I is equal to 2. So, the m takes the value of 1 and i takes value of 0 only. By substituting I, m and i in (4.5), P_{FEP} of a 2-PAM system can be written as

$$P_{FEP} \leq \sum_{N_{e|m}=1}^{N_S} \frac{1}{2} \left(1 - \sqrt{\frac{\bar{\gamma}_{1,2} N_{e|m}}{2 + \bar{\gamma}_{1,2} N_{e|m}}} \right). \tag{4.6}$$

Similarly, the interuser FEP for 4-PAM systems can be written as

$$\begin{aligned} P_{FEP} \leq \sum_{N_{e|m}=1}^{N_S} \frac{1}{8} \Bigg(& 4 - 3\sqrt{\frac{\bar{\gamma}_{1,2} N_{e|m}}{5 + \bar{\gamma}_{1,2} N_{e|m}}} \\ & - 2\sqrt{\frac{9\bar{\gamma}_{1,2} N_{e|m}}{5 + 9\bar{\gamma}_{1,2} N_{e|m}}} + \sqrt{\frac{25\bar{\gamma}_{1,2} N_{e|m}}{5 + 25\bar{\gamma}_{1,2} N_{e|m}}} \Bigg). \end{aligned} \tag{4.7}$$

4.2.2 Average BEP of CD system of I-PAM when the partner helps

In this subsection, we derive the BEP, P_{MRC}, when the relay forwards the information. First, we derive the analytical expression for the probability of error, P_m, for bit m, $m = 1, 2, ..., \log_2 I$ for I-PAM when the partner helps in the cooperation. The conditional probability of error for bit m, $P_m(h_{1,B}, h_{2,B})$, can be written using the Log-likelihood

ratio (LLR) method of [66]:

$$P_m(h_{1,B}, h_{2,B}) = \sum_{i=0}^{(1-2^{-m})I-1} \frac{\lambda(I,m,i)}{I} \times Q\left((2i+1)\sqrt{\frac{3\log_2 I E_b}{4(I^2-1)N_0}(|h_{1,B}|^2+|h_{2,B}|^2)}\right). \tag{4.8}$$

So, the conditional bit error probability of the CD system, which is equivalent to maximal ratio combining for an I-PAM system, can be written as

$$P_{MRC}(h_{1,B}, h_{2,B}) = \sum_{m=1}^{\log_2 I} \sum_{i=0}^{(1-2^{-m})I-1} \frac{\lambda(I,m,i)}{I\log_2 I} \times Q\left((2i+1)\sqrt{\frac{3\log_2 I E_b}{4(I^2-1)N_0}(|h_{1,B}|^2+|h_{2,B}|^2)}\right).$$

Define $\bar{\gamma}_1 = \sigma_{1,B}^2 \frac{E_b}{N_0}$ and $\bar{\gamma}_2 = \sigma_{2,B}^2 \frac{E_b}{N_0}$, where $\sigma_{1,B}^2 = \mathrm{E}\{|h_{1,B}|^2\}$ and $\sigma_{2,B}^2 = \mathrm{E}\{|h_{2,B}|^2\}$. Based on the signal-to-noise ratios $\bar{\gamma}_1$ and $\bar{\gamma}_2$, we can derive the unconditional probability of error P_{MRC}.

4.2.2.1 Similar Uplink channel ($\bar{\gamma_1} = \bar{\gamma_2}$)

Assume that $\mathrm{E}\{|h_{1,B}|^2\}$ and $\mathrm{E}\{|h_{2,B}|^2\}$ are equal. The P_{MRC} of (4.9) is given as [63],

$$P_{MRC} = \frac{1}{I\log_2 I} \sum_{m=1}^{\log_2 I} \sum_{i=0}^{(1-2^{-m})I-1} \lambda(I,m,i) \left(\frac{1-\mu_1(I,i)}{2}\right)^2 (2+\mu_1(I,i)) \tag{4.9}$$

where $\mu_1(I,i) = \sqrt{\frac{3\log_2 I.(2i+1)^2\bar{\gamma}_1}{2(I^2-1)+3\log_2 I.(2i+1)^2\bar{\gamma}_1}}$.

For a 2-PAM system, the P_{MRC} can be written as

$$\begin{aligned} P_{MRC} &= (2+\mu_1(2,0))\left[\frac{1}{2}(1-\mu_1(2,0))\right]^2 \\ &= \left(2+\sqrt{\frac{\bar{\gamma}_1}{2+\bar{\gamma}_1}}\right)\left[\frac{1}{2}\left(1-\sqrt{\frac{\bar{\gamma}_1}{2+\bar{\gamma}_1}}\right)\right]^2. \end{aligned} \tag{4.10}$$

which is equivalent to ([78], (8)). Similarly, for a 4-PAM system, P_{MRC} can be obtained as

$$P_{MRC} = \frac{1}{4}\Bigg\{ \frac{3}{4}\left(1-\mu_1(4,0)\right)^2\left(2+\mu_1(4,0)\right) + \frac{1}{2}\left(1-\mu_1(4,1)\right)^2\left(2+\mu_1(4,1)\right) - \frac{1}{4}\left(1-\mu_1(4,2)\right)^2\left(2+\mu_1(4,2)\right)\Bigg\}. \quad (4.11)$$

4.2.2.2 Dissimilar Uplink channel ($\bar{\gamma_1} \neq \bar{\gamma_2}$)

Assume that $\mathrm{E}\{|h_{1,B}|^2\}$ is not equal to $\mathrm{E}\{|h_{2,B}|^2\}$. The unconditional error probability of (4.9) is given by

$$\begin{aligned} P_{MRC} = \frac{1}{I\log_2 I}\sum_{m=1}^{\log_2 I}\sum_{i=0}^{(1-2^{-m})I-1}\lambda(I,m,i) \\ \times\left[\frac{\bar{\gamma_1}}{\bar{\gamma_1}-\bar{\gamma_2}}(1-\mu_1(I,i)) + \frac{\bar{\gamma_1}}{\bar{\gamma_1}-\bar{\gamma_2}}(1-\mu_2(I,i))\right] \end{aligned} \quad (4.12)$$

where $\mu_2(I,i) = \sqrt{\frac{3\log_2 I.(2i+1)^2\bar{\gamma_2}}{2(I^2-1)+3\log_2 I.(2i+1)^2\bar{\gamma_2}}}$.

By substituting I=2 for a 2-PAM system, the P_{MRC} can be written as

$$\begin{aligned} P_{MRC} &= \frac{1}{2}\left[\frac{\bar{\gamma_1}}{\bar{\gamma_1}-\bar{\gamma_2}}\left(1-\mu_1(2,0)\right) + \frac{\bar{\gamma_2}}{\bar{\gamma_2}-\bar{\gamma_1}}\left(1-\mu_2(2,0)\right)\right] \\ &= \frac{1}{2}\left[\frac{\bar{\gamma_1}}{\bar{\gamma_1}-\bar{\gamma_2}}\left(1-\sqrt{\frac{\bar{\gamma_1}}{2+\bar{\gamma_1}}}\right) + \frac{\bar{\gamma_2}}{\bar{\gamma_2}-\bar{\gamma_1}}\left(1-\sqrt{\frac{\bar{\gamma_2}}{2+\bar{\gamma_2}}}\right)\right] \end{aligned} \quad (4.13)$$

which is equivalent to ([78], (7)). Similarly for a 4-PAM system, the P_{MRC} can be obtained as

$$P_{MRC} = \frac{1}{8}\Bigg\{ \frac{\bar{\gamma_1}}{\bar{\gamma_1}-\bar{\gamma_2}}(4-3\mu_1(4,0)-2\mu_1(4,1)+\mu_1(4,2)) + \frac{\bar{\gamma_2}}{\bar{\gamma_2}-\bar{\gamma_1}}(4-3\mu_2(4,0)-2\mu_2(4,1)+\mu_2(4,2))\Bigg\}. \quad (4.14)$$

4.2.3 Average BEP of cooperation scheme of I-PAM when the partner does not help

In this subsection, we derive the analytical expression for the probability of error, P_{NH}, for I-PAM signaling when the partner does not help in forwarding the information in the cooperation. The P_{NH} can be written as

$$P_{NH} = \frac{1}{I \log_2 I} \sum_{m=1}^{\log_2 I} \sum_{i=0}^{(1-2^{-m})I-1} \lambda(I, m, i)(1 - \mu_1(I, i)). \tag{4.15}$$

For the case of 2-PAM and 4-PAM systems, the P_{NH} can be written as

$$P_{NH} = \frac{1}{2}\left(1 - \sqrt{\frac{\bar{\gamma}_1}{2 + \bar{\gamma}_1}}\right) \tag{4.16}$$

and

$$P_{NH} = \frac{1}{8}(4 - 3\mu_1(4, 0) - 2\mu_1(4, 1) + \mu_1(4, 2)), \tag{4.17}$$

respectively.

4.2.4 Average BEP of the CD system

From the above derivation, the average BEP of the CD system, P_e, can be written as

$$P_e = (1 - P_{FEP})P_{MRC} + P_{FEP}P_{NH}. \tag{4.18}$$

By substituting (4.5), (4.9) or (4.12) and (4.15) into (4.18), the BEP can be written for similar and dissimilar channel towards the BS.

For the CD system with 4-QAM signaling i.e., 2-PAM per user, by substituting (4.10) or (4.13) and (4.16) into (4.18), the BEP can be written for similar and dissimilar channel towards the BS as

$$\begin{aligned} P_e = (1 - P_{FEP}) &\left(2 + \sqrt{\frac{\bar{\gamma}_1}{2 + \bar{\gamma}_1}}\right) \left[\frac{1}{2}\left(1 - \sqrt{\frac{\bar{\gamma}_1}{2 + \bar{\gamma}_1}}\right)\right]^2 \\ &+ P_{FEP}\frac{1}{2}\left(1 - \sqrt{\frac{\bar{\gamma}_1}{2 + \bar{\gamma}_1}}\right) \end{aligned} \tag{4.19}$$

and

$$P_e = (1 - P_{FEP})\frac{1}{2}\left[\frac{\bar{\gamma}_1}{\bar{\gamma}_1 - \bar{\gamma}_2}\left(1 - \sqrt{\frac{\bar{\gamma}_1}{2 + \bar{\gamma}_1}}\right) + \frac{\bar{\gamma}_2}{\bar{\gamma}_2 - \bar{\gamma}_1}\left(1 - \sqrt{\frac{\bar{\gamma}_2}{2 + \bar{\gamma}_2}}\right)\right] + P_{FEP}\frac{1}{2}\left(1 - \sqrt{\frac{\bar{\gamma}_1}{2 + \bar{\gamma}_1}}\right), \quad (4.20)$$

respectively. By substituting (4.11) or (4.14) and (4.17) into (4.18), a closed-form solution can be derived for the BEP of the 16-QAM adaptive CD system for similar and dissimilar channels towards the BS as

$$P_e = (1-P_{FEP})\frac{1}{4}\left\{\frac{3}{4}\left(1 - \mu_1(4,0)\right)^2\left(2 + \mu_1(4,0)\right) + \frac{1}{2}\left(1 - \mu_1(4,1)\right)^2\left(2 + \mu_1(4,1)\right) - \frac{1}{4}\left(1 - \mu_1(4,2)\right)^2\left(2 + \mu_1(4,2)\right)\right\} + P_{FEP}\frac{1}{8}(4 - 3\mu_1(4,0) - 2\mu_1(4,1) + \mu_1(4,2)), \quad (4.21)$$

and

$$P_e = (1 - P_{FEP})\frac{1}{8}\left\{\frac{\bar{\gamma}_1}{\bar{\gamma}_1 - \bar{\gamma}_2}(4 - 3\mu_1(4,0) - 2\mu_1(4,1) + \mu_1(4,2)) + \frac{\bar{\gamma}_2}{\bar{\gamma}_2 - \bar{\gamma}_1}(4 - 3\mu_2(4,0) - 2\mu_2(4,1) + \mu_2(4,2))\right\} + P_{FEP}\frac{1}{8}(4 - 3\mu_1(4,0) - 2\mu_1(4,1) + \mu_1(4,2)), \quad (4.22)$$

respectively.

4.2.5 Average BEP of non-cooperative system

In this chapter, NCD system are referred to the conventional direct communication system between user-to-destination. NCD system uses standard I-PAM modulation with bit energy equal to E_b.

The average BEP of the non-cooperative system is given by [57]:

$$P_{NC} = \frac{1}{I \log_2 I} \sum_{m=1}^{\log_2 I} \sum_{i=0}^{(1-2^{-m})I-1} \lambda(I, m, i)(1 - \hat{\mu}_1(I, i)), \tag{4.23}$$

where $\hat{\mu}_1(I, i) = \sqrt{\frac{3 \log_2 I.(2i+1)^2 \bar{\gamma_1}}{(I^2-1)+3 \log_2 I.(2i+1)^2 \bar{\gamma_1}}}$.

4.3 Numerical Results

In this section, we present numerical results to demonstrate the performance of the proposed CD system. The BEP is evaluated analytically and via simulation. In our simulation, a frame consisting of 128 information symbols is transmitted through a Rayleigh flat fading channel. In a cooperative session, 100 frames are considered. The noise is assumed to be a zero mean complex Gaussian process with variance $N_0/2$ per dimension. The channel is also considered as slow fading that remains constant over a frame interval. We assume that the fading channel coefficients is available at the respective receivers for decoding the received signal.

4.3.1 BEP of the CD system with dissimilar channel towards the BS

The BEPs as a function of user 1's SNR of the proposed CD system with 4-QAM/QPSK for dissimilar channels are plotted in Fig. 4.2. Here, $\bar{\gamma}_2$ is fixed at 15dB and $\bar{\gamma}_1$ varies from 0 to 30 dB for the cases in which the ISNR are $\bar{\gamma}_{1,2}$=15dB and 30dB. The proposed CD system provides better bit error performance not only for user 1 but also for the stronger user 2 over the NCD system (standard BPSK) for ISNR=15dB. Furthermore, the BEP of the CD system gradually decreases when ISNR increases, i.e., ISNR=30dB. In addition, Fig. 4.2 shows that the analytical results for upper bound virtually coincide with the simulation results. This is because the difference between the exact FEP and the upper bound of FEP is insignificant in the calculation of the overall BEP.

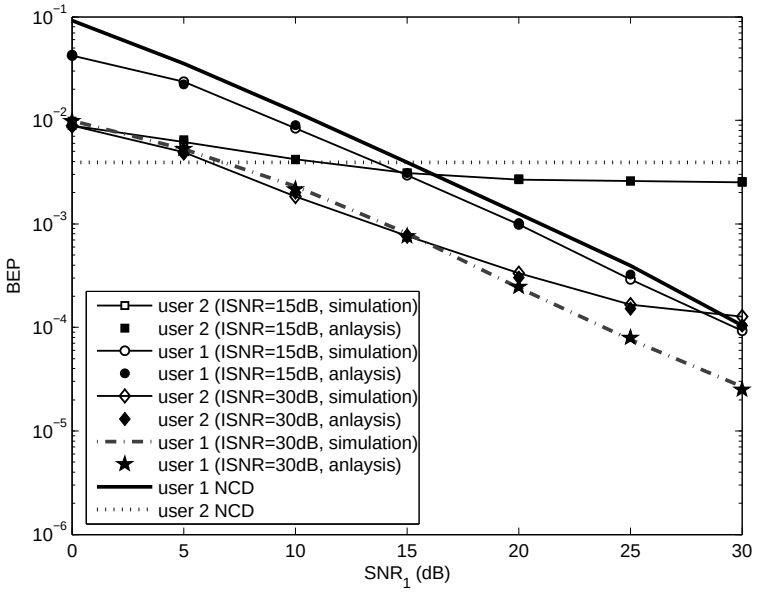

Figure 4.2: Bit error probability of the CD system with 4-QAM/QPSK for dissimilar channel towards BS ($SNR_2 = 15dB$)

The simulation and analytical results of the proposed CD system for 16-QAM are given for ISNR=15dB and 30dB, respectively in Figs. 4.3 and 4.4. For the NCD system, 4-PAM modulation is considered. For the curve shown in Fig. 4.3, $\bar{\gamma}_2$ is fixed at 15dB and $\bar{\gamma}_1$ varies from 0 to 30 dB. It can be seen that the BEP of both users is enhanced significantly by the proposed scheme. This means that cooperation enhances not only the performance of the user far away from the BS but also the user near to the BS. In addition, the BEP improves with the interuser channel quality, as shown in Fig. 4.4 for ISNR=30dB. Thus, the BEP performance of the proposed scheme improves as the ISNR increases. For ideal cooperation (assuming that the partner's information is perfectly decoded), the performance of the proposed scheme is the same as that of the conventional MRC scheme with one transmitting and two receiving antennas. For the CD system with 16-QAM, the BEP upper bound is very close to the simulation results.

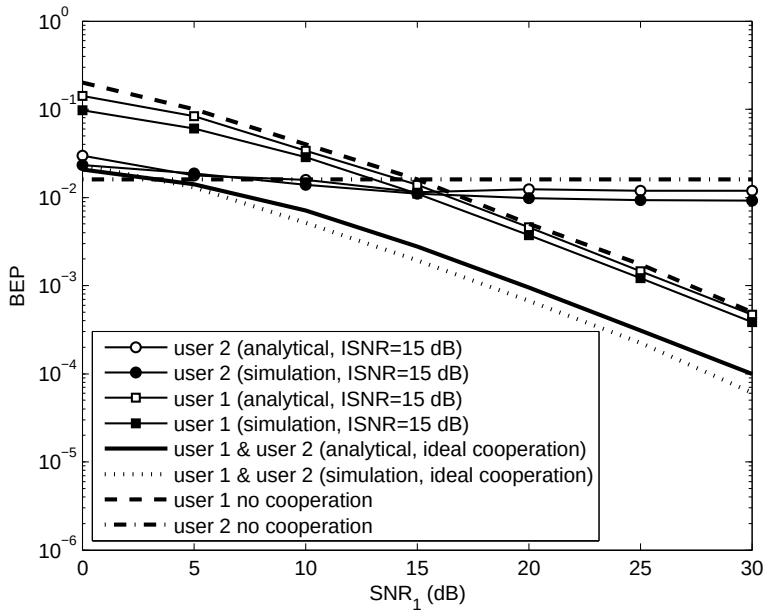

Figure 4.3: Bit error probability of the CD system with 16-QAM for dissimilar channel towards BS ($SNR_2 = 15dB$)

From all of the above figures, we can observe that the error floor for user 2 due to $\bar{\gamma}_2$ is fixed at 15dB. The level of the error floor is a function of the interuser channel quality, e.g., 3.6×10^{-3} when ISNR=15dB, and 2×10^{-4} when ISNR=30dB in Fig. 4.2.

4.3.2 BEP of the CD system with similar channel towards the BS

In the case of similar channel towards the BS ($\bar{\gamma}_1 = \bar{\gamma}_2$), both users experience the same BEP as shown in Figs. 4.5 and 4.6. In Fig. 4.5, the BEPs of the proposed scheme with 4-QAM/QPSK for various ISNR are compared with those of the non-cooperative diversity scheme and the ideal cooperation scheme. The BEP performance of the CD system with 16-QAM and similar channel towards the BS is plotted in Fig. 4.6. The proposed scheme gives a 2 dB gain over the non-cooperative diversity scheme when ISNR is 10 dB. When ISNR increases, the BEP decreases. Furthermore, the CD system achieves diversity order

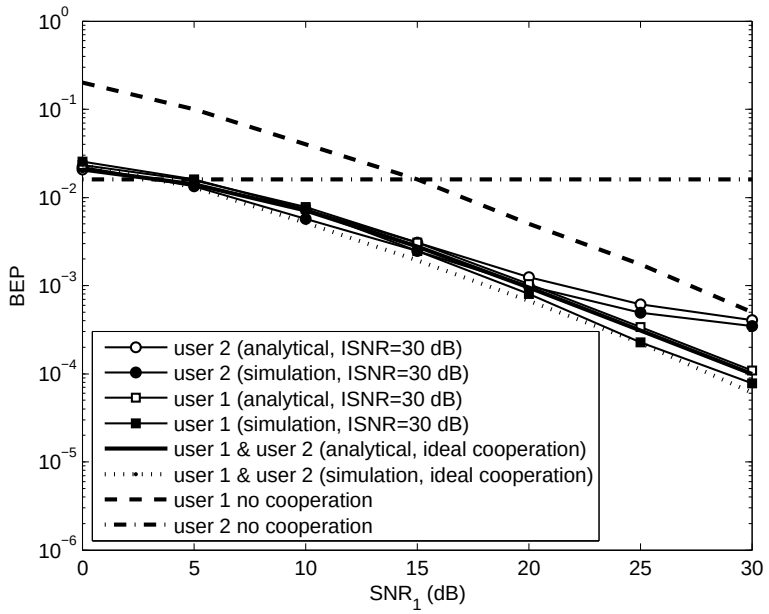

Figure 4.4: Bit error probability of the CD system with 16-QAM for dissimilar channel towards BS ($SNR_2 = 30dB$)

of two when ideal cooperation takes place; similar performance can be achieved when ISNR is 30 dB. In contrast to the fixed *regenerate and forward* CD system in Chapter 3, it is observed that cooperation is beneficial even when the interuser channel is worse than the channel between the user and the BS.

4.4 Summary

An adaptive *regenerate and forward* CD system using quadrature signaling to send M-QAM signals is proposed and analyzed. The bit error performance of the scheme has been evaluated analytically and via simulation for 4-QAM/QPSK and 16-QAM modulations. Numerical results show that the derived analytical upper bound is quite tight. The derived analytical upper bound of the BEP follows the simulated BEP and the proposed

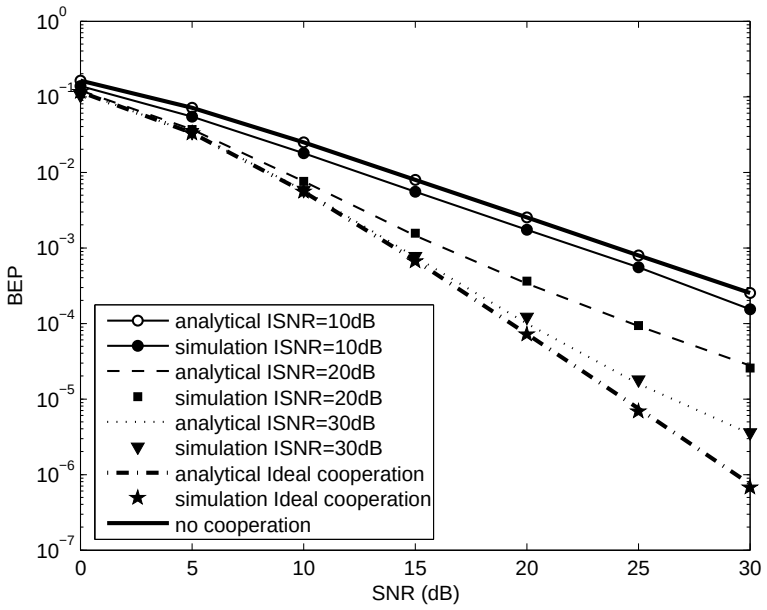

Figure 4.5: Bit error probability of the CD system with 4-QAM/QPSK for similar channel towards BS

CD system exhibits a similar behavior regardless of the size of the QAM signal constellation. Thus, the proposed CD system can achieve similar BEP performance for higher order QAM modulation. In addition, the performance of the proposed scheme can be improved when the interuser channel signal strength increases and the proposed scheme can achieve maximum diversity order of two. Furthermore, the cooperation is beneficial not only for a user far from the BS but also for a user near the BS. In contrast to a fixed CD system, the proposed CD system performs better than an NCD system even when the interuser channel is worse than the user to BS channel.

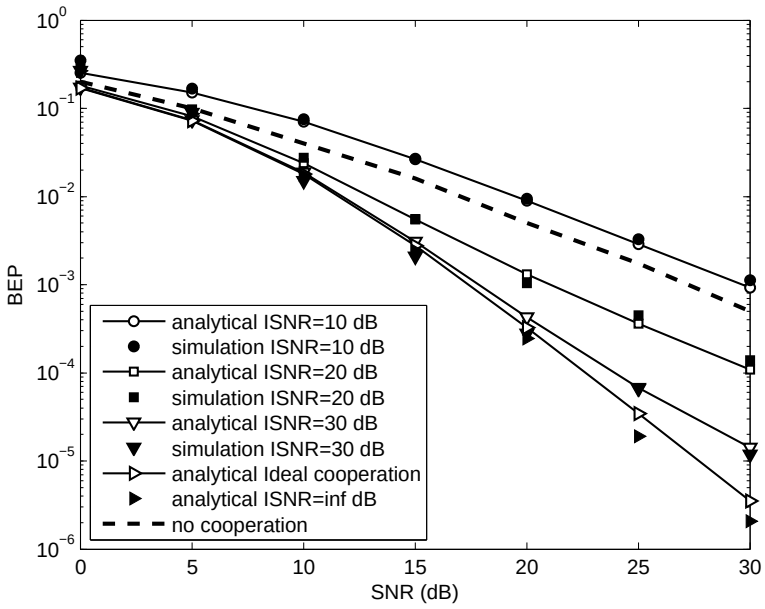

Figure 4.6: Bit error probability of the CD system with 16-QAM for similar channel towards BS

Chapter 5

Cross-Layer Performance Study of Cooperative Diversity System with ARQ

5.1 Introduction

In the previous chapters, we studied the performance of the CD systems at the bit level (physical layer) and assumed the communication channel is independent from one frame to the next frame. In reality, the channel is time-selective. This leads to burst frame error when the channel exhibits deep fading. The burst frame errors impacts the performance in the upper layer. It could be mitigated by automatic repeat request schemes. So, in this chapter, we jointly study the CD system at the physical layer with the ARQ scheme for time selective cooperative channels.

As mentioned earlier, adaptive relaying can be selection or incremental. Selection relaying forwards if the frame of information bits received is error free which can be done by error detecting codes such as CRC. On the other hand, in incremental relaying,

the partner forwards the information if any request is made from the destination and received frame is error free.

From an information theoretic point of view, incremental relaying is more bandwidth efficient than that of selection relaying [7]. On the other hand, incremental relaying has implementation problems in CD systems. If a transmission is requested by the destination, the radio resources should be allocated for the partner-to-destination link for short durations i.e., a period of a frame. Allocating radio resources such as multiple access channel for short duration requires significant signaling overhead. Further, an ARQ scheme is a must at the link level and all cooperating users should be aware about the feedback from the destination. In contrast, for selection relaying, the partner-to-destination channel could be assigned for long duration, which reduces the channel allocation overhead. Even though the data link layer is equipped with ARQ, the partners do not have to be aware of it; so this will reduce the signaling overhead and the complexity at the partner's device.

From the above, it is clear that there is a performance-complexity tradeoff among the relaying schemes in CD systems. Therefore, it is important to thoroughly study and understand the performance of a CD system with ARQ (CD-ARQ) in various wireless network environments. However, there are limited studies on performance of CD-ARQ schemes in the open literature [28–30]. In [28], cooperative energy gain of DSTBC-CD-ARQ scheme is studied for incremental relaying with optimal power allocation and delay constraints. However, the effects in the upper layers due to ARQ, such as packet loss rate, average delay, jitter, etc., are not considered. Incremental relaying is applied for DSTBC in [29]. The throughput of the system is analyzed with the assumption that ideal synchronization is available at the destination. But, power allocation and code allocation among the partners are not considered. In [30], a selection combining (SC) based CD-ARQ (SC-CD-ARQ) scheme is developed for an ad-hoc network which selects only one branch at the destination.

In this chapter, a cross layer communication system, in which an adaptive QS-CD at the physical layer and truncated stop-and-await ARQ at the link layer are combined, is proposed. The proposed QS-CD-ARQ system is studied analytically by developing a Markov model to capture the behavior of the Nakagami-m correlated fading among the partners and partner-to-destination channels and compared with simulation. The performance metrics such as channel efficiency, packet loss rate, throughput or average delay and jitter are considered in the study and the proposed QS-CD-ARQ system is compared with existing schemes in the literature that consider incremental relaying at the partner. From the numerical results, we can observe that selection relaying outperforms incremental relaying schemes when it has a good partner. The QS-CD-ARQ also exhibits the robustness even if one channel is in deep fading. In addition, the proposed QS-CD-ARQ system is less complex in terms of implementation compared with a system employing incremental relaying.

The main contributions of the chapter are three-fold. First, we propose a QS-CD-ARQ system employing selection relaying at the partner by considering the Nakagami-m fading channels. Second, effects of user mobility is taken into account in the performance analysis of the QS-CD-ARQ schemes. Third, DSTBC-ARQ, SC-CD-ARQ and non-cooperative diversity ARQ (NCD-ARQ) systems are compared with the proposed QS-CD-ARQ system under a generalized framework for correlated Nakagami-m fading channels.

The remainder of the chapter is organized as follows. Sec. 5.2 introduces the proposed QS-CD-ARQ system. The performance analysis of the QS-CD-ARQ system is given in Sec. 5.3. Numerical results of the proposed system is presented in Sec. 5.4. In Sec. 5.5, performance of the proposed system is compared with the existing CD-ARQ systems. Finally, the chapter is concluded in Sec. 5.6.

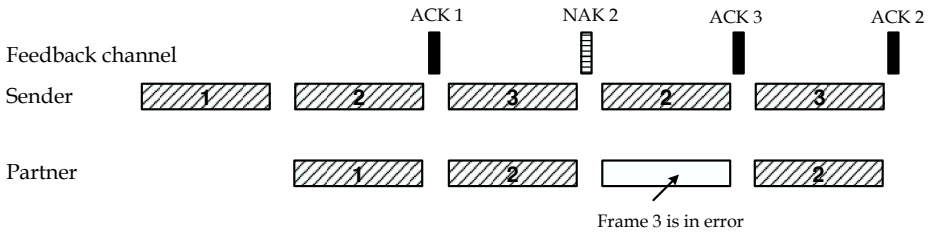

Figure 5.1: QS-CD-ARQ Scheme

5.2 Proposed CD-ARQ System

In this section, we propose the QS-CD-ARQ system by combining adaptive QS-CD system at the physical layer with truncated stop-and-wait ARQ at the data link layer.

5.2.1 System Description

Consider the adaptive QS-CD system proposed in Chapter 4. The *user 1* (sender) broadcasts the frame of bits to the destination and *user 2* (partner) in multiple access *channel 1*. *user 2* detects the signal from *user 1* and decodes the frame of bits to check the correctness of the bits using CRC. According to the selection relaying mechanism, if the received frame is error free, *user 2* forwards the information in multiple access *channel 2*. At the BS, the signals from *user 1* and *user 2* are combined using MRC and decodes the frame. The correctness of the frame is checked using CRC. If the frame is error free, an acknowledgement ('ACK') message is sent to *user 1*. Otherwise, a negative acknowledgement ('NAK') message is sent to *user 1*. If *user 1* receives 'NAK', he/she retransmits the frame if the number of retransmission does not exceed the maximum retry limit (N_r^{max}). In this protocol, *user 2* is not aware about feedback from the destination. This reduces the complexity of the partnering device. Details of the protocol is described in Table I. The graphical representation is given in Fig. 5.1. In non-cooperative transmission, E_{b1} and E_{b2} are the bit-energies spent by *user 1* and *user 2*, respectively.

In cooperative transmission, the energy spent by each user to transmit own information is E_{bi}^S and energy spent for partner's information is equal E_{bi}^R. For a fair comparison, $E_{bi} = E_{bi}^S + E_{bi}^R$.

For the regenerate and forward mode, it is easy to make decision on frame error at the partner and the BS using CRC. In order to facilitate the performance study at a high level independent of the underlying channel coding and modulation schemes, frame error is decided by a signal-to-noise ratio threshold (SNR_T). SNR_T is the minimum received SNR required for receiving a frame correctly. Thus, if the received SNR is below the threshold, the received frame is considered to be erroneous and dropped.

5.2.2 Nakagami fading channel

The channels between *user 1* and *user 2*, {1,2}, *user 1* and BS, {1,BS}, and *user 2* and BS, {2,BS}, are assumed to be Nakagami-m fading and constant over a frame duration. But, the channel is time correlated among adjacent frames due to the Doppler effect, as captured by Jake's model. We also assume that channel state information is available at the respective receivers.

The probability density function of the Nakagami-m distribution is given by [67]

$$f(h) = \frac{2m^m h^{2m-1}}{\Gamma(m)\Omega^m} \exp^{-\frac{mh^2}{\Omega}}, \tag{5.1}$$

where h is the fading channel coefficient, $m = \mathbf{E}^2[h^2]/var(h^2)$, $\Omega = \mathbf{E}[h^2]$ and $\Gamma(m) = \int_0^\infty x^{m-1} \exp^{-x} dx$ is the Gamma function. The corresponding cumulative distribution function (CDF) can be written as

$$F(h) = \frac{\gamma(m, mh^2/\Omega)}{\Gamma(m)}, \tag{5.2}$$

where $\gamma(a, b) = \int_0^b y^{a-1} \exp^{-y} dy$ is the incomplete gamma function.

Table 5.1: Protocol of QS-CD-ARQ

Sender (user 1) Retry counter of each frame is initialized to zero.

1. A new frame is transmitted by *user 1* to the BS and *user 2* in its own multiple access channel (*user 1* channel) with bit energy $E_{b1}^{S} = E_{b1}/2$.

2. In the next time slot,

   (a) if the time slot is 2 or it receives a 'ACK', go to 1).

   (b) if the retry counter does not exceed the maximum retry limit N_R^{max}. the corrupted ('NAK' received) frame is re-transmitted in the *user 1* channel with bit energy $E_{b1}^{S} = E_{b1}/2$, retry counter is increased the by 1 and go to 2).

   (c) Otherwise, the frame is dropped and go to 1).

Partner (user 2) If *user 2* receives the frame correctly, in the next time slot, received frame is forwarded using *user 2* channel with bit energy $E_{b2}^{R} = E_{b2}/2$. Otherwise, *user 2* remains silent.

Destination (BS) At end of each time slot from second time slot, the message signal received from *user 1* and *user 2* is combined by the BS using MRC. Depending on the received frame correctness, an 'ACK' or a 'NAK' is sent in the feedback channel to the source.

The joint PDF of $h(t)$ and $h(t+\tau)$ is obtained as in [67]

$$f(h(t),h(t+\tau)) = \frac{4m^{m+1}(h(t)h(t+\tau))^m}{\Gamma(m)\Omega^{m+1}(1-\rho)\rho^{m-1}} \quad (5.3)$$

$$\times \exp\left(\frac{-m}{1-\rho}\left[\frac{h(t)^2+h(t+\tau)^2}{\Omega}\right]\right) \quad (5.4)$$

$$\times I_{m-1}\left(\frac{2\sqrt{\rho}mh(t)h(t+\tau)}{\Omega(1-\rho)}\right) \quad (5.5)$$

where ρ is the correlation coefficient and I_ν denotes ν^{th} order modified Bessel function. The joint CDF can be written, using the technique in [70], as

$$\begin{aligned} F_{h(t),h(t+\tau)}(\Delta,\Delta) &= P(h(t)\le\Delta, h(t+\tau)\le\Delta) \\ &= \frac{1}{2}-\frac{2}{\pi}\int_0^{\pi/2}\Im\left\{\psi(-j\tan\theta)e^{-j\Delta^2\tan\theta}\right\}\frac{1}{\sin 2\theta}d\theta \end{aligned} \quad (5.6)$$

where $\psi(s)=\frac{2^{2m+1}\Gamma(2m)}{\Gamma(m)\Gamma(m+1)}\frac{(A^2(s)m)^m}{[(1+B(s))B(s)\Omega]^m}{}_2F_1\left(1-m,m;1+m;\frac{1}{2}-\frac{1}{2B(s)}\right)$. ${}_2F_1$ is Gauss hypergeometric function, $A(s)=\frac{1}{s}\sqrt{\frac{m}{2\Omega(1-\rho)}}$ and $B(s)=\frac{\sqrt{[s\Omega(1-\rho)+2m]^2-4\rho m^2}}{s\Omega(1-\rho)}$.

5.3 Performance analysis

In this section, performance analysis of the proposed QS-CD-ARQ system is derived by modeling the system as a Markov process at frame level. The Markov process takes physical layer parameters into account. From the Markov process, we derive the performance metrics at the frame level and packet level where a packet from upper layer is divided into frames at the data link layer.

5.3.1 Signal reception

To model the system as a Markov process, the characteristics of the received signal at the partner's device and the destination should be known. Therefore, in this subsection, the signals at the individual receivers are given.

5.3.1.1 Received signal by partner

The signal received by *user 2*'s device at time t can be written as,

$$r_{1,2}(t) = \sqrt{E_{b1}^S} h_{1,2}(t) s_1(t) + \eta_{1,2}(t) \tag{5.7}$$

where E_{b1}^S is the bit energy spent by *user 1*, $h_{1,2}$ is the Nakagami fading channel coefficient between *user 1* and *user 2* (with parameters $m_{1,2}$ and $\Omega_{1,2}$, maximum Doppler frequency shift, $f_{1,2}$), $s_1(t)$ is the transmitted symbol at time t by the *user 1*, and $\eta_{1,2}(t)$ is additive white Gaussian noise at the *user 2*'s device with zero mean and two-sided power spectral density $N_0/2$.

5.3.1.2 Received signal at the destination

The transmitted signals from *user 1* and *user 2* traverse through two different Nakagami fading channels. The received signals are combined by using MRC to attain diversity gain. In a cooperative situation, the channels are non-identical but independently distributed (non-i.i.d.) due to unequal fading figures (m), signal power (Ω), or maximum Doppler shifts (f_d). The received signal at the BS can be written as

$$r_{1,B}(t) = \sqrt{E_{b1}^S} h_{1,B}(t - T_f) s_1(t - T_f) + \eta_{1,B}(t - T_f) \tag{5.8}$$

$$r_{2,B}(t) = \sqrt{E_{b2}^R} h_{2,B}(t) s_2(t) + \eta_{2,B}(t) \tag{5.9}$$

where E_{b2}^R is bit energy spent for relaying by *user 2*, T_f is frame duration, $\eta_{i,B}(t)$ is additive white Gaussian noise at the BS with zero mean and two-sided power spectral density $N_0/2$, $h_{1,B}$ and $h_{2,B}$ are the Nakagami fading channel coefficients of {1, BS} (with parameters $m_{1,B}$ and $\Omega_{1,B}$, maximum Doppler frequency shift, $f_{1,B}$) and {2, BS} (with parameters $m_{2,B}$ and $\Omega_{2,B}$, maximum doppler frequency shift, $f_{2,B}$), respectively.

When *user 2* helps, the received signal power can be written in terms of received

signal envelops from each user, $r^2_{1,B}(t) = \sum_{k=1}^{m_{1,B}} r^2_{1,B,k}(t)$ and $r^2_{2,B}(t) = \sum_{k=1}^{m_{2,B}} r^2_{1,B,k}(t)$,

$$R^2(t) \;=\; \sum_{k=1}^{m_{1,B}} r^2_{1,B,k}(t) + \sum_{l=1}^{m_{2,B}} r^2_{2,B,l}(t) \tag{5.10}$$

where $r^2_{1,B,k}(t)$, $k = 1..m_{1,B}$, and $r^2_{2,B,l}(t)$, $l = 1..m_{2,B}$, are independent and exponentially distributed with $E\{r^2_{1,B,k}(t)\} = \Omega_{1,B}E^S_{b1}$ and $E\{r^2_{2,B,l}(t)\} = \Omega_{2,B}E^R_{b2}$, respectively. $r^2_{1,B,k}(t)$, and $r^2_{1,B,k}(t+\tau)$, $k = 1..m_{1,B}$, are correlated with correlation coefficient given by

$$\rho_{1,B} = \frac{E\{r^2_{1,B,k}(t)r^2_{1,B,k}(t+\tau)\} - E\{r^2_{1,B,k}(t)\}E\{r^2_{1,B,k}(t+\tau)\}}{\sqrt{var\{r^2_{1,B,k}(t)\}var\{r^2_{1,B,k}(t+\tau)\}}} \tag{5.11}$$

for all k. Similarly we can write the correlation between $r^2_{2,B,l}(t)$, and $r^2_{2,B,l}(t+\tau)$, $l = 1..m_{2,B}$ as

$$\rho_{2,B} = \frac{E\{r^2_{2,B,l}(t)r^2_{2,B,l}(t+\tau)\} - E\{r^2_{2,B,l}(t)\}E\{r^2_{2,B,l}(t+\tau)\}}{\sqrt{var\{r^2_{2,B,l}(t)\}var\{r^2_{2,B,l}(t+\tau)\}}} \tag{5.12}$$

for all l.

From Jakes channel model,

$$\rho_{1,B} = J_0^2(2\pi f_{1,B}T_f) \tag{5.13}$$

and

$$\rho_{2,B} = J_0^2(2\pi f_{2,B}T_f) \tag{5.14}$$

where $J_0(.)$ is zeroth-order Bessel function of the first kind.

The output of the MRC with two Nakagami channel inputs can be effectively modeled as a single Nakagami channel. So, the Equation (5.10) can be written as

$$R^2(t) \;=\; \sum_{k=1}^{m_C} r^2_{C,k}(t) \tag{5.15}$$

where $r^2_{C,k}$, $k = 1..m_C$, are independent and exponentially distributed with $E\{r^2_{C,k}(t)\} = \Omega_C$. $r^2_{C,k}(t)$, and $r^2_{C,k}(t+\tau)$, $k = 1..m_C$, are correlated and the correlation coefficient is

given by ρ_C. The m_C, Ω_C and ρ_C can be derived as

$$m_C = m_{1,B} + m_{2,B}, \tag{5.16}$$

$$\Omega_C = \sqrt{(m_{1,B} + m_{2,B}) \left(\frac{(E_{b1}^S)^2 \Omega_{1,B}^2}{m_{1,B}} + \frac{(E_{b2}^R)^2 \Omega_{2,B}^2}{m_{2,B}} \right)} \tag{5.17}$$

and

$$\rho_C = \frac{\frac{(E_{b1}^S)^2 \Omega_{1,B}^2}{m_{1,B}} \rho_{1,B} + \frac{(E_{b2}^R)^2 \Omega_{2,B}^2}{m_{2,B}} \rho_{2,B}}{\left(\frac{(E_{b1}^S)^2 \Omega_{1,B}^2}{m_{1,B}} + \frac{(E_{b2}^R)^2 \Omega_{2,B}^2}{m_{2,B}} \right)}. \tag{5.18}$$

In a situation where the *user 2* does not help, the BS detects the signal as in a conventional system which is similar to detection at the *user 2*'s device. In this case, the received signal power is

$$R^2(t) = r_1^2(t). \tag{5.19}$$

5.3.2 Markov modelling

At the frame level, the channel is modelled as a Markov process. In this subsection, the Markov modelling of non-cooperative and the cooperative systems are given.

5.3.2.1 Two state model of Nakagami fading channel

The received signal, $R(t)$, is sampled once in each frame interval which is denoted as $R(nT_f)$ and it is assumed that channel does not change significantly in a frame duration, T_f. A sampled process is modelled as a Gillbert-Elliot two-state discrete time Markov process as shown in Fig. 5.2. If the received signal is below the threshold Δ, the frame is erroneous. Otherwise, the frame is error free. Therefore, the system can be categorized as good, 'G', and bad, 'B' state if the received signal envelope falls into the regions, (0,Δ) and (Δ, ∞), respectively. The system state is defined by $S(n)$, $n = 0, 1, 2, ...$, which takes value 'G' and 'B' for good and bad state, respectively.

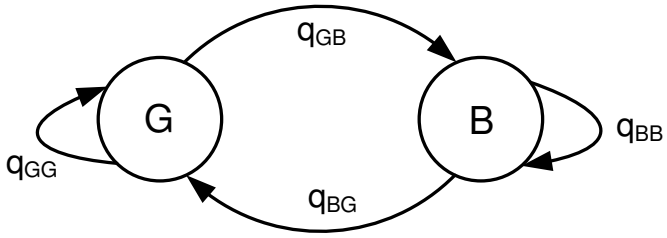

Figure 5.2: Two state Markov model

The transition probabilities of the Markov process can be given by

$$\begin{aligned} q_{GG} &= \text{Prob}(S(n) = G | S(n-1) = G) \\ &= \frac{\text{Prob}(S(n) = G, S(n-1) = G)}{\text{Prob}(S(n-1) = G)} \\ &= \frac{\int_{R_1=\Delta}^{\infty} \int_{R_2=\Delta}^{\infty} f(R_1, R_2) dR_1 dR_2}{\int_{R_1=\Delta}^{\infty} f(R_1) dR_1} \end{aligned} \tag{5.20}$$

and

$$\begin{aligned} q_{BB} &= \text{Prob}(S(n) = B | S(n-1) = B) \\ &= \frac{\text{Prob}(S(n) = B, S(n-1) = B)}{\text{Prob}(S(n-1) = B)} \\ &= \frac{\int_{R_1=0}^{\Delta} \int_{R_2=0}^{\Delta} f(R_1, R_2) dR_1 dR_2}{\int_{R_1=0}^{\Delta} f(R_1) dR_1} \end{aligned} \tag{5.21}$$

where $R_1 = R(t)$ and $R_2 = R(t + \tau)$. Further, q_{GG} and q_{BB} can be simplified as

$$q_{GG} = \frac{1 - 2F(\Delta) + F(\Delta, \Delta)}{1 - F(\Delta)} \tag{5.22}$$

and

$$q_{BB} = \frac{F(\Delta, \Delta)}{F(\Delta)}, \tag{5.23}$$

respectively. Therefore, the transition probability matrix, $\bar{T}$, of the steady state Markov process is given by

$$\bar{T} = \begin{bmatrix} q_{GG} & q_{GB} \\ q_{GB} & q_{BB} \end{bmatrix} \tag{5.24}$$

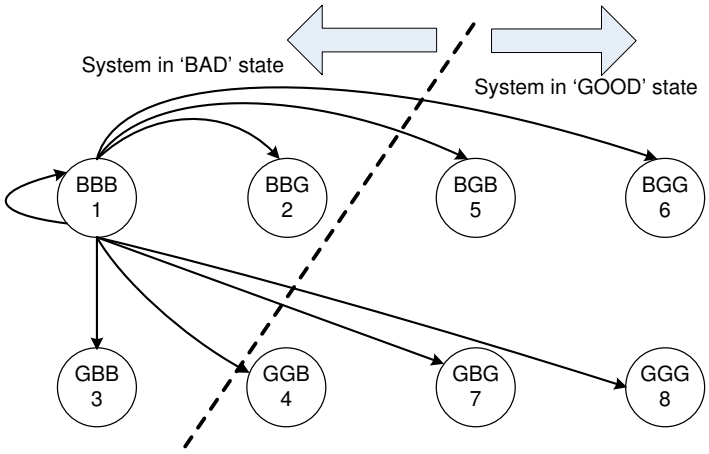

Figure 5.3: Markov model of the proposed system. The system state is denoted by $\{S_{1,2}S_{1,B}S_C\}$

where $q_{GB} = 1 - q_{GG}$ and $q_{GB} = 1 - q_{BB}$. The steady state probability of being in the good state, π_G and the steady state probability of being in the bad state, π_B can be derived as

$$\pi_G = \frac{q_{GB}}{q_{GB} + q_{BG}} \tag{5.25}$$

and

$$\pi_B = \frac{q_{BG}}{q_{GB} + q_{BG}}. \tag{5.26}$$

5.3.2.2 Proposed QS-CD-ARQ system

The performance of the CD system is influenced by {1, BS}, {1, 2} and {2, BS} channels. As mentioned earlier, each channel is modelled by a two-state Markov process. *user 2* only helps when he/she has an error free frame. When *user 2* helps, the BS receives the combined signal that denoted by {C}. Otherwise, it receives from *user 1* only. This situation can be modelled by a modulated Markov process as given in Fig. 5.3 where the {1, 2} channel is modulating the {1, BS} and {C} channels. The Markov state

is denoted by $\{S_{1,2}S_{1,B}S_C\}$. When the direct link is in the good state ($S_{1,B} = G$), the destination decodes the frame without any error. So, states 4, 5, 6 and 8 yield the overall system in good state. When the direct link is in the bad state ($S_{1,B} = B$), the destination decodes the frame without any error if and only if $S_{1,2} = G$ and $S_C = G$. Ultimately, the states 1, 2 and 3 belong to frame error and the system is in the bad state. The remaining five states belong to the good state.

Therefore, this eight-state Markov process can be mapped to a 2-state Markov process. The transition probabilities of the new 2-state system can be given as

$$q_{GG} = \frac{\sum_{i=4}^{8}\sum_{j=4}^{8} T^2[i,j]}{\sum_{i=4}^{8}\sum_{j=1}^{8} T^2[i,j]} \tag{5.27}$$

and

$$q_{BB} = \frac{\sum_{i=1}^{3}\sum_{j=1}^{3} T^2[i,j]}{\sum_{i=1}^{3}\sum_{j=1}^{8} T^2[i,j]} \tag{5.28}$$

where T^2 is square of transition probability matrix T. $T^2[i,j]$ gives transition probability from state i to state j after two time slot and it can be written in terms of transition probabilities of channels {1, 2}, {1, BS} and {C}. The square term comes into play since the proposed CD system retransmits a particular frame in alternate slots as shown in Fig. 5.1.

5.3.3 Derivation of performance metrics

In this subsection, the analytical derivation of performance metrics such as channel efficiency, ξ, packet loss rate, PLR, and throughput, ζ, are given based on the two-state Markov model. It can be applied to CD-ARQ system or NCD-ARQ system. The channel efficiency is defined in the frame level as ratio of the sum of error free frames to the total number of frames transmitted. Since a large packet from the upper layer could not be transmitted in one frame in the physical layer, the packet is usually fragmented. Similar to [30], we assume that fixed size packet from the upper layers is fragmented to N_f

frames in the data link layer. Then, the packet loss rate is defined as the ratio of the sum of dropped packets to the total number of packets transmitted. The throughput of the system is given by the ratio between the total number of successful packets transmitted and the total number of slots taken.

The channel efficiency is equivalent to the probability of the system being in a good state which is given by

$$\xi = \frac{q_{GB}}{q_{GB} + q_{BG}}. \tag{5.29}$$

The average packet loss rate is derived as

$$PLR = 1 - \left(\pi_G + \pi_B(1 - q_{BB}^{N_r^{max}})\right)\left(q_{GG} + q_{GB}(1 - q_{BB}^{N_r^{max}})\right)^{N_f - 1}. \tag{5.30}$$

The throughput is given as

$$\zeta = \frac{1 - PLR}{1 + \pi_B\left(\frac{1 - q_{BB}^{N_r^{max}}}{1 - q_{BB}}\right)} \quad \text{packet/slot.} \tag{5.31}$$

5.4 Numerical results

In this section, the analysis of the proposed QS-CD-ARQ system is validated with simulation results. In addition, the performance of the QS-CD-ARQ is compared with that of the NCD-ARQ system. A detailed description of NCD-ARQ system can be found in [60]. For the simulation, we first utilize an improved Jakes' simulator, proposed in [68], to generate correlated Rayleigh fading traces and then use an efficient method proposed in [69] to generate correlated Nakagami-m fading envelope from the generated Rayleigh traces.

We simulate non identical and independent correlated fading envelopes and using them according to the CD-ARQ schemes. To obtain accurate results, we use a sampling duration $T_f = 10^{-3}$ sec. and collect 10^5 samples for each random seed. The simulation results are obtained by considering the carrier frequency $f_c = 900$ MHz. For a

given f_dT_f, the relative velocity, v, of the {1,2}, {1,BS} and {2,BS} links can be calculated using the equation $v = f_dc/f_c$ where c is the velocity of light. To generalize the performance study, the average signal power in each link and threshold Δ are written in terms of average SNR and SNR threshold, SNR_T, respectively. By defining noise power spectral density $N_0 = 1$, the average SNRs can be written as $SNR_{1,2} = E_{b1}^S\Omega_{1,2}$, $SNR_{1,B} = E_{b1}^S\Omega_{1,B}$, $SNR_{2,B} = E_{b2}^R\Omega_{2,B}$ and $SNR_T = \Delta^2$.

The following system parameters are used unless explicitly stated in Figs. 5.4 - 5.8. The Nakagami fading figures, $m_{1,B} = 1$, $m_{2,B} = 1$ and $m_{1,2} = 2$, the normalized doppler frequency $f_dT_f = 0.1$ for all links, the normalized average SNRs, $SNR_{1,2}/SNR_T = 5dB$, $SNR_{1,B}/SNR_T = 5dB$, and $SNR_{2,B}/SNR_T = 5dB$, the number frames per packet, $N_f = 100$, and the retry limit of a frame, $N_r^{max} = 4$.

5.4.1 Effects of ARQ Parameters

In this subsection, we study the impact of ARQ protocol parameters on performance by considering the packet size (N_f) and the maximum number of retransmission (N_r^{max}). The PLR and the throughput of the QS-CD-ARQ system is compared with those of the NCD-ARQ system in Fig. 5.4. From Fig. 5.4, we can observe that the overall performance of the QS-CD-ARQ is far better than the NCD-ARQ. That means cooperation provides less PLR and higher throughput to the communication system. As expected, the performance of both QS-CD-ARQ and NCD-ARQ degrades in terms of PLR and throughput as the packet size increases, which is shown in subfigures (a) and (b). The rate of change of QS-CD-ARQ is slower than that of NCD-ARQ. This means that a variable packet size system is more robust with QS-CD-ARQ than NCD-ARQ. In subfigures (c) and (d), the maximum number of retries is varied from 0 to 6. From the results, the NCD-ARQ system keeps improving as N_r^{max} increases. The performance improvement of the QS-CD-ARQ system is not significant beyond $N_r^{max} = 4$. In addition, the analytical and simulation results coincide for both systems when $N_f = 100$. In this section, we

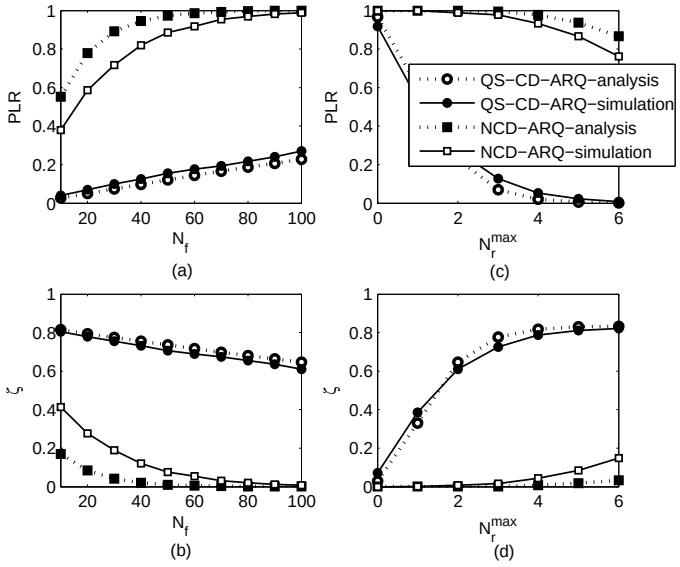

Figure 5.4: Packet loss rate and throughput of the proposed scheme compared with non-cooperative scheme by varying packet size and maximum number of retransmission

use $N_r^{max} = 4$ and $N_f = 100$ to study the effects of other parameters.

5.4.2 Effects of Channel Condition

In this subsection, we study the effects of channel conditions with respect to the normalized SNRs, fading figures and normalized doppler frequencies.

The channel efficiency, packet loss rate and throughput of both QS-CD-ARQ and NCD-ARQ are presented in Figs. 5.5, 5.6 and 5.7, respectively, for different system parameters in subfigures (a), (b), (c) and (d). In subfigures (a) and (b), the $SNR_{1,B}/SNR_T$ is varied from -5dB to 10dB for $m_{2,B} = 1$ and $m_{2,B} = 2$, respectively. $SNR_{2,B}/SNR_T$ and $SNR_{1,2}/SNR_T$ are varied from -5dB to 10dB in subfigures (c) and (d), respectively.

In Fig. 5.5 for all scenarios, the channel efficiency of QS-CD-ARQ increases as the normalized SNRs increase. In subfigures (a) and (b), the channel efficiency of QS-CD-

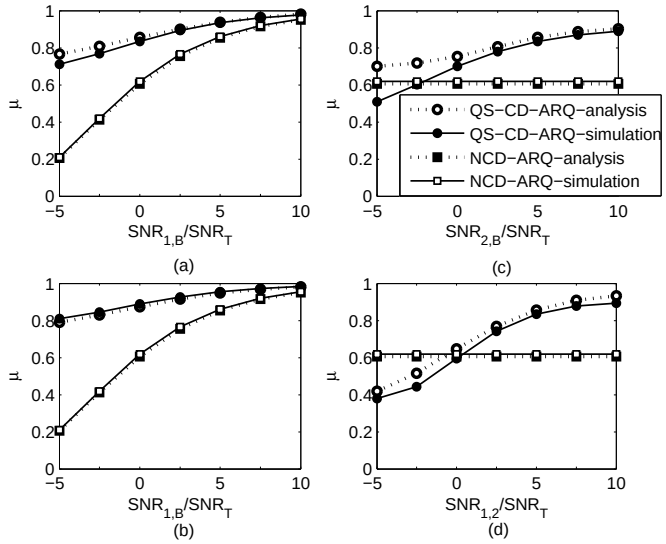

Figure 5.5: Efficiency of the proposed scheme compared with non-cooperative scheme. [For (b), $m_{2,B}$ is changed to 2]

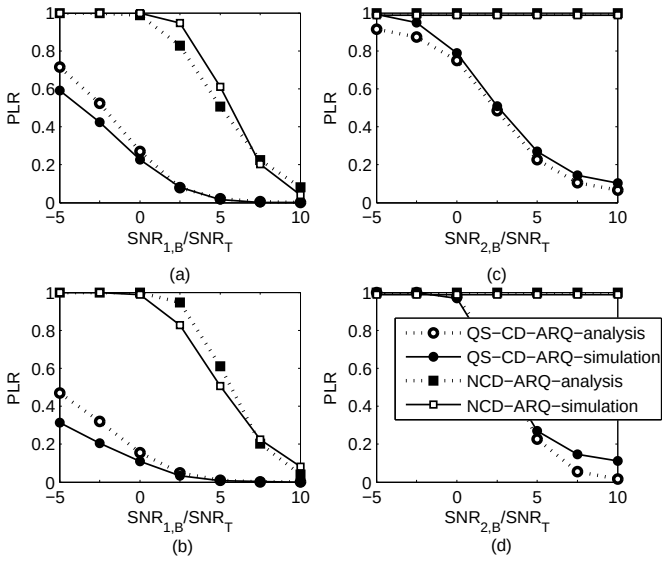

Figure 5.6: Packet loss rate of the proposed scheme compared with non-cooperative scheme. [For (b), $m_{2,B}$ is changed to 2]

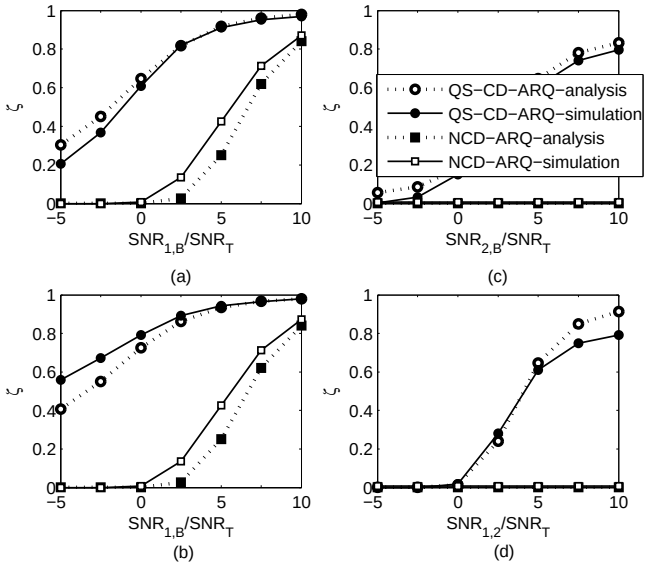

Figure 5.7: Throughput of the proposed scheme compared with non-cooperative scheme. [For (b), $m_{2,B}$ is changed to 2]

ARQ is better than that of NCD-ARQ and improves when the fading figure of *user 2* is changed from 1 to 2. This is due to the fact that frame error rate decreases with improving cooperative channels. In subfigures (c) and (d), the QS-CD-ARQ system outperforms the NCD-ARQ system when normalized SNRs are greater than 0dB, which means that the average received signal power at the receivers should be above the SNR_T.

The PLR is presented in Fig. 5.6. In all cases, the proposed QS-CD-ARQ gives lower PLR than NCD-ARQ, and PLR decreases as the normalized SNRs increases. From the subfigures (a) and (b) of Fig. 5.6, it can be observed that increasing the fading figure of the {2,B} channel improves the PLR performance significantly. In addition, the throughput of the QS-CD-ARQ system given in Fig. 5.7 also exhibits similar performance characteristics as PLR in Fig. 5.6. This behavior of the QS-CD-ARQ is due to the diversity provided by cooperation and improved channel quality with SNR.

From Figs. 5.5, 5.6 and 5.7, we can conclude that increasing the normalized SNRs

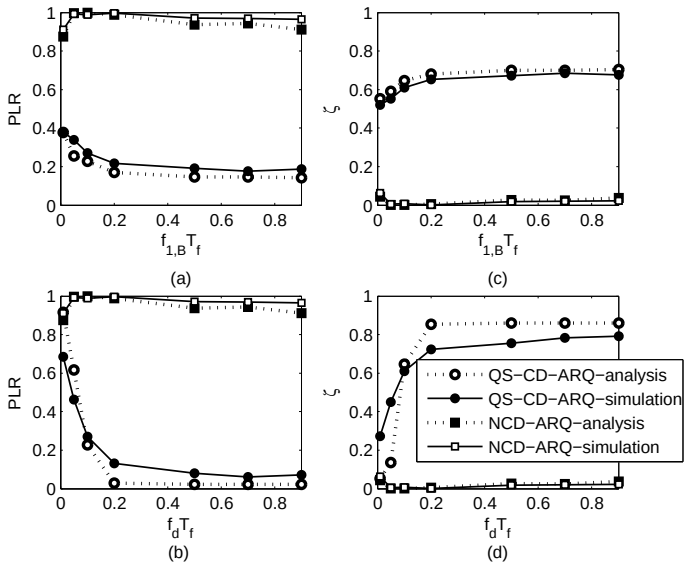

Figure 5.8: Packet loss rate and throughput of the proposed scheme compared with non-cooperative scheme for various speed of the users.

improves the QS-CD-ARQ system performances. The fading figure of the {2,BS} channel significantly affects the upper layer performance. When average received SNR of all the channels are above the SNR_T, the proposed QS-CD-ARQ system outperforms the NCD-ARQ system. Finally, our analytical approach is validated from the figures that simulation results closely follow the analytical results.

In Fig. 5.8, the PLR and throughput are plotted for various values of normalized Doppler frequencies, f_dT_f. The normalized Doppler frequency of the {1,B} channel $f_{1,B}T_f$ is varied from 0.01 to 0.9 in subfigures (a) and (c). On the other hand, in subfigures (b) and (d), the normalized frequencies of all the channels are changed simultaneously from 0.01 to 0.9. Even though NCD-ARQ performs poorly for the given system parameters in terms of PLR and throughput, the QS-CD-ARQ scheme performs better in all cases. When the normalized frequency is larger than 0.2, the PLR of the QS-CD-ARQ is almost saturated to 0.2 for subfigure (a) and 0.05 for subfigures (b). This also

reflects in the performance of throughput in subfigures (c) and (d), which means that the throughput is saturated when the normalized frequency is larger 0.2. Since the normalized Doppler frequency of all the channel are equal in subfigures (b) and (d), the effective channel exhibits more uncorrected than the effective channel in the case of subfigures (a) and (c). Therefore, the QS-CD-ARQ system provides lower PLR and higher throughput for subfigure (b) than subfigure (a), respectively. Similar to (a) and (c), the effect of individual channel correlation can be studied.

From Figs. 5.4 - 5.8, the analytical study is validated by simulation not only for the proposed QS-CS-ARQ system but also for NCD-ARQ. The proposed system can outperform the conventional non-cooperative ARQ system by selecting a good partner for cooperation.

5.5 Related Work and Comparative Study

In this section, the performance of DSTBC-CD-ARQ, SC-CD-ARQ and NCD-ARQ systems are compared with the our proposed QS-CD-ARQ system. In all cases, we use a two-user based cooperative diversity and stop-and-wait ARQ mechanism. The description of each scheme is given as follows.

5.5.1 System Description

In the DSTBC-CD-ARQ system, relay is equipped with incremental relaying and destination is combining signal according to the space time block coding employed. This scheme is similar to the scheme proposed in [28, 29]. The protocol of DSTBC-CD-ARQ is given in Table II and illustrated in Fig. 5.9. The SC-CD-ARQ is similar to DSTBC-CD-ARQ except the relays forward without any coding technique (decode and repeat) and the destination uses SC instead of DSTBC. This scheme is equivalent to the node

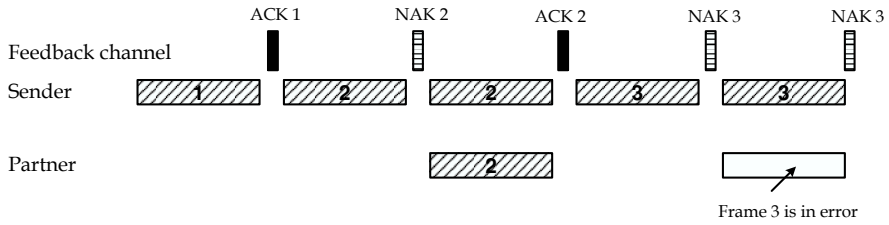

Figure 5.9: DSTBC-CD-ARQ Scheme

cooperative ARQ scheme proposed in [30]. NCD-ARQ is a conventional stop and wait ARQ scheme without cooperation as mentioned in earlier section.

A comparative study is performed based on simulation. In this section, we consider $m_{1,B} = m_{2,B} = 1$ and $m_{1,2} = 2$. To obtain accurate results, we use a sampling time of 10^{-3} sec and collect 10×10^5 samples for each random seed. In the simulation study, we consider the following system parameters. The carrier frequency f_c is equal to 900 MHz. The relative velocity of the {1,2}, {1,BS} and {2,BS} links are 10 Km/hr, 30 Km/hr, and 30 Km/hr, respectively. Unless explicitly stated, the following parameters are used. The normalized SNRs, $SNR_{1,2}/SNR_T = 15dB$, $SNR_{1,B}/SNR_T = 5dB$, and $SNR_{2,B}/SNR_T = 5dB$, the number frames per packet, $N_f = 10$, and the retry limit of a frame, $N_r^{max} = 9$.

The metrics of interest in evaluating the performance of the CD-ARQ schemes are efficiency, packet loss rate, average delay and delay jitter. The efficiency and packet loss rate are similar to earlier definitions. Instead of throughput, we introduce average delay and jitter in this section. The average delay of the packet is given by the ratio of the total number of successful packets to the total number of slots used. The jitter is the variance of the packet delay.

Table 5.2: Protocol of DSTBC-CD-ARQ

Source Flag=New frame; retry counter of each frame is initialized to zero.

1. Broadcast mode: A frame (depending on Flag) is transmitted by *user 1* to both the BS and *user 2* in the user-1 channel with bit energy $E_{b1}^S = E_{b1}$,

   (a) if an 'ACK'is received, Flag=New frame; go to 1).

   (b) if a 'NAK' is received and the retry counter does not exceed the retry limit, go to 2).

   (c) otherwise, the frame is dropped; Flag=New frame; go to 1).

2. Cooperation mode: The same frame is re-transmitted by *user 1* in the user-1's channel with bit energy $E_{b1}^S = E_{b1}/2$, the retry counter of the frame is increased by 1, and

   (a) if an 'ACK' is received, Flag=New frame; go to 1).

   (b) if a 'NAK' is received and the retry counter does not exceed the retry limit, Flag=current frame; go to 1)

   (c) otherwise, the frame is dropped; Flag=New frame; go to 1).

Partner

1. (Listening mode): The *user 2* listens the transmission and decodes it, and

   (a) if the received frame is in error, stay in 1).

   (b) otherwise, go to 2).

2. (Transmission mode):

   (a) if a 'NAK' is received from the BS, the *user 2* transmits with the *user 1* simultaneously in user-1's channel with power $E_{b2}^R = E_{b2}/2$ and go to 1).

   (b) otherwise, go to 1).

Destination

1. (Conventional mode): The BS decodes the signal from *user 1* and checks for correctness, and

   (a) if the received frame is in error, a 'NAK' is sent in the reverse channel and go to 2).

   (b) otherwise, an 'ACK' is sent in the feedback channel and stay in 1).

2. (Cooperation mode): received signal is decoded according to the DSTBC detection; check for correctness and

   (a) if the received frame is in error, a 'NAK' is sent in the feedback channel and go to 1).

   (b) otherwise, an 'ACK' is sent in the feedback channel and go to 1).

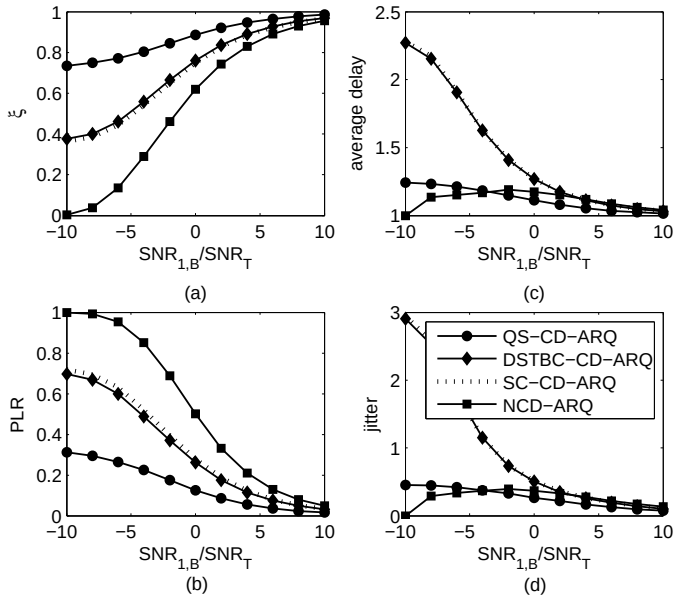

Figure 5.10: Performance of CD-ARQ systems with varying $SNR_{1,B}/SNR_T$ from -10 to 10dB

5.5.2 Effects of Channel Condition

In this subsection, we study the effects of channel conditions by using the normalized SNRs.

Figs. 5.10, 5.11 and 5.12, are plotted as a function of the $SNR_{1,B}/SNR_T$, $SNR_{2,B}/SNR_T$ and $SNR_{1,2}/SNR_T$, respectively. The performance metrics such as channel efficiency, PLR, average delay and jitter are presented in subfigures (a), (b), (c) and (d), respectively.

By utilizing selection relaying in the cooperation, even though the sender to destination channel is poor, a good partner (with good interuser and partner to destination channels) helps for successful transmission in the first attempt. But, in the incremental relaying based schemes, the partner helps only if the first attempt failes. This is the reason for QS-CD-ARQ outperforms all other schemes in Fig. 5.10. Further, NCD-ARQ has low delay and jitter, comparably to those of DSTBC-CD-ARQ and SC-CD-ARQ

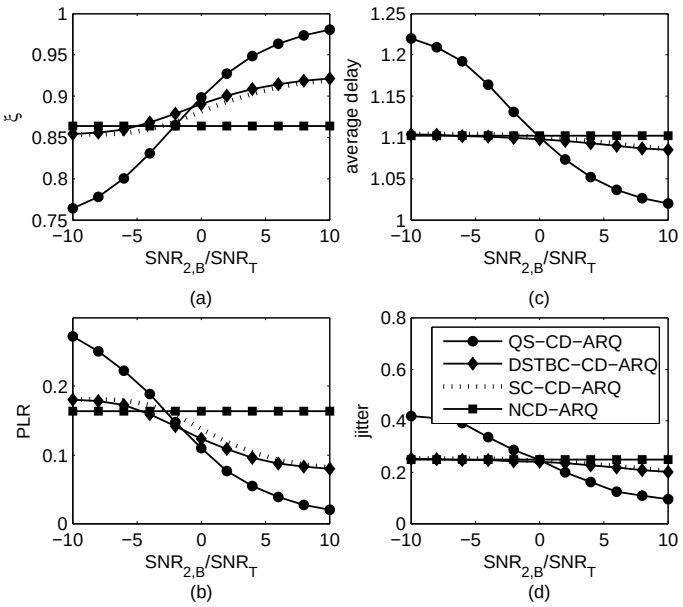

Figure 5.11: Performance of CD-ARQ systems with varying $SNR_{2,B}/SNR_T$ from -10 to 10dB

at the expense of higher packet loss rate. The proposed QS-CD-ARQ outperforms all other schemes when $SNR_{2,B}/SNR_T$ is greater than 0 dB in Figs. 5.10 and 5.11, and $SNR_{1,2}/SNR_T$ is greater than $SNR_{1,B}/SNR_T$ in Fig. 5.12. This is due to the fact that QS-CD-ARQ always gets help from *user 2*. So, the {1,2} and {2,BS} links should be good enough. In addition, SC-CD-ARQ closely follows the DSTBC-CD-ARQ in Figs. 5.10, 5.11 and 5.12 since both are equipped with incremental relaying and the effect of signal combing techniques at the destination is not significant for correlated frame losses. It means that the performance difference between SC and DSTBC is minor in the upper layers.

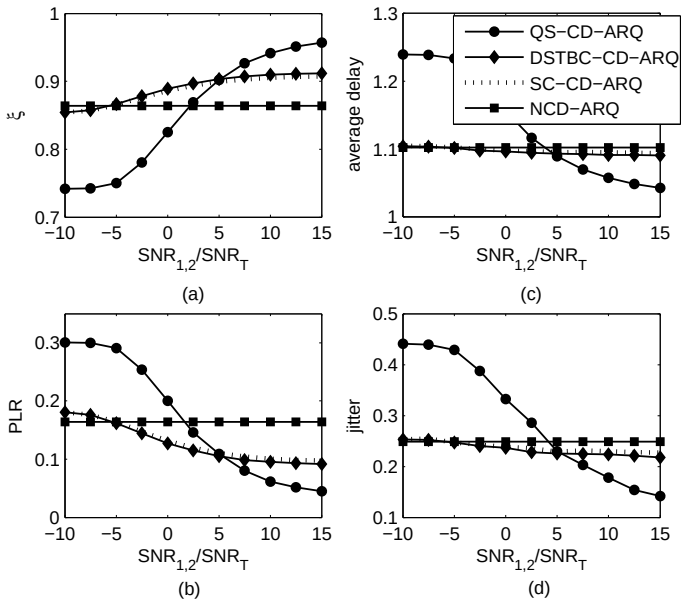

Figure 5.12: Performance of CD-ARQ systems with varying $SNR_{1,2}/SNR_T$ from -10 to 15dB

5.5.3 Effects of ARQ Parameters

In this subsection, we study the impact of ARQ protocol parameters such as N_f and N_r^{max}.

The effects of N_f are studied in Fig. 5.13. Since the channel parameters is not changed, the efficiency and average delay is not changed with packet size. The packet loss rate is increased with N_f for all schemes but the rate of changes is the smallest for QS-CD-ARQ. In addition, the performance of QS-CD-ARQ is better than other schemes that we can observe from all four performance metrics. As discussed earlier, the QS-CD-ARQ performs better due to the incremental relaying mechanism.

The performances of the schemes are plotted against N_r^{max} in Fig. 5.14. The efficiency of the channel employing each scheme is similar to that in Fig. 5.13 except at $N_r^{max} = 0$. With no ARQ mechanism ($N_r^{max} = 0$), DSTBC-CD-ARQ and SC-CD-ARQ

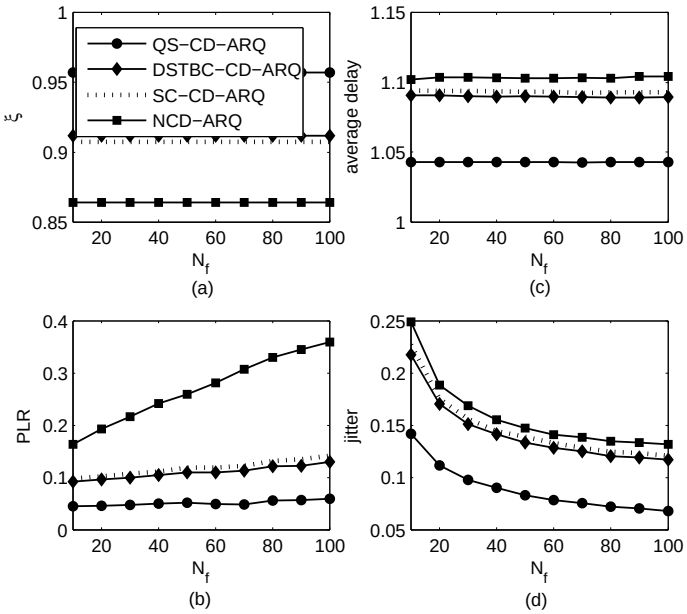

Figure 5.13: Performance of CD-ARQ systems with varying N_f from 10 to 100

have a channel efficiency similar to that of NCD-ARQ since there is no help from the partner. On the other hand, the efficiency of QS-CD-ARQ is better than others even for $N_r^{max} = 0$ because the relay in the QS-CD-ARQ system always forwards if it has error free frame and is unaware of any ARQ mechanism. This leads QS-CD-ARQ to have comparable very low packet loss rate at $N_r^{max} = 0$. For all the schemes, the average delay is increased with increasing N_r^{max} due to increasing retransmissions of a frame or reduce the packet loss rate. The overall performance of the QS-CD-ARQ is better than other schemes and rate of change of both average delay and jitter are minimal compared with other schemes when N_r^{max} is greater than 4. From the results, we can conclude that the proposed QS-CD-ARQ scheme is more favorable for QoS guaranteed applications.

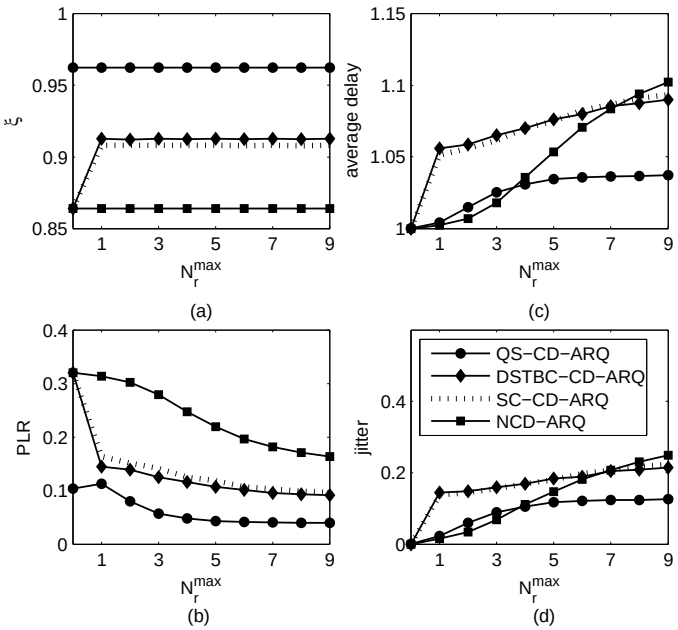

Figure 5.14: Performance of CD-ARQ systems with varying maximum retransmission limit, N_r^{max}, from 0 to 9

5.6 Summary

In this chapter, we introduce a common framework for analyzing adaptive relaying schemes in CD-ARQ systems for time-selective channels. The performance of the schemes is studied and the complexity of the schemes is discussed. From the numerical results, we can observe that the proposed QS-CD-ARQ outperforms other schemes when the sender is cooperating with a partner who provides a good sender-to-partner and partner-to-destination link. In addition, the less complex SC-CD-ARQ performs similarly to DSTBC-CD-ARQ. From the implementation point of view, QS-CD-ARQ is more favorable since radio resources can be allocated for a long duration and the partner does not need to be aware of the ARQ. Moreover, the results of this study shows the importance of the partner selection in CD systems which will be addressed in the next two chapters.

Chapter 6

Matching Algorithms for Cooperative Diversity Systems

As shown in the previous chapters, the performance of CD systems heavily depends on partner location. Given a pair of users, if the interuser transmissions are error free, the CD system can achieve full diversity order, which is equal to the number of terminals participating in the cooperation. In reality, interuser channels are also erroneous. On the other hand, wireless mobile devices are battery powered. It is important to minimize the energy consumption in order to maximize the time the wireless device can be functional without recharging or replacing the battery. Although cooperative diversity energy gain for a single group of users has become an active research topic, how much energy gain can be achieved for a network that employs a CD scheme, and how the diversity gain can be maximized for the whole network are still open issues. In wireless mobile networks, user mobility further complicates the grouping problem. The mobile users' velocities and direction of motion can change over time, which affect the cooperative diversity gain of a pair of users. To the best of our knowledge, there is no research work reported in the literature on how to group mobile users.

In a densely populated network, partner selection that maximizes the number of

matchings is important. In practice, service or network providers will do their best to maximize user capacity in order to maximize the revenue. Based on this premise, it is reasonable to assume that the population size of a cell would be relatively large. The partner selection algorithm proposed in this chapter, based on the criterion of maximizing cell energy, is in a direction to maximize the number of matchings in the partner selection process.

Each individual user has its own preference in choosing its partner. The objective of an individual user (maximizing its own energy gain by cooperation) may conflict with the objective of the network (maximizing the energy gain of the whole network). For user mobility, the best grouping at the current time instant may not be the best at a future time instant. In this chapter, our objective is to group active users in a radio cell, taking cell energy gain and user mobility into consideration. This problem requires the joint efforts from both the *physical layer*, which determines how a pair of users cooperate with each other, and the *network layer*, which determines how to group users in a radio cell. To solve the problem, we first focus on how to optimally group static users in a radio cell, and then study how to match users in a radio cell in the presence of user mobility.

Given the cooperative diversity energy gain of any pair of users, how to maximize it in a radio cell by optimally grouping all the active users can be formulated as a non-bipartite maximum weighted matching problem, which can be solved in polynomial time, $O(n^3)$. Then, well known heuristic based Greedy matching algorithm, which can be solved in polynomial time, $O(n^2 \log n)$, is considered. Due to user mobility and intermittent traffic, the matching algorithm should be periodically executed in real time. Thus, it is important to reduce the computational and implementation complexity of the matching algorithm without compromising too much energy gain. We propose a Worst-Link-First (WLF) algorithm which gives the user with the worse channel condition and higher energy consumption rate a higher priority to choose its partner. The computational complexity of the proposed WLF algorithm is $O(n^2)$. Later, we will show that the WLF is also easier to implement. In this chapter, all the matching algorithms consider the energy gain

achieved by a pair of users as a weight of the vertex and maximizing the total gain of the network is the objective. Therefore, the proposed WLF algorithm that maximizes the energy gain is called WLF-MaxGain. In addition, we derive a theoretical upper bound of energy gain achievable by the matching algorithms.

With user mobility, the population size of a radio cell of the network varies with time, and frequently updating the matching will introduce significant overhead. We propose how to incorporate the mobility information in the matching algorithm to reduce the overhead. It is shown that, by intelligently incorporating user mobility, the MW matching and the WLF matching algorithms can maintain high cell energy gain with reduced overhead.

The main contributions of this chapter are three-fold. First, we formulate the problem of maximizing the cell energy gain in a radio cell as a classic a non-bipartite maximum weighted-matching problem. Then, we study the performance of the four matching algorithms, the MW algorithm, the Greedy matching algorithm, the proposed WLF algorithm and the benchmark random matching algorithm, and compare their computational complexity and cell energy gain tradeoff. Second, we derive theoretical upper bounds of energy gain by cooperation in a radio cell. Third, we propose how to optimally group mobile users, taking user mobility into consideration.

The remainder of the chapter is organized as follows. Section 6.1 presents the operational functions of the MW algorithm, the Greedy matching algorithm, the proposed WLF algorithm and the benchmark random matching algorithm. Section 6.2 describes the network setup. Section 6.3 gives analysis and numerical evaluation of the matching algorithms in a static network. How to group mobile users by considering mobility information is presented in Section 6.4. A summary of the chapter is given in Section 6.5.

6.1 Matching Algorithms

Choosing pairs of cooperating users is known as *matching* on graphs [72, 73]. Let $\mathcal{G} = \{\mathcal{V}, \mathcal{E}\}$ be a graph, where $\mathcal{V}$ is a set of vertices and $\mathcal{E} \subseteq \mathcal{V} \times \mathcal{V}$ is a set of edges between vertices. Each mobile user in a cell is represented as a vertex. The $(i,j)^{th}$ edge $e_{i,j} \in \mathcal{E}$ has a weight $w(e_{i,j})$, which equals the energy gained by cooperation between users i and j over no cooperation. If there is no cooperative energy gain, the two users will just use the non-cooperative scheme, and the weight of the edge linking them is zero. Thus, the weight is always non-negative, and a positive weight represents the energy gain of cooperation over no cooperation.

A subset $\mathcal{S}$ of $\mathcal{E}$ is called a *matching* subset if there are no two edges in $\mathcal{S}$ sharing the same vertex. The overall energy gain in the network is the sum of the positive weights of all edges in $\mathcal{S}$.

6.1.1 Maximum Weighted-Matching

Maximizing the energy gain by cooperation is equivalent to maximizing $w(\mathcal{S}) = \sum_{e_{i,j} \in \mathcal{S}} w(e_{i,j})$ among all possible matchings, which is a non-bipartite weighted-matching problem. The number of matchings with $|\mathcal{S}| = \lfloor \frac{n}{2} \rfloor !$ equals $n!/(2^{\lfloor \frac{n}{2} \rfloor} \lfloor \frac{n}{2} \rfloor !)$, which exponentially increases with n, where $n = |\mathcal{V}|$ is the cardinality of the set $\mathcal{V}$ or the number of users in the network. Comparing all possible matching by Brute Force search is very time consuming when the number of active users is large.

The maximum weighted-matching algorithm developed in [61] can yield the optimal solution for the non-bipartite weighted-matching problem in polynomial time, $O(n^3)$. This state-of-the-art algorithm can be used to obtain the upper-bound of energy gain in a wireless network.

6.1.2 Greedy Matching

The heuristic Greedy matching algorithm [62] is given in Table 6.1. The Greedy matching algorithm requires sorting the weights of all edges in $\mathcal{E}$, so its complexity is $O(n^2 \log n)$.

Table 6.1: Greedy Matching Algorithm

1. The BS selects a user pair i and j such that energy gain $w(e_{i,j})$ is the largest among $w(e)$ for $e \in \mathcal{E}$. $e_{i,j}$ is added to the matching set.
2. Remove all edges incident to $e_{i,j}$ from $\mathcal{E}$.
3. Repeat 1) and 2) until the number of unmatched users is less than two.

6.1.3 Worst-Link-First Matching by Maximizing Gain

With user mobility and intermittent traffic, the matching algorithm should be periodically executed in real time. Thus, it is important to further reduce the computational complexity of the matching algorithm without compromising too much energy gain.

Since the user with the worse channel quality (far from the BS) consumes more energy than the one with a better channel quality (near the BS) in a conventional transmission system, cooperation generally gives more energy gain to the far user than the near user. Therefore, when considering the radio cell, those users with worse channel quality and higher energy consumption rate should be given a higher priority. This motivates us to develop the WLF-MaxGain matching algorithm that is given in Table 6.2.

Table 6.2: WLF-MaxGain Matching Algorithm

1. The BS selects an unmatched user i with the worst channel quality among all unmatched users.
2. The BS selects an unmatched user j such that energy gain $w(e_{i,j})$ provided by the cooperation of user i and user j over no cooperation is the maximum one among all $w(e_{i,k})$, where k is an unmatched user other than i. $e_{i,j}$ is added to the matching set.
3. Repeat 1) and 2) until the number of unmatched users is less than two.

6.1.4 Random Matching

The random matching algorithm is the simplest one and is used as the benchmark. The algorithm randomly selects an unmatched user i and matches it with another unmatched user j, until there are fewer than two unmatched users remaining. Although the computational complexity of the random matching algorithm is $O(n)$, due to the randomness in matching, a significant number of pairs cannot obtain positive energy gain by cooperation. Therefore, random matching provides very limited energy gain.

6.2 Network Setup

We study the performance of an infrastructure-based wireless network, *e.g.*, wireless cellular systems or infrastructure-based wireless LANs (WLANs). The BS of a radio cell, (or an access point in a WLAN) supports N_U mobile users, as shown in Fig. 6.1.

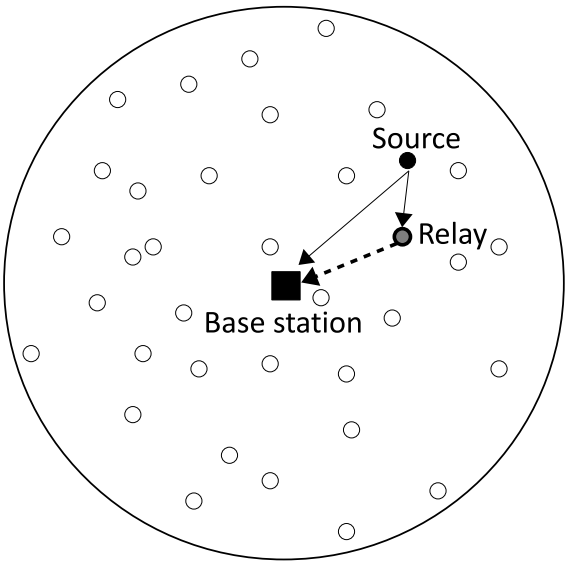

Figure 6.1: Network setup

We consider the scenario in which any user is capable of cooperating with another user, *i.e.*, cooperation between two active users.

Both the interuser channels and the channel between a user and the BS are assumed as quasi-static flat Rayleigh fading. Channel state information, *i.e.*, the variance of channel fading coefficient, is assumed available at the respective receivers. The users estimate the interuser CSIs with their potential partners and forward them to the BS. If estimating interuser CSIs is very time and power consuming by the mobile users, the BS can estimate the interuser CSIs using the locations of the users and the path loss model available for the respective areas. Matching can be done by the BS according to the $N_U(N_U-1)/2$ CSIs, and the users can be grouped according to the matching results. Since cooperation is not always beneficial, a pair of users can choose not to cooperate if there is no cooperative diversity energy gain for them, and they communicate with the BS using a conventional non-cooperative scheme.

In the fixed CD scheme that is studied in Chapter 3, the partner always relays the information to the destination. In contrast, the partner of an adaptive CD scheme that is

proposed in Chapter 4 decides whether or not to forward the information based on the CRC of the received frame of bits. Since the relay should store frames and check the CRC, and inform the BS whether the partner's bits should be relayed or not, additional processing and signaling are introduced. However, error performance of the adaptive CD scheme is generally superior to that of the fixed CD scheme, especially when the interuser channel is highly erroneous. In this chapter, the cell energy gain of both fixed CD system reported in chapter 3 and the adaptive CD system reported in chapter 4 are analyzed with each matching algorithm.

In general, wireless networks have a mixture of static and mobile users. In the following, the performance of the proposed matching algorithms will be analyzed and evaluated for a static-user network and a network with mixed static and mobile users.

6.3 Performance in Static-User Network

Given the required BER of each user, we first calculate the energy consumptions with and without cooperation and the maximum energy gain for a pair of cooperating users. We then obtain the cell energy gain over a non-cooperative system, and its theoretical upper bounds.

6.3.1 Analysis

6.3.1.1 Energy Consumption of Non-cooperative Scheme

In signal transmission using a given modulation scheme over a Rayleigh fading channel, the bit error probability can be expressed as a function of SNR. The bit error probability of the non-cooperative (standard) BPSK scheme for user i can be written as [63]

$$P_{bi} = \frac{1}{2}\left(1 - \sqrt{\frac{\bar{\gamma}_i^{nc}}{1+\bar{\gamma}_i^{nc}}}\right), \tag{6.1}$$

where $\bar{\gamma}_i^{nc} = \sigma_{i,B}^2 \frac{E_{bi}}{N_0}$ is the SNR. E_{bi} is the energy expended in transmitting one bit using the non-cooperative scheme, $\sigma_{i,B}^2$ is the variance of the channel fading coefficient and N_0 is the one-sided power spectral density of additive white Gaussian noise. Therefore, to ensure the BEP of user i to be no less than P_{bi}, the minimal required bit energy is

$$E_{bi} = \frac{N_0}{\sigma_{i,B}^2} \left[\frac{(1-2P_{bi})^2}{1-(1-2P_{bi})^2} \right]. \tag{6.2}$$

6.3.1.2 Energy Consumption of CD Schemes

6.3.1.2.1 Fixed regenerate-and-forward CD scheme For user i partnering with user j, the bit error probability with the fixed regenerate-and-forward CD scheme can be given as in Eq. (3.38),

$$P_{bi} = \frac{1}{2\bar{\gamma}_{i,j}} \frac{\bar{\gamma}_j}{\bar{\gamma}_i + \bar{\gamma}_j} + \frac{3}{4\bar{\gamma}_i\bar{\gamma}_j} + \frac{1}{2\bar{\gamma}_{i,j}} \frac{\bar{\gamma}_i - \bar{\gamma}_j}{(\bar{\gamma}_i + \bar{\gamma}_j)^2} - \frac{1}{2\bar{\gamma}_{i,j}} \frac{3}{4\bar{\gamma}_i\bar{\gamma}_j} \tag{6.3}$$

where $\bar{\gamma}_i = \sigma_{i,B}^2 \frac{2E_{bi}^S}{N_0}$, $\bar{\gamma}_j = \sigma_{j,B}^2 \frac{2E_{bj}^R}{N_0}$, and $\bar{\gamma}_{i,j} = \sigma_{i,j}^2 \frac{2E_{bi}^S}{N_0}$. E_{bi}^S and E_{bj}^R are respectively the energies spent by the source (user i) and the relay (user j) in transmitting one bit for user i.

Let $k = E_{b_j}^R / E_{b_i}^S$. We can write (6.3) as

$$\begin{aligned} 0 &= P_{bi}(E_{b_i}^S)^3 - \left[\frac{k\sigma_j^2 N_0}{4\sigma_{i,j}^2(\sigma_i^2 + k\sigma_j^2)} \right] (E_{b_i}^S)^2 + \frac{3N_0^3}{64k\sigma_{i,j}^2\sigma_i^2\sigma_j^2} \\ &- \left[\frac{3}{16k\sigma_i^2\sigma_j^2} + \frac{\sigma_i^2 - k\sigma_j^2}{8\sigma_{i,j}^2(\sigma_i^2 + k\sigma_j^2)^2} \right] N_0^2 E_{b_i}^S. \end{aligned} \tag{6.4}$$

The above equation has a real solution for $E_{b_i}^S$, which can be expressed as a function of P_{bi}, N_0, k, $\sigma_{i,B}^2$, $\sigma_{j,B}^2$ and $\sigma_{i,j}^2$:

$$E_{b_i}^S = f_1(P_{bi}, N_0, k, \sigma_{i,B}^2, \sigma_{j,B}^2, \sigma_{i,j}^2). \tag{6.5}$$

$f_1(\cdot,\cdot,\cdot,\cdot,\cdot,\cdot)$ is a relatively complex function of its arguments. It can be solved numerically. Given E_{bi}^S, E_{bj}^R can be found using $E_{bj}^R = kE_{bi}^S$. Thus, the energy required for user i in cooperation with user j, $(E_{bi}^S + E_{bj}^R)$, can be determined. Similarly, the energy required for user j in cooperation with user i, $(E_{bj}^S + E_{bi}^R)$, can be derived.

6.3.1.2.2 Adaptive Regenerate-and-Forward CD Scheme By considering cooperative and non-cooperative modes of the adaptive CD scheme in the high SNR regime, the bit error probability of user i can be written as

$$P_{bi} = \left(1 - \frac{K_N}{2\bar{\gamma}_{i,j}}\right) \frac{3}{4\bar{\gamma}_i\bar{\gamma}_j} + \frac{K_N}{4\bar{\gamma}_{i,j}} \frac{1}{\bar{\gamma}_i} \tag{6.6}$$

where $K_N = \sum_{e_b=1}^{N_S} \frac{1}{e_b}$, N_S is the number of symbols in a frame and e_b is the number of bit errors between the transmitted and received frames. Equation (6.6) can be written as

$$0 = P_{bi}(E_{bi}^S)^3 - \frac{N_0^2}{16\sigma_{i,B}^2} \left[\frac{3}{k\sigma_{j,B}^2} + \frac{K_N}{\sigma_{i,j}^2}\right] E_{b_i}^S + \frac{K_N N_0^3}{64k\sigma_{i,B}^2\sigma_{j,B}^2\sigma_{i,j}^2} \tag{6.7}$$

Similar to the fixed CD scheme, the energy required for cooperative transmission can be expressed as a function of P_{bi}, k, N_S, N_0, $\sigma_{i,B}^2$, $\sigma_{j,B}^2$ and $\sigma_{i,j}^2$.

6.3.1.3 Analytical Upper Bound

The cooperative diversity gain of the network depends largely on user deployment, e.g. how many active users in the network, their locations, etc. A tight theoretical upper bound is important for quantifying the performance of different CD schemes and matching algorithms.

Network energy gain, which is the energy gain of a cell with user cooperation over a cell without user cooperation, is defined as

$$G_E = 10\log_{10}\left(\frac{\sum_{i=1}^{N_U} E_{bi}}{\sum_{i=1}^{N_P}(E_{b_i}^S + E_{b_i}^R) + \sum_{i=N_P+1}^{N_U} E_{bi}}\right), \tag{6.8}$$

where the first N_P users are paired to have cooperation and the remaining $(N_U - N_P)$ users have no partners. Since $\sum_{i=1}^{N_U} E_{bi}$ is a constant independent of matching, G_E is maximized when $\sum_{i=1}^{N_P}(E_{b_i}^S + E_{b_i}^R)$ is minimized.

Consider user i located at distance $d_{i,B}$ from the BS and user j at distance $d_{j,B}$ from the BS. The average CSIs $\sigma_{i,B}^2 \propto d_{i,B}^{-\alpha}$, $\sigma_{j,B}^2 \propto d_{j,B}^{-\alpha}$ and $\sigma_{i,j}^2 \propto d_{i,j}^{-\alpha}$, where the path loss

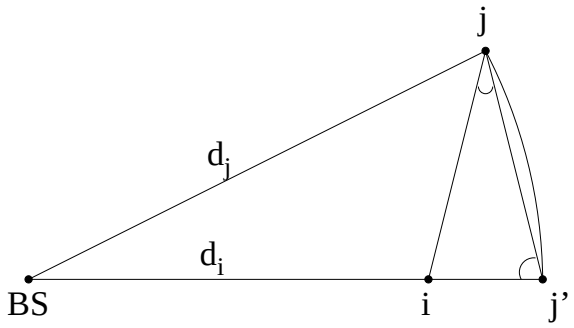

Figure 6.2: Geographical setting of users for the derivation of upper bound

exponent α takes the value between 2 to 6. We first demonstrate that the energy gained by cooperation between users i and j is no larger than the energy gained by cooperation between users i and j', where user j' is located on the straight line beginning at the BS and passing through i, and the distance between j' and the BS is also $d_{j,B}$. Obviously, $E_{bj} = E_{bj'}$. For user i located anywhere between the BS and user j' (see Fig. 6.2), $\angle ijj' < \angle ij'j$, and the distance between i and j is larger than the distance between i and j'. Therefore, $\sigma^2_{i,j} < \sigma^2_{i,j'}$. Consequently, given the BER requirements, the total energy consumption by cooperating users i and j' is smaller than that by users i and j.

Therefore, to obtain an upper bound of cell energy gain, it is sufficient to consider the one-dimensional case. That is, all users lie on the same straight line beginning at the BS, such that the distance between users i and j, $d_{i,j}$, equals $|d_{i,B} - d_{j,B}|$.

6.3.1.3.1 Fixed Regenerate-and-Forward CD Scheme As an example, by substituting $k = 1$, $P_{b1} = P_{b2} = 10^{-3}$, $N_S = 128$, $N_0 = 1$ unit power/Hz, the CSIs in terms of distance, and $\alpha = 3$ into (6.5) and rearranging, we get $E_{bi} + E_{bj} - E^S_{bi} - E^R_{bj} - E^S_{bj} - E^R_{bi}$ in terms of $d_{i,B}$ and $d_{j,B}$, which is maximized when $d_{j,B} = 0.85 d_{i,B}$ or $d_{j,B} = d_{i,B}/0.85$. It means that the most favorable matching for user i is a user located $0.85 d_{i,B}$ or $d_{i,B}/0.85$ away from the BS and on the line between user i and the BS. Therefore, to maximize the cooperative energy gain of the pair, $G_{i,j} = 10 \log_{10} \left(\frac{E_{bi}+E_{bj}}{E^S_{bi}+E^S_{bj}+E^R_{bi}+E^R_{bj}} \right)$ should be maxi-

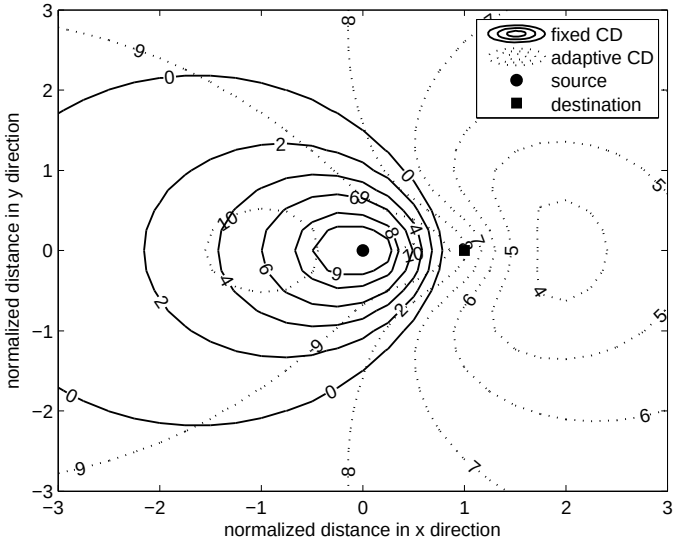

Figure 6.3: Energy gain for a pair of users using fixed CD scheme and adaptive CD scheme

mized. For a given $d_{i,B}$, the maximum cooperative energy gain, $\max\{G_{i,j}\} = 9.63$ dB, is achieved when $d_{j,B} = 0.85 d_{i,B}$ or $d_{j,B} = d_{i,B}/0.85$.

It is noted that $\max\{G_{i,j}\}$ depends on the ratio of $d_{i,B}$ and $d_{j,B}$ only, and it is independent of the values of $d_{i,B}$ and $d_{j,B}$. The upper bound on the cell energy gain can be achieved when all the users have cooperative partners ($N_P = N_U$ even number) and the cooperating pair are located according to the ratio. Therefore, with the fixed CD scheme and other parameters, (α, k, P_{bi}, N_S, N_0), as specified, (7.22) yields the upper bound of the network energy gain, which equals 9.63 dB. The energy gain contours are plotted in the Fig. 6.3: if the source node paired with a node located at the G dB contour, G dB cooperative energy gain can be achieved.

6.3.1.3.2 Adaptive Regenerate-and-Forward CD Scheme Similarly, with the adaptive CD scheme, for a given $d_{i,B}$, $E_{bi} + E_{bj} - E_{bi}^S - E_{bj}^R - E_{bj}^S - E_{bi}^R$ is maximized when

$d_{j,B} = 0.54 d_{i,B}$ or $d_{j,B} = d_{i,B}/0.54$. For a given $d_{i,B}$, the maximum cooperative energy gain, $\max\{G_{i,j}\} = 10.22$ dB, is achieved when $d_{j,B} = 0.54 d_{i,B}$ or $d_{j,B} = d_{i,B}/0.54$, and the upper bound of the cell energy gain with the adaptive CD scheme is 10.22 dB. Both the fixed and adaptive CD schemes have the same energy gain, 9.60 dB, when cooperative users are co-located and their inter-channel is error free. The energy gain contours with the adaptive CD scheme are also plotted in Fig. 6.3.

Comparing the contours of fixed CD and adaptive CD schemes in Fig. 6.3, since the fixed CD scheme is more sensitive to interuser transmission errors, the cooperative energy gain for a particular user decreases quickly when the partner is far away from the user. For the adaptive CD scheme, the pair can still achieve quite significant energy gain even when they are far away from each other. As shown in Fig. 6.3 for adaptive CD scheme, the cooperative region (in which a partner is located with certain dB cooperative energy gain) of the adaptive CD scheme is much larger than that of the fixed CD scheme.

6.3.2 Numerical Results

In this subsection, numerical results are presented for the four matching algorithms with both the fixed and adaptive CD schemes in a network with static users. We generate a wireless network where the coordinates of the BS are $(0, 0)$. N_U users are randomly placed on a unit disk centered at the BS as given in Fig. 6.1, with their coordinates x and y uniformly distributed in $[-1, 1]$. The average CSIs are inversely proportional to d^{α}, where d is the distance between the sender and the receiver, and the path loss exponent α takes the value 3 in the simulation. The required BER is 10^{-3}.

Different user deployments are generated by using different random seeds. We assume that the BS can track the user locations, and thus determine their pair-wise distances and CSIs. From the CSIs, the average energy required for no cooperation and cooperation schemes are calculated, using (6.2) and (6.4), respectively. We change the number of active users in the network from 10 to 100 in order to consider both the low-density and

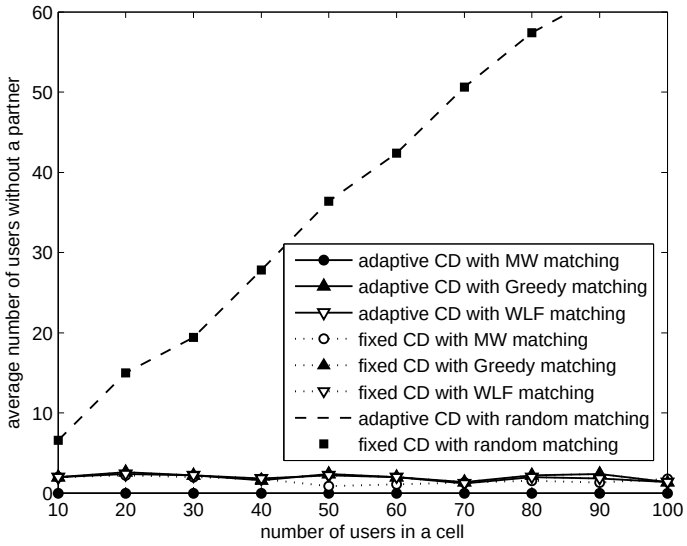

Figure 6.4: Average number of users without a partner vs number of users in the cell

high-density scenarios. The number of users without a partner and the average cell energy gains with the four matching algorithms are shown in Figs. 6.4 and 6.5, respectively. All the results are obtained by averaging the performance parameters over 25 different user deployments.

As shown in Fig. 6.4, for both the fixed and the adaptive CD schemes with the MW, Greedy, and WLF matching algorithms, the number of users without a partner are independent of the number of active users in the network. Thus, the chance for a user without a partner is very low for a high-density network. On the other hand, with the random matching algorithm, the number of users without partner increases proportionally with the number of users in the network. This is because each user has a cooperative region, as shown in Fig. 6.3, only users in the cooperative region grouped together can obtain positive cooperative diversity gain. The probability of two randomly chosen users are within each other's cooperative region is constant, independent of the network density.

Fig. 6.5 shows that the average cell energy gains for the four matching algorithms.

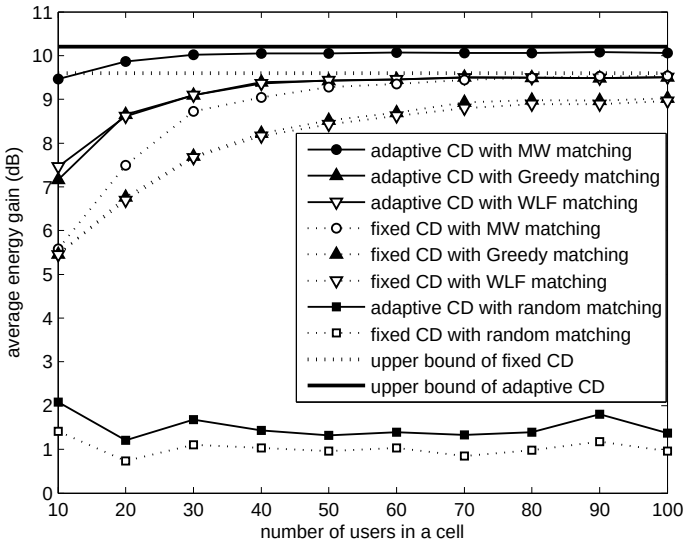

Figure 6.5: Average energy gain, G_E, versus number of users in the cell

The gains of the MW, Greedy, and WLF matching algorithms increase with the number of users. This is because, as shown in Fig. 6.4, in a lower-density network, the chance for a user without a partner is higher, so the average cell energy gain is lower. To approach the analytical upper bound, the network should have a sufficiently large number of users, so every user can be grouped with an optimal partner. As shown in Fig. 6.3, the higher energy gain regions become smaller, so the energy gain of the cell increases slower when the number of active users is larger. In contrast, the random matching algorithm provides almost constant gain, independent of the number of users in the network.

From the numerical results, if a BS does not have the knowledge of the CSIs and just randomly matches users for cooperation, only about 1 dB or 1.5 dB cell energy gain over no cooperation can be achieved with the fixed CD scheme or the adaptive CD scheme, respectively. If the CSIs were available or could be estimated, the WM, Greedy, and WLF matching algorithms would achieve $5.5 \sim 9$ dB cell energy gain with the fixed CD scheme and $7 \sim 10$ dB cell energy gain with the adaptive CD scheme. In addition, the

adaptive CD scheme outperforms the fixed CD scheme by about $1 \sim 2$ dB.

Although the WLF algorithm does not guarantee the worst case performance, extensive simulations demonstrate that, the performance of the WLF algorithm is close to that of the Greedy algorithm, and their average energy gains in a cell are about 1 dB less than that with the MW algorithm. The WLF algorithm is easier to implemente than the MW and Greedy algorithms: the latter two require the matching gains of any pair of active users ($N_U(N_U - 1)/2$ pairs) which are difficult to obtain. With the WLF, the BS can choose an unmatched active user with the farthest distance to the BS (or the worst channel condition to the BS) first. Then, according to Fig. 6.3, the BS selects an unmatched user in the high-dB-gain region to be its partner. In addition, the WLF algorithm can potentially be implemented in a distributed manner: each user chooses its desired partner; if there is any conflict, the user farther away from the BS (or with worse channel condition to the BS) has a higher priority.

6.4 Performance in Mobile Network

In mobile networks, user mobility complicates the matching problem. Since users may move in different directions at different velocities, and the velocities and directions change over time, their absolute and relative locations keep on changing. The currently best matching strategy may be less attractive or even no longer applicable after a while. Therefore, the matching algorithm should be periodically executed according to the current user locations and channel conditions.

6.4.1 Matching Algorithms Considering Mobility

Although more frequently updating the matching can more accurately track the locations and channel conditions of random and high-mobility users, it introduces significant

overhead to not only the BS, but also the mobile users. Furthermore, mobile users need to synchronize with their new cooperative partners frequently. To reduce the overhead without significantly sacrificing performance, it is proposed to predict the future cooperative diversity energy gain of mobile users based on their current location and mobility information, and match users accordingly. How a BS detects the location and speed of active mobile users has been extensively studied in the literature, and the technologies have been used for E-911 service and other location dependent services.

Table 6.3: Modified WLF-MaxGain Matching Algorithm considering mobility

```
1  at time t, sort V according to CSIs
2  for each i ∈ V
3     MaxW = 0; partner(i) = 0
4     for (j = i + 1; j < N_U; j++)
5        if v_j ∈ V
6           w(e_{i,j}) = f(w(e_{i,j}(t)), T)
7           if w(e_{i,j}) > MaxW
8              partner(i) = j;
                MaxW = w(e_{i,j})
9     remove i and partner(i) from V;
      add e_{i,partner(i)} to S
```

The WLF matching algorithm considering mobility, which is periodically executed every T seconds, is given in Table 6.3. At time t, the set of N_U active users, $\mathcal{V}$, are sorted according to their channel conditions (CSIs), such that the user with the worst channel condition is considered first, as shown in Line 1. All users being grouped are removed from $\mathcal{V}$ (Line 9). For each unmatched user i, the BS calculates the cooperative diversity gain of i and another un-matched user j, $w(e_{i,j})$, (Lines 4, 5, 6). Note that $w(e_{i,j})$ is a function of $w(e_{i,j}(t))$ and T. $w(e_{i,j}(t))$ is the energy gain according to users i and

j's current channel conditions or user locations (at time t). Assuming that the velocities and directions of i and j remain the same in the next T seconds, the BS can predict their future locations and channel conditions. $w(e_{i,j}(t+\delta))$ is the predicted energy gain according to the predicted user locations and channel conditions at time $t+\delta$. Function f in Line 6 calculates the average energy gain during t to $t+T$:

$$f(w(e_{i,j}(t)),T) = 1/T \int_{t}^{t+T} w(e_{i,j}(x))dx. \tag{6.9}$$

To simplify the calculation, when T is small, $f(w(e_{i,j}(t)),T)$ can be approximated as $[w(e_{i,j}(t))+w(e_{i,j}(t+T))]/2$. Similarly, the MW and Greedy algorithms can be modified by using the average cooperative diversity gain during $[t, t+T]$ as the weight.

There are certain implications that the system designers may consider. First, to reduce the overhead by lengthening T, the prediction of future user channel conditions and locations become less accurate, which will degrade the overall cell energy gain. Second, even if all active users keep their current velocities and directions for a long time, less frequently updating of the matching will also reduce the overall cell energy gain. This can be illustrated as follows. Observe l consecutive time slots, $t_1, t_2, ..., t_l$, where each slot has a very short duration ϵ. Assume that the user locations and channel conditions remain the same in each slot. If the maximum weighted-matching algorithm is executed at each slot, the energy gain in that slot will always be the highest among any matchings. Therefore, by executing the MW algorithm at each slot, the energy gain is always better than or equal to matching once for a period of l time slots. Third, if the matching algorithm is executed only once per T sec, and user mobility estimation is accurate, using $w(e_{i,j}) = f(w(e_{i,j}(t)),T) = 1/T \int_{t}^{t+T} w(e_{i,j}(x))dx$ in the MW algorithm also leads to optimal matching for overall energy gain of the cell during t to $t+T$. This is because the overall energy gain of the cell during t to $t+T$ is $\int_{t}^{t+T} \sum_{e_{i,j}\in\mathcal{S}} w(e_{i,j}(x))dx = \sum_{e_{i,j}\in\mathcal{S}} \int_{t}^{t+T} w(e_{i,j}(x))dx$, which is maximized using the MW algorithm.

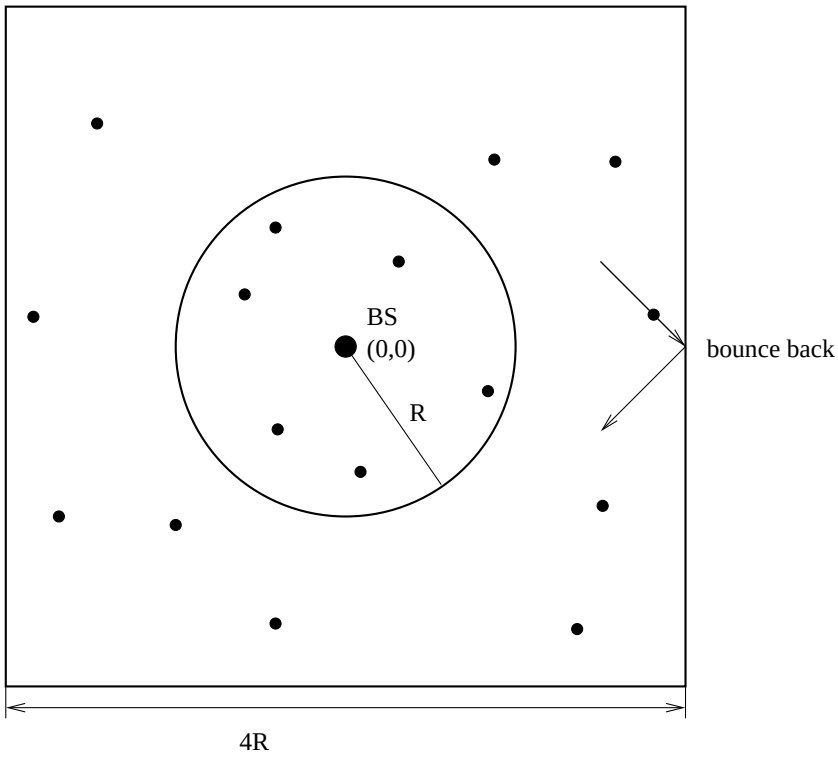

Figure 6.6: Mobility model

6.4.2 Numerical Results

We consider a wireless mobile network in which the users are uniformly distributed over a $(4R)^2$ square area, as shown in Fig. 6.6. The BS is located at the center of the square, covering all active users in the disk centered at the BS with radius R. The mobile users move at constant velocities and the directions of motion are independent and identically distributed (i.i.d.) with uniform distribution in the range $[0, 2\pi)$. If a mobile user reaches the edge of the square, it will be bounced back and move with the same velocity. The velocity is a uniformly distributed random variable in the range $[0, V_{\max}]$. In the simulation, a user chooses a direction and a velocity, and moves in that direction (unless being bounced back) at the constant velocity for a time duration t_d, which is also uniformly distributed in the range $(0, t_{\max})$ slots. After t_d, the process repeats. The matching al-

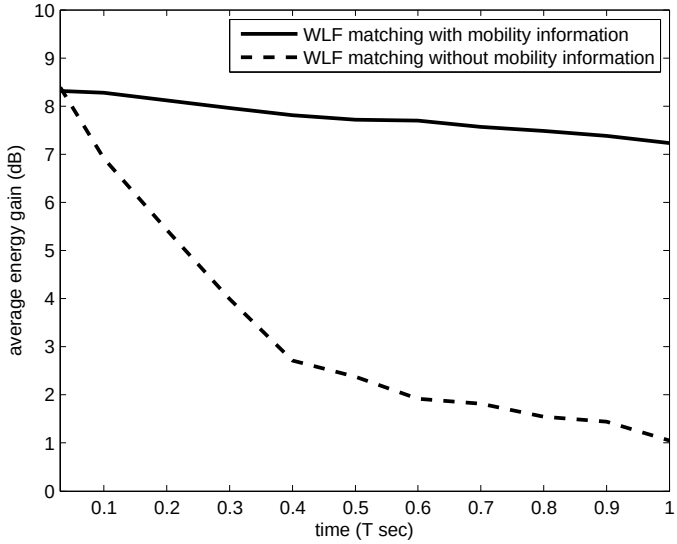

Figure 6.7: Average energy gain, G_E, of WLF matching with and without mobility information

gorithm will be executed every T seconds. The grouped pairs will cooperate with each other until new matching results separate them, or when any of them moves out of the cell or when there is no longer any cooperative diversity gain between them. We use the following parameters in the simulations. The number of active users in the square area is 200. The normalized velocity V_{norm}, which is defined by $V_{norm} = \frac{V_{\max}T}{R}$, is set to 0, 0.25, 0.5, 0.75, 1, which cover the static, low mobility, and high mobility cases.

The energy gain achieved by the WLF matching algorithm for the adaptive CD scheme with and without mobility are shown in Fig. 6.7. It can be seen that for $V_{norm} = 1.0$, from the time after the matching ($t = 0$) to the time just before the next matching ($t = T$), the cell energy gain with the WLF algorithm without mobility information quickly drops from 9 dB to 1 dB. On the other hand, with the same user deployment, the WLF algorithm with mobility information maintains a high cell energy gain (above 7 dB). The simulation results confirm that if we intelligently apply the mobility informa-

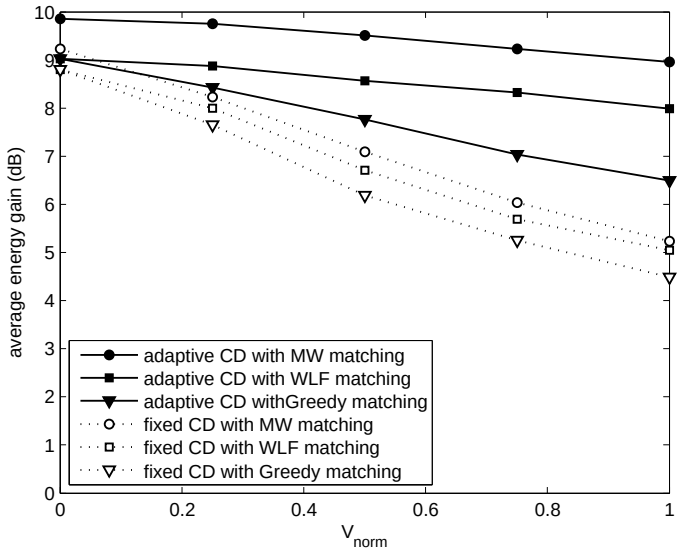

Figure 6.8: Average energy gain, G_E, vs. normalized velocity

tion in the matching algorithm, a significant cell energy gain can be achieved for mobile networks. Similar results are obtained for both the adaptive CD scheme and the fixed CD scheme, with the MW, WLF and Greedy algorithms. In the following, we focus on matching algorithms with mobility information, and compare their performance metrics.

The percentage of in-cell users participating in the cooperation (specifically in the matching process) is approximately $(1-0.3V_{norm})$. In the low mobility situation ($V_{norm} < 0.25$), more than 90% of the in-cell users participate in the cooperation. It is reduced to 70% for the high mobility situation, i.e., $V_{norm} = 1$. On the other hand, the average energy gain decreases as V_{norm} increases, as shown in Fig. 6.8. With other CD scheme or matching algorithms, the same trend can be observed for the average energy gain versus V_{norm} curve. This is due to two factors. First, the percentage of participating users remaining in the cell for a given duration T decreases as V_{norm} increases. Second, with high mobility, even if the matching is ideal at the beginning of a slot, it becomes less favorable or even impractical at the end of the slot.

Fig. 6.8 demonstrates the tradeoff between the performance and overhead. If the BS updates the matching more frequently, *i.e.*, T is shorter, V_{norm} can be reduced and higher cell energy gain can be achieved; otherwise, the BS updates the matching less frequently with less overhead and less energy gain.

The simulation results show that the WLF algorithm outperforms the Greedy algorithm in mobile networks. The performance of the WLF and MW algorithms degrade gracefully when V_{norm} is higher, and the performance of Greedy matching algorithm degrades quickly with higher mobility. In addition, the adaptive CD scheme outperforms the fixed CD scheme by a larger margin with higher mobility. This is because, according to Fig. 6.3, the high gain area is much smaller with the fixed CD scheme than that with the adaptive CD scheme, so the partners easily move outside the high gain area with the fixed CD scheme.

6.5 Summary

Matching theory and algorithms have been extensively investigated in the past for other applications, *e.g.,* scheduling, assignment. Both the state-of-the-art algorithms to obtain the optimal matching, and the approximation algorithms have been reported. The proposed WLF matching algorithm considers the fact that the nodes with worse channel condition generally get more benefits from the cooperation, which is not obvious in other applications. Furthermore, there are some characteristics which are unique in CD systems; thus, it is worth to re-investigate matching algorithms for this particular problem.

We have studied the energy gain provided by four matching algorithms, the MW, Greedy, random, and the proposed WLF matching algorithms, with computational complexity of $O(N_U^3)$,$O(N_U^2 \log N_U)$, $O(N_U)$, and $O(N_U^2)$, respectively, for both fixed and adaptive CD systems. We have further proposed how to optimally match mobile users considering user mobility. Simulation results demonstrate that, by intelligently applying

user mobility information in the matching algorithm, high energy gain with moderate overhead is achievable in mobile networks. It is conjectured that our study provides insights into the tradeoff between matching overhead and energy gain in a wireless network, which is an important step toward practically deploying CD systems in wireless networks.

Chapter 7

Joint Power Allocation and Partner Selection of the Cooperative Diversity System

In the previous chapter, we propose the WLF matching algorithm and compare it with existing matching algorithms by considering equal power transmission from sender and partner. In this chapter, our objective is to minimize the overall energy consumption rate in the network by appropriately grouping users and setting their power levels according to their QoS requirements. Since mobile users in wireless networks change their locations from time to time, by minimizing the energy spent by all users in the cell, the long term energy consumption rate of each user can be minimized so that the average battery recharge time can be significantly prolonged. In addition, the power allocation and matching algorithm should be with low overhead, low computational complexity, and easy implementation.

We first formulate and solve the power allocation problems of 2-user cooperation in cellular networks, considering both the *regenerate and forward* CD systems (including our proposed QS-CD system) and the *amplify and forward* systems. We also extend

the optimal power allocation problems with the constraint that the relaying power at the partner be equal to the source's transmission power. We refer to this as the equal power constraint, which is desired for static wireless networks like sensor networks, in which nodes are equipped with the same initial energy. The objective is to maximize the lifetime of the network; it is therefore necessary to minimize the energy consumption of the nodes with the maximum energy consumption rate. In this situation, equal power allocation (EPA) can maximize the lifetime of the pair. We then study the location of the optimal partner for a user and how to match users to maximize the energy gain of the whole network.

The main contributions of the chapter are three-fold. First, we formulate the optimization problem to maximize cooperative diversity gain in a wireless network, taking into consideration the operational characteristics of different layers. Second, we obtain optimal power allocation solutions for general CD systems to minimize the total energy consumption for a cooperating pair, with and without the EPA constraint, and then substantiate the analysis by calculating the optimal powers for the *amplify and forward* CD system proposed in [49] and our proposed QS-CD (*adaptive regenerate and forward*) system. We further determine the locations of a user's best partner to minimize the energy consumption of the user and to maximize the CD energy gain of the pair. Third, the analytical results motivate us to improve the WLF matching algorithm referred as WLF-MinMaxEnergy. The WLF-MinMaxEnergy can achieve near optimal performance by minimizing the maximum energy requested for cooperative transmission as a weight for the matching algorithm. The power allocation strategies can be directly applied to various CD systems proposed in the literature and the proposed matching algorithm can be easily implemented in a centralized or distributed manner.

The remainder of the chapter is organized as follows. Sec. 7.1 introduces the system model and the CD systems considered. How to optimize the power allocation and the best partner's location are studied in Sec. 7.2. Improved WLF matching algorithms is presented in Sec. 7.3. Numerical results are presented in Sec. 7.4, followed by summary

in Sec. 7.5.

7.1 Network Setup

We consider similar network setup as in Chapter 6. For the sake of completeness, it is briefly described here. Fig. 6.1 shows a wireless cellular network where the BS of a radio cell supports N_U mobile users. A user is capable of cooperating with another user, *i.e.*, cooperation between two active users. The BS and the mobile devices each has a single antenna. The uplink signals transmitted by the sender and relayed by the partner are combined at the BS using MRC. The cooperative diversity system thus emulates a "two inputs one output" (2I1O) situation.

The interuser and the user to BS channels are assumed to exhibit frequency non-selective Rayleigh fading and independent of each other. They are also static over a frame interval and change independently from frame to frame, and each frame consists of B bits. In addition, it is assumed that channel state information is available at the respective receivers and proper synchronization has been established.

7.1.1 Regenerate and forward CD system

We consider the QS-CD system proposed in Chapter 4 in which the partner's device employs CRC to check the correctness of the received frame before making a decision of whether or not to forward the message. According to Eq. 4.20 in chapter 4, the approximate bit error probability of user 1 (P_{b1}), using quadrature phase shift keying (QPSK) modulation, is rewritten for high SNR as

$$P_{b1} = \frac{K_N}{4\bar{\gamma}_1\bar{\gamma}_{1,2}} + \frac{3}{4\bar{\gamma}_1\bar{\gamma}_2} - \frac{3K_N}{8\bar{\gamma}_1\bar{\gamma}_2\bar{\gamma}_{1,2}} \tag{7.1}$$

where $K_N = \sum_{n=1}^{N_S} \frac{1}{n}$ for N_S-symbols frame. The approximate bit error probability of user 2 (P_{b2}) can be similarly expressed. The average received SNR at the destination of

the signals from user 1 and user 2 are $\bar{\gamma}_1 = \sigma^2_{1,B}\frac{2E^S_{b1}}{N_0}$ and $\bar{\gamma}_2 = \sigma^2_{2,B}\frac{2E^R_{b2}}{N_0}$, respectively; and the average received SNR at user 1 of the signal from user 2 is $\bar{\gamma}_{1,2} = \sigma^2_{1,2}\frac{2E^S_{b1}}{N_0}$. The σ^2's are the variances of the respective Rayleigh fading channel coefficients which are defined as the average channel state information. E^S_{b1} and E^R_{b2} are respectively the energies spent by the source (user 1) and the relay (user 2) in transmitting one bit for user 1.

Using the QS-CD system, both the transmitting and relaying bit energy at the respective user should be equal in order to avoid power imbalance in the in-phase and quadrature signaling. This is not the situation in other *regenerate and forward* CD systems reported in the literature e.g., [47, 50, 51, 73].

7.1.2 Amplify and forward CD system

With the *amplify and forward* CD system, the partner amplifies the signal received from the sender and retransmits it to the destination. The *amplify and forward* CD system proposed in [49] is used here. Binary phase shift keying (BPSK) modulation is applied and each receiver accumulates channel state information and employs coherent detection. Each of the cooperating users is allocated different frequency bands (centered at f_1 and f_2) and, in each band, a user transmits signals in two time frames: one frame is dedicated for its own bits and the other is for relaying the partner's bits. According to Eq. (13) in [49], the approximate bit error probability of user 1 for high SNR can be written as

$$P_{b1} = \frac{3}{4\bar{\gamma}_1\bar{\gamma}_2} + \frac{3}{4\bar{\gamma}_1\bar{\gamma}_{1,2}}. \tag{7.2}$$

The approximate bit error probability of user 2 (P_{b2}) can similarly be expressed.

7.2 Optimal Power Allocation and Partner Location

Given the locations of the source and the relay, to satisfy the BEP requirements, the required power of the cooperating users depends on the quality of the interuser channel

and the user-to-destination channels. How to minimize the total power consumption for the pair by appropriate power allocation is still an open issue. We first derive the optimal power allocation (OPA) and equal power allocation strategies for a general CD system, and then substantiate the analysis by calculating the optimal powers for the *regenerate and forward* (QS-CD system) and the *amplify and forward* CD system in [49].

7.2.1 Power allocation for regenerate and forward CD system

Since power and energy are directly related, in what follows, we use the term power allocation even though the optimization problem is formulated as a minimization of the energy.

7.2.1.1 Optimal power allocation

In a practical situation, when a user must have the same power level for transmitting and relaying due to implementation concern of QS-CD system, the power allocation problem can be formulated as the following convex optimization problem:

$$\min\left(E_{c1}+E_{c2}\right) \tag{7.3}$$
$$s.t.\ P_{b1}(E_{c1},E_{c2})\leq\beta_1 \text{ and } P_{b2}(E_{c1},E_{c2})\leq\beta_2$$

where β_1 and β_2 are the maximum tolerable BEP for user 1 and user 2, respectively, $E_{b1}^S = E_{b2}^R = E_{c1}$, and $E_{b2}^S = E_{b1}^R = E_{c2}$. The optimization problem can be solved as follows. As mentioned earlier, the transmission power of the user is always a non-increasing continuous convex function of the relay power of its partner. For a given BEP, if E_{c1} is smaller, E_{c2} must be larger, and vice versa. As shown in Fig. 7.1, to guarantee $P_{b1}\leq\beta_1$ and $P_{b2}\leq\beta_2$, the energy levels of the two users should be in the intersection of the region above[1] the dotted and the solid curves which is shown as the shaded area. To

[1]When a point is "above" another point, we mean that the total energy consumption of the two users corresponding to the former one is higher.

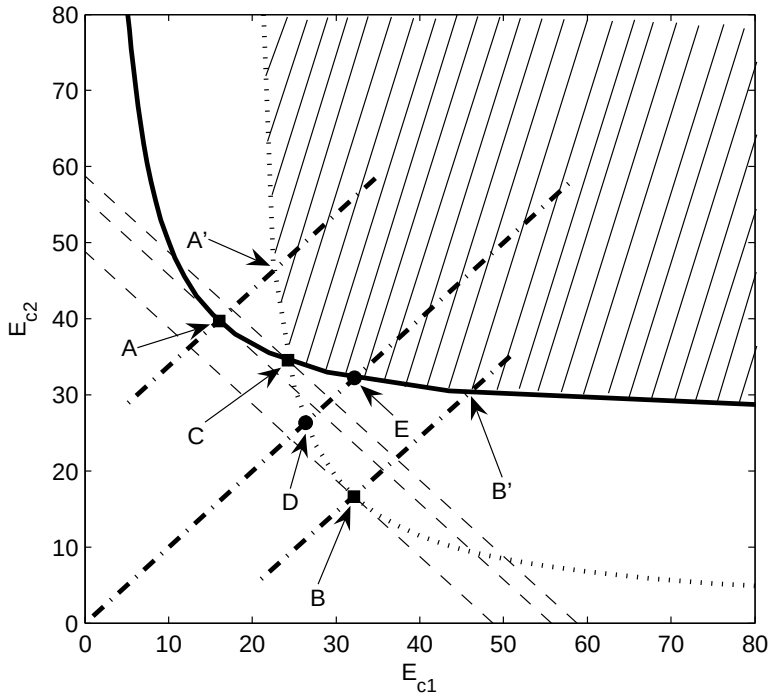

Figure 7.1: Power allocation problem of *regenerate and forward*

select the optimum operating point that minimizes the energy consumption $(E_{c1} + E_{c2})$ with the constraints $P_{b1} \leq \beta_1$ and $P_{b2} \leq \beta_2$, we should consider the following three cases.

Case I: The optimal operating point that satisfies $P_{b1} = \beta_1$ only is the tangent point of the dotted curve touched by the line with slope -1, i.e., point B in Fig. 7.1. This is because all the points on the line with slope -1 (dashed lines) correspond to the same value of $(E_{c1} + E_{c2})$, and all other points on the dotted curve have higher total energy levels than that of point B. If point B also satisfies $P_{b2} \leq \beta_2$, point B is the optimal solution for the OPA problem.

Case II: If the condition in case I is not satisfied, we can identify the optimal operating point to minimize the total energy with the constraint $P_{b2} = \beta_2$ only, which is the tangent

point of the solid curve touched by the line with slope -1, i.e., point A in Fig. 7.1. If point A also satisfies $P_{b1} \leq \beta_1$, point A is the optimal solution for the OPA problem.

Case III: if the conditions in both cases I and II are not satisfied, according to the following theorem, the two curves must intersect at a point which is the optimal operating point of the OPA problem.

Theorem 1 *Let point A (E_{c1}^A, E_{c2}^A) be the tangent point of $P_{b2}(E_{c1}, E_{c2}) = \beta_2$ (the solid curve in Fig. 7.1) touched by the line with slope -1, and B (E_{c1}^B, E_{c2}^B) be the tangent point of $P_{b1}(E_{c1}, E_{c2}) = \beta_1$ (the dotted curve in Fig. 7.1) touched by the line with slope -1. If $P_{b1}(E_{c1}^A, E_{c2}^A) > \beta_1$ and $P_{b2}(E_{c1}^B, E_{c2}^B) > \beta_2$, the two functions $P_{b1}(E_{c1}, E_{c2}) = \beta_1$ and $P_{b2}(E_{c1}, E_{c2}) = \beta_2$ must intersect at a point labeled C. C is located between the two parallel lines with slope 1, one passing through point A and the other passing through point B, and C is the optimal solution of the OPA problem in (7.7).*

Proof of Theorem 1 *The line passing through point A with slope 1 intersects the solid curve at point A' which must be above point A; otherwise, point A will satisfy the condition $P_{b1} \leq \beta_1$ (case I), which contradicts the condition of the theorem. The line passing through point B with slope 1 intersects the solid curve at point B' which must be above point B; otherwise, point B will satisfy the condition $P_{b2} \leq \beta_2$ (case II), which contradicts the condition of the theorem. Given $P_{b1}(E_{c1}, E_{c2}) = \beta_1$ and $P_{b2}(E_{c1}, E_{c2}) = \beta_2$ are continuous convex functions, AB' and BA' must intersect at one and only one point, i.e., point C. On the solid curve, from point A to point B', $E_{c1} + E_{c2}$ monotonically increases, and any point between A and C cannot satisfying $P_{b1}(E_{c1}, E_{c2}) \leq \beta_1$. Thus, C is the point with the minimum $E_{c1} + E_{c2}$ and satisfies both constraints, and it is the optimum solution.*

Using the proposed QS-CD system, (7.1) can be written as

$$E_{c2} = \frac{\left(12k_1k_2\sigma_{1,B}^2N_0^2E_{c1} - 3K_Nk_2N_0^3\right)}{\left(64k_1^2P_{b1}\sigma_{1,B}^6E_{c1}^2 - 8K_Nk_1N_0^2\sigma_{1,B}^2\right)}. \tag{7.4}$$

The coordinates of point B can be obtained by solving $\frac{\mathrm{d}E_{c2}}{\mathrm{d}Ec1} = -1$.

Similarly, for user 2,

$$E_{c1} = \frac{\left(12k_1k_2\sigma_{1,B}^2N_0^2E_{c2} - 3K_Nk_2N_0^3\right)}{\left(64k_1^2\sigma_{1,B}^6P_{b2}E_{c2}^2 - 8K_Nk_2N_0^2\sigma_{1,B}^2\right)}. \tag{7.5}$$

The coordinates of point A can be obtained by solving $\frac{\mathrm{d}E_{c1}}{\mathrm{d}E_{c2}} = -1$.

The coordinates of the intersection point of $P_{b1} = \beta_1$ and $P_{b2} = \beta_2$, point C, can be obtained from the solutions of a fifth order polynomial, obtained by substituting E_{c2} in (7.4) by the RHS of (7.5). The coordinates of points A, B and C can be solved numerically.

7.2.1.2 Equal power allocation

For the case of EPA, both users are transmitting at equal power level. This requires one more constraints to the OPA given above, and the optimization problem can be formulated as

$$\begin{aligned} &\min\left(E_{c1} + E_{c2}\right) \\ s.t.\ &P_{b1}(E_{c1}, E_{c2}) \leq \beta_1, P_{b2}(E_{c1}, E_{c2}) \leq \beta_2 \\ &\text{and } E_{c1} - E_{c2} = 0. \end{aligned} \tag{7.6}$$

As shown in Fig. 7.1, the shaded area can guarantee the BEPs of the pair of users, and the intersection point of the equal power line with the boundary of the shaded area, point E, corresponds to the optimal solution.

Using the QS-CD system, by substituting $E_{c1} = E_{c2}$ into (7.4) and (7.5), the coordinates of points D and E can be obtained, respectively. Between D and E, the point with the higher power level can satisfy both conditions $P_{b1} \leq \beta_1$ and $P_{b2} \leq \beta_2$, and it will be the optimal equal-power solution for the QS-CD system proposed in chapter 4.

Remarks: For *regenerate and forward* CD systems, if the user can have different power levels for transmission and relaying [47, 50, 51, 73], the optimization problem can be solved using the approach is in the next subsection for *amplify and forward* CD systems.

7.2.2 Power allocation for amplify and forward CD systems

7.2.2.1 Optimal power allocation

Let $E_{b_i}^S$ and $E_{b_i}^R$ be the energy spent by user i to transmit and relay a bit, respectively. For the *amplify and forward* CD system, the OPA problem is

$$\begin{aligned} &\min \left(E_{b1}^S + E_{b1}^R + E_{b2}^S + E_{b2}^R\right) \\ &s.t.\ P_{b1} \leq \beta_1 \text{ and } P_{b2} \leq \beta_2. \end{aligned} \tag{7.7}$$

Here, β_1 and β_2 are the maximum tolerable BEP for user 1 and user 2, respectively.

P_{b1} is a function of E_{b1}^S and E_{b2}^R, and P_{b2} is a function of E_{b2}^S and E_{b1}^R. Since each user can use different power levels for transmitting and relaying, E_{bi}^S and E_{bi}^R are independent of each other. Therefore, the optimization problem can be decomposed into two independent optimization problems

$$\begin{aligned} &\min \left(E_{b1}^S + E_{b2}^R\right) \\ &s.t.\ P_{b1}(E_{b1}^S, E_{b2}^R) \leq \beta_1, \end{aligned} \tag{7.8}$$

and

$$\begin{aligned} &\min \left(E_{b2}^S + E_{b1}^R\right) \\ &s.t.\ P_{b2}(E_{b2}^S, E_{b1}^R) \leq \beta_2. \end{aligned} \tag{7.9}$$

Notice that for a given BEP of a user, the transmission power of the user is always a non-increasing continuous convex function of the relay power of its partner, and vice

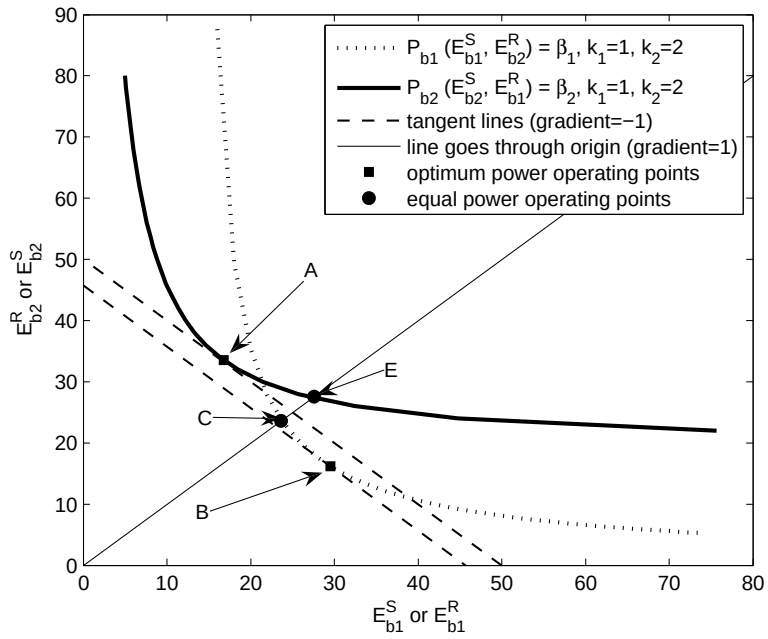

Figure 7.2: Power allocation problem of *amplify and forward*

versa, as shown in Fig. 7.2. To minimize the energy consumption $(E_{b1}^S + E_{b2}^R)$ with constraint $P_{b1} \leq \beta_1$, the optimal operating point is the tangent point of the dotted curve touched by the line with slope -1, i.e., point B in Fig. 7.2. This is because all the points on the line with slope -1 correspond to the same value of $(E_{b1}^S + E_{b2}^R)$, and all other points on the dotted curve have higher total energy level than that of point B. Similarly, the solution for problem (7.9) is the tangent point of the solid curve touched by the line with slope -1, i.e., point A in Fig. 7.2.

We verify this by using the *amplify and forward* CD system proposed in [49]. Let $k_1 = \frac{\sigma_{1,2}^2}{\sigma_{1,B}^2}$ and $k_2 = \frac{\sigma_{2,1}^2}{\sigma_{2,B}^2}$. Because of the broadcast nature of the channel, $\bar{\gamma}_{1,2} = k_1\bar{\gamma}_1$ and $\bar{\gamma}_{2,1} = k_2\bar{\gamma}_2$. Furthermore, $\sigma_{2,B}^2 = \frac{k1}{k2}\sigma_{1,B}^2$ because of the reciprocity of the interuser channel ($\sigma_{1,2}^2 = \sigma_{2,1}^2$). The minimal relay power can be obtained as a function of the

transmission power and the required BEP:

$$E_{b2}^{R} = \frac{3k_2 N_0^2 E_{b1}^{S}}{\left(16k_1 P_{b1}\sigma_{1,B}^4 (E_{b1}^{S})^2 - 3N_0^2\right)}. \tag{7.10}$$

By solving $\frac{\mathrm{d}E_{b2}^{R}}{\mathrm{d}E_{b1}^{S}} = -1$, the optimal solutions of E_{b1}^{S} and E_{b2}^{R} can be written as

$$E_{b1}^{S} = \frac{N_0}{\sigma_{1,B}^2}\left(\frac{6+3k_2+\sqrt{9k_2^2+72k_2}}{32k_1 P_{b1}}\right)^{1/2} \text{ and} \tag{7.11}$$

$$E_{b2}^{R} = \left(\frac{2k_2}{k_2+\sqrt{k_2^2+8k_2}}\right)\frac{N_0}{\sigma_{1,B}^2} \tag{7.12}$$

$$\times\left(\frac{6+3k_2+\sqrt{9k_2^2+72k_2}}{32k_1 P_{b1}}\right)^{1/2}. \tag{7.13}$$

Similarly, for user 2,

$$E_{b1}^{R} = \frac{3k_1 k_2 N_0^2 E_{b2}^{S}}{\left(16k_1^2 P_{b2}\sigma_{1,B}^4 (E_{b2}^{S})^2 - 3k_2 N_0^2\right)}. \tag{7.14}$$

By solving $\frac{\mathrm{d}E_{b1}^{R}}{\mathrm{d}E_{b2}^{S}} = -1$, the optimal solutions of E_{b2}^{S} and E_{b1}^{R} can be written as

$$E_{b2}^{S} = \frac{N_0}{\sigma_{1,B}^2}\left(\frac{6k_2+3k_1k_2+\sqrt{9k_2^2k_1^2+72k_2^2k_1}}{32k_1^2 P_{b1}}\right)^{1/2} \tag{7.15}$$

and

$$E_{b1}^{R} = \left(\frac{2k_1}{k_1+\sqrt{k_1^2+8k_1}}\right)\frac{N_0}{\sigma_{1,B}^2}\times \tag{7.16}$$

$$\left(\frac{6k_2+3k_1k_2+\sqrt{9k_2^2k_1^2+72k_2^2k_1}}{32k_1^2 P_{b1}}\right)^{1/2}. \tag{7.17}$$

7.2.2.2 Equal power allocation

To maximize the lifetime of the cooperative pair in static networks, equal power allocation is preferred. Since energy usage level of both users are the same, we should add

another constraint to the OPA. The optimization problem with equal power constraints can be formulated as

$$\begin{aligned} &\min \left(E_{b1}^{S}+E_{b2}^{R}\right) \\ s.t.\ &P_{b1}(E_{b1}^{S},E_{b2}^{R}) \leq \beta_1 \text{ and } E_{b1}^{S}-E_{b2}^{R}=0, \end{aligned} \tag{7.18}$$

and

$$\begin{aligned} &\min \left(E_{b2}^{S}+E_{b1}^{R}\right) \\ s.t.\ &P_{b2}(E_{b2}^{S},E_{b1}^{R}) \leq \beta_2 \text{ and } E_{b2}^{S}-E_{b1}^{R}=0. \end{aligned} \tag{7.19}$$

Obviously, for (7.18), the optimal operating point is the intersection of the equal power line (the line with slope 1 and passing through the origin) and the dotted curve, i.e., point C in Fig. 7.2. For the CD system in [49], the optimal solution is given by

$$E_{b1}^{S}=E_{b2}^{R}=\sqrt{\frac{3N_0^2(1+k_2)}{16k_1P_{b1}\sigma_{1,B}^4}} \tag{7.20}$$

For (7.19), the intersection point D in Fig. 7.2 corresponds to the optimal solution given by

$$E_{b2}^{S}=E_{b1}^{R}=\sqrt{\frac{3N_0^2k_2(1+k_1)}{16k_1^2P_{b2}\sigma_{1,4}^4}} \tag{7.21}$$

7.2.3 Optimal partner location

To facilitate the derivation of the matching algorithm, we study the location of the optimal partner based on OPA. It is trivial to prove that the optimal partners' locations which maximize the cooperative energy gain of the pair and minimize the power consumption rate of the user are both on the line connecting the source and the destination (BS). Therefore, in the following, we determine the optimal locations of the partners in the one-dimensional line segment between the source and the destination.

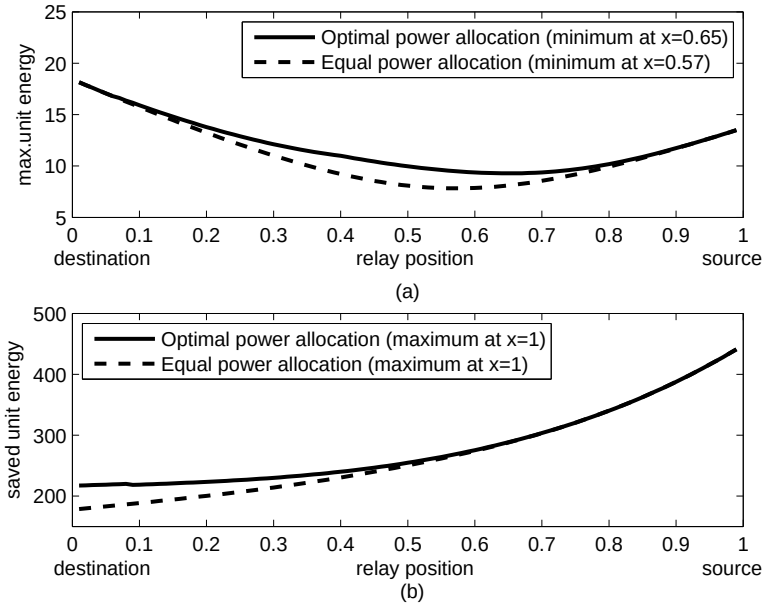

Figure 7.3: 1-D analysis of *regenerate and forward* CD Scheme

Assume that the average CSI is proportional to the respective distance raised to the power α, i.e., $\sigma_{1,B}^2 \propto d_{1,B}^{-\alpha}$, $\sigma_{2,B}^2 \propto d_{2,B}^{-\alpha}$ and $\sigma_{1,2}^2 \propto d_{1,2}^{-\alpha}$, where the path loss exponent α takes the value between 2 to 6. Define *maximum unit energy*$= \max\{E_{b1}^S, E_{b2}^S, E_{b1}^R, E_{b2}^R\}$, and *saved unit energy* $= E_{b1} + E_{b2} - E_{b1}^S - E_{b2}^S - E_{b1}^R - E_{b2}^R$. Consider a pair of users, user 2 is located on the line between the BS and user 1. By substituting $P_{b1} = P_{b2} = 10^{-3}$, $B = 128$, $N_0 = 1$ unit power/Hz, the CSIs in terms of normalized distance, and $\alpha = 3$, we demonstrate the trends of *maximum unit energy* and *saved unit energy* for the CD systems with OPA and EPA, respectively.

In Figs. 7.3 and 7.4, the x-axis represents the location of the partner, while the destination is located at $x = 0$, and the source is located at $x = 1$ (the source-destination distance is normalized to one unit). The y-axis of Fig. 7.3(a) represents the *maximum unit energy* of the pair with the *regenerate and forward* CD system, and the optimal location of the partner for minimizing the energy consumption of the source are $x = 0.65$ and $x = 0.57$ for OPA and EPA, respectively. Fig. 7.3(b) shows that the *saved unit energy* of

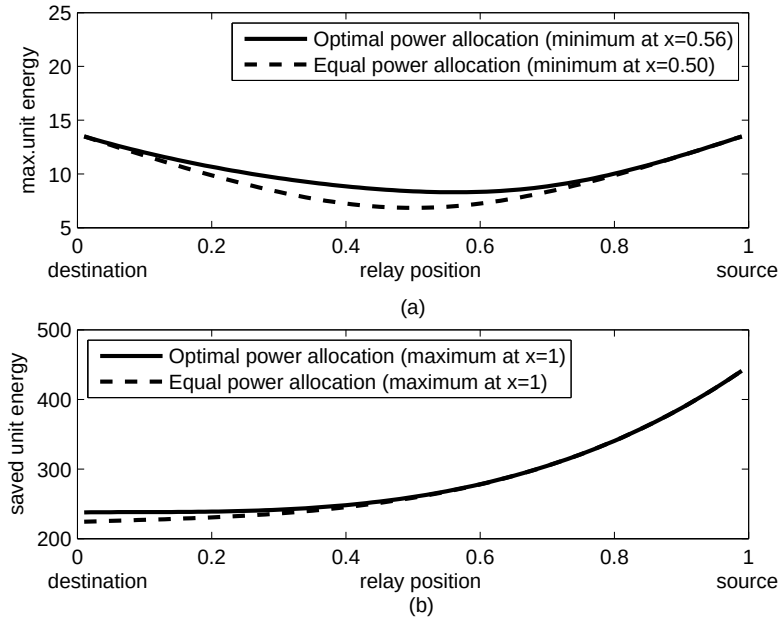

Figure 7.4: 1-D analysis of *amplify and forward* CD system

the cooperative pair for both power allocation systems is maximized when $x = 1$. From a user's point of view, its optimal partner's location is close to the mid-point between itself and the destination; on the other hand, to maximize the total energy saving for the pair of users, the two users should be collocated. As shown in Fig. 7.4(a) for the case of *amplify and forward* CD system, *maximum unit energy* is minimized when $x = 0.58$ and $x = 0.50$ for OPA and EPA, respectively, and the behavior of *saved unit energy* in Fig. 7.4(b) is similar to that of the *regenerate and forward* based CD system.

A two dimensional plot of cooperative region of both *amplify and forward* and *regenerate and forward* systems, considering the source's gain, is shown in Figs. 7.5 and 7.6, respectively. The solid curves in the figures correspond to the case with OPA, and the dotted curves correspond to the case with EPA. It can be seen that the OPA enlarges the cooperative region contour with fixed CD gain for the pair, especially when the partner is far away from the source, and their optimal power levels are quite different. The contours

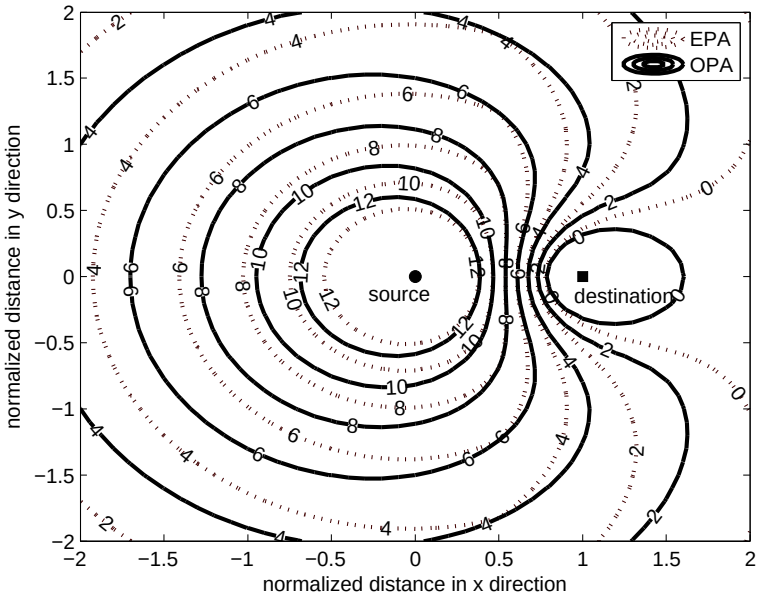

Figure 7.5: Cooperative region of *regenerate and forward* system for both power allocation

of the cooperative region in these figures can help to locate the best partner of any user and to explain the numerical results presented in section 7.4.

7.3 Improved WLF Matching Algorithm

A worst-link-first matching algorithm which maximizes the total energy gain of the pair (WLF-MaxGain) is proposed in Chapter 6. The WLF-MaxGain algorithm gives the user with the worse channel condition and higher energy consumption rate a higher priority to choose its partner. The computational complexity of the WLF-MaxGain algorithm is $O(n^2)$. The WLF-MaxGain algorithm performs better than the Greedy matching algorithm in [62] for mobile networks, while exhibiting similar performance in static net-

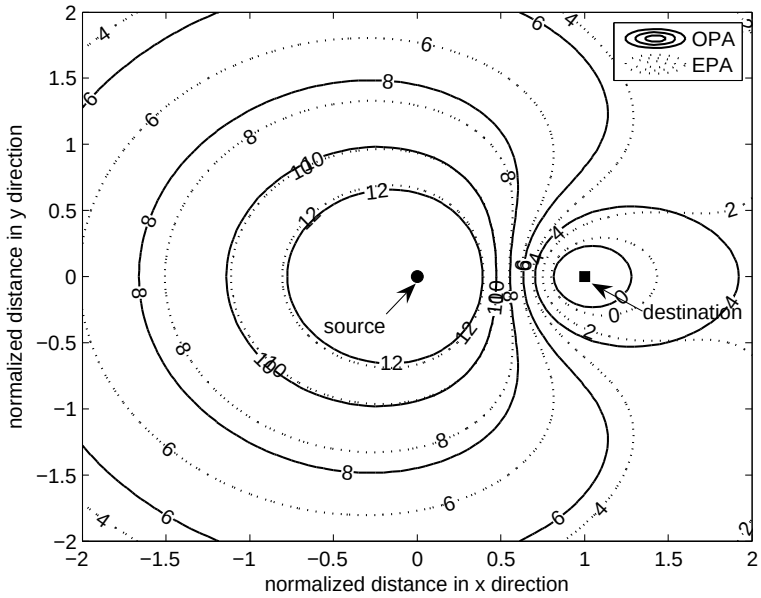

Figure 7.6: Cooperative region of *amplify and forward* system for both power allocation

works.

For the cases of MW and WLF-MaxGain, the weight of a pair of users is the energy saved by cooperation between users i and j over no cooperation. If there is no energy saved, the two users will just use the non-cooperative scheme, and the weight of the edge linking them is zero. Thus, the weight is always non-negative, and a positive weight represents the energy gain of cooperation over no cooperation.

The question is whether using the energy gain of a pair as the weight is the best choice for WLF matching or not. Consider a scenario with four users: users u_1 and u_2 be collocated at the point $x = 1$, and users u_3 and u_4 be collocated at $x = 0.5$. According to Fig. 7.4, with the WLF-MaxGain, u_1 and u_2 will be grouped since the energy saved by them, $w(e_{1,2}) \approx 440$ units, is the maximum among all pairs ($w(e_{1,3})$, $w(e_{1,4})$, $w(e_{2,3})$, $w(e_{2,4})$, and $w(e_{3,4})$), and u_3 and u_4 will be grouped thereafter. The total energy saved by the two pairs is around $440(1 + 0.5^{\alpha}) = 495$ units. If u_1 is grouped with u_3, and u_2

is grouped with u_4, the total energy saved is around $265 \times 2 = 530$ units. Therefore, maximizing the energy saved by a pair does not lead to maximizing the energy saved in the network. Motivated by this example, we propose to use the maximum energy spent by the pair of users as a weight for matching, and we refer to this scheme as WLF-MinMaxEnergy matching. The WLF-MaxGain matching algorithm is given in Table 7.1.

Table 7.1: WLF-MinMaxEnergy Matching Algorithm:

1. The BS selects an unmatched user i with the worst channel quality among all unmatched users.

2. The BS selects an unmatched user j such that $\max(E_{bi}^S + E_{bi}^R, E_{bj}^S + E_{bj}^R)$ is minimized among all $\max(E_{bi}^S + E_{bi}^R, E_{bk}^S + E_{bk}^R)$, where k is an unmatched user other than i.

3. Repeat steps 1) and 2) until the number of unmatched users is less than two.

The numerical results in the next section demonstrate that the performance of the WLF-MinMaxEnergy algorithm is very close to that of the optimal MW matching algorithm, and it outperforms the WLF-MaxGain algorithm by a large margin.

Since WLF-MaxGain tends to maximize the energy saving by a pair of users, not necessary the energy saving by the user with the worst link according to the results in sub section 7.2.3, we use the maximum energy spent by the cooperating users as the weight, $w(e_{i,k})$. The matching algorithm of WLF-MinMaxEnergy is similar to that of WLF-MaxGain, except that the weights used for the pair of users being matched in step 2) are different: The BS selects an unmatched user j such that $\max(E_{bi}^S + E_{bi}^R, E_{bj}^S + E_{bj}^R)$ is minimized among all $\max(E_{bi}^S + E_{bi}^R, E_{bk}^S + E_{bk}^R)$, where k is an unmatched user other

than i. Both the WLF-MaxGain and WLF-MinMaxEnergy algorithms have computational complexity of $O(n^2)$. In step (2) of both algorithms, if it is difficult to obtain the instantaneous interuser channel condition, the BS can use the location information and the cooperative region obtained in the previous section to choose the best partner for the user. In addition, the WLF algorithms can potentially be implemented in a distributed manner: each user chooses its desired partner; if there is any conflict, the user far away from the BS (or has worst channel condition to the BS) has a higher priority. The unpaired users will continue to choose their desired partners from the remained unpaired users, and the procedure repeats till we cannot pair any users among the remaining unpaired ones.

It is easy to prove that the distributed WLF matching result is stable. First, the algorithm terminates with at most $\lfloor N_U/2 \rfloor$ iterations, since each iteration will result in at least one pair. Second, for any unpaired user, it cannot break the existing pairs since at least one user of any existing pair has higher priority than the unpaired user. Third, for any two pairs of users, (u_{11}, u_{12}) and (u_{21}, u_{22}), they cannot exchange partners. Without loss of generality, we assume u_{i1} has higher priority than u_{i2} for $i = 1, 2$, and u_{11} has higher priority than u_{21}. Since u_{11} has the highest priority among all users, it can choose its desired partner u_{12}, and no other users can choose u_{12}. Thus, the matching is stable.

7.4 Numerical Results

We present the numerical results of the three matching algorithms with the OPA and the EPA for both CD schemes in a network. We simulate a wireless network where the coordinates of the BS are $(0, 0)$. N_U users are randomly placed on a unit disk centered at the BS as given in Fig. 6.1. Both the interuser channels (channels between two users) and the channel between a user and the BS are assumed to have quasi-static flat Rayleigh fading. We assume that the BS can track the user locations, and thus estimate their pair-

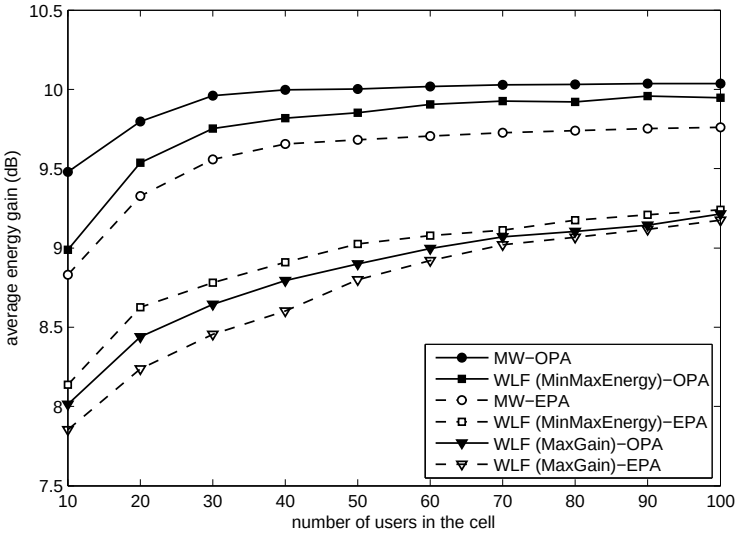

Figure 7.7: Average energy gain, G_E, of *regenerate and forward* schemes for both OPA and EPA

wise distances and average CSIs which are inversely proportional to d^{α}. By substituting $\beta_1 = \beta_2 = 10^{-3}$, $N_S = 128$, $N_0 = 1$ unit power/Hz and $\alpha = 3$, the average energy required for no cooperation and with cooperation are calculated. Matching is performed by the BS according to the N_U^2 weights, and the users will be grouped according to the matching results. The weights used in the MW and WLF-MaxGain matching algorithms are the cooperative diversity energy gains of each pair of users using the OPA strategy; and the weights used in the WLF-MinMaxEnergy matching algorithm are the maximum energy levels of the pair of cooperative users. Since cooperation is not always beneficial, a pair can choose not to cooperate if there is no cooperative diversity energy gain for them, and they communicate with the BS using a conventional non-cooperative scheme. Cell cooperative diversity gain, which is the energy gain of a cell with user cooperation over a cell without user cooperation, is defined as in Chapter 6

$$G_E = 10 \log_{10} \left(\frac{\sum_{i=1}^{N_U} E_{bi}^{no}}{\sum_{i=1}^{N_P} (E_{bi}^{S} + E_{bi}^{R}) + \sum_{i=N_P+1}^{N_U} E_{bi}^{no}} \right), \tag{7.22}$$

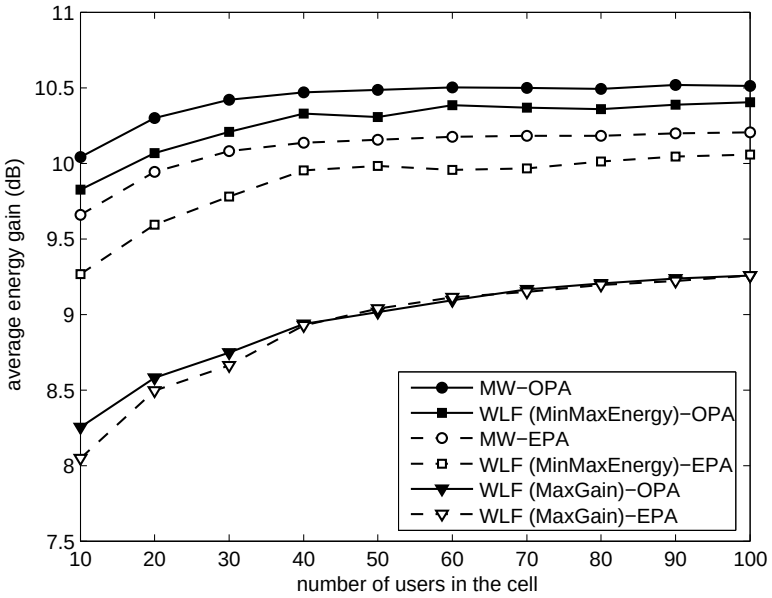

Figure 7.8: Average energy gain, G_E, of *amplify and forward* scheme for both OPA and EPA

where the first N_P users are paired to have cooperation and the remaining $(N_U - N_P)$ users have no partners. Since $\sum_{i=1}^{N_U} E_{bi}^{no}$ is a constant independent of matching, G_E is maximized when $\sum_{i=1}^{N_P}(E_{bi}^{S} + E_{bi}^{R})$ is minimized. Different user deployments are generated by using different random seeds. We vary the number of active users in the network from 10 to 100 in order to consider both the low-density and high-density scenarios. The average energy gain vs. number of users is shown in Figs. 7.7 and 7.8 for both *regenerate and forward* and *amplify and forward* CD schemes, respectively.

In the figures, the solid curves are those with OPA and the dotted curves are those with EPA. Both figures show that with the MW or WLF-MinMaxEnergy matching algorithms, the OPA can enhance the total energy gain by about 0.5 dB to 1 dB (or around 10% to 25% improvement) over EPA. The gap for the *regenerate and forward* CD scheme is larger than that for the *amplify and forward* CD scheme.

With the WLF-MaxGain matching algorithm, the difference in performance between the two power allocation schemes is negligible, especially when the number of users in the cell is large. This is because, with the WLF-MaxGain algorithm, the BS tends to choose a partner close to the user for cooperation to maximize their cooperative energy gain. When the two users are close, their OPA result is similar to that of EPA.

On the other hand, the figures show that the performance of the WLF-MinMaxEnergy is close to that of the optimal MW matching algorithm, when the OPA scheme is used. For the *amplify and forward* CD scheme, the performance of WLF-MinMaxEnergy with the EPA is much worse. This is because the BS tends to choose a partner sitting close to the mid-point between the user and the BS, and the results with EPA and OPA are quite different. The numerical results also demonstrate that the WLF-MaxGain performs much worse than the WLF-MinMaxEnergy, as shown in Figs. 7.7 and 7.8. Furthermore, the average G_E increases with the number of users in the low user density region and saturates in the higher user density region.

7.5 Summary

We have derived optimal power allocation strategies for both the *regenerate and forward* and the *amplify and forward* CD schemes, with and without the equal power allocation constraint, and studied the optimal location of a partner. Based on the analytical results, we have also proposed a non-bipartite stable matching algorithm that can achieve close to optimal cooperative diversity gain in a wireless cellular network. We have demonstrated the effectiveness and the efficiency of the proposed WLF-MinMaxEnergy matching algorithm using the optimal power allocation strategy. It is shown that a $9 \sim 10$ dB cooperative diversity gain can be achieved, which is equivalent to prolonging the cell phone battery recharge time by about 10 times.

In addition, the numerical results demonstrate the importance of the combination

of power allocation and partner selection. In order to achieve high energy gain for the cell, the combination of OPA with the WLF-MinMaxEnergy matching algorithm is more desirable from an implementation point of view.

Chapter 8

Conclusions and Future Work

In this chapter, the dissertation is concluded by summarizing the contributions and proposing the future research directions.

8.1 Summary of Contributions

8.1.1 Quadrature Signaling based CD Systems

Firstly, an energy and power efficient *fixed regenerate and forward* quadrature signaling based cooperative diversity (QS-CD) system has been proposed. Secondly, an *adaptive regenerate and forward* QS-CD system to send M-QAM signals is proposed and analyzed. Both QS-CD systems can easily be switched between the cooperative and the non-cooperative modes of operation. The bit error performance of both QS-CD systems can be improved when the interuser channel signal strength increases and the proposed scheme can achieve maximum diversity order of two. In addition, the cooperation is beneficial not only for a user far from the BS but also for a user near the BS. In contrast to a fixed QS-CD system, the adaptive QS-CD system with the expense of additional

signaling performs better than an NCD system even when the interuser channel is worse than the user-to-BS channel. Notably, the QS-CD system is less complex and easy to implement compared with the existing CD systems in the literature.

8.1.2 QS-CD-ARQ System

We have introduced a generalized framework for analyzing the performance of adaptive relaying schemes in CD-ARQ systems. The framework is applied to our QS-CD system and compared with existing CD-ARQ schemes in the literature such as SC-CD-ARQ and DSTBC-CD-ARQ. The performance of the CD-ARQ schemes is studied and the complexity of the schemes is discussed. It is shown that our QS-CD-ARQ outperforms other schemes when the sender is cooperating with a partner who provides a good sender-to-partner and partner-to-destination link. From the implementation point of view, QS-CD-ARQ is more favorable since radio resources can be allocated for long duration and the partner does not need to be aware of the ARQ.

8.1.3 WLF Matching Algorithm

We have studied the energy gain provided by four matching algorithms, the MW, Greedy, random, and the proposed WLF-MaxGain matching algorithms, with computational complexity of $O(N_U^3)$,$O(N_U^2 \log N_U)$, $O(N_U)$, and $O(N_U^2)$, respectively, for both fixed and adaptive CD systems. We have further proposed how to optimally match mobile users considering user mobility. It is shown that by intelligently applying user mobility information in the matching algorithm, high energy gain is achievable with moderate overhead in mobile networks. In addition, our study provides insights into the tradeoff between matching overhead and energy gain in a wireless network, which is an important step toward practically deploying CD systems in wireless networks. Moreover, the adaptive CD system outperforms the fixed CD system by 1-2 dB.

8.1.4 Joint Power Allocation and Partner Selection

We have derived optimal power allocation strategies for both the *regenerate and forward* and the *amplify and forward* CD schemes, with and without the equal power allocation constraint, and studied the optimal location of a partner. By jointly considering the power allocation and matching, the modified WLF matching algorithm, referred to WLF-MinMaxEnergy, can achieve close-to-optimal cooperative diversity gain in a wireless network. We have demonstrated the effectiveness and the efficiency of the proposed WLF-MinMaxEnergy matching algorithm using the optimal power allocation strategy. It is shown that a $9 \sim 10$ dB cooperative diversity gain can be achieved, which is equivalent to prolonging the cell phone battery recharge time by nearly 10 times. In addition, the numerical results demonstrate the importance of the combination of power allocation and partner selection. In order to achieve high energy gain for the cell, the combination of OPA with the WLF-MinMaxEnergy matching algorithm is more desirable to implement.

8.2 Future Work

Even though several research contributions has been made in this dissertation for cooperative communication systems, there are a number of research topics need to be explored as extensions of this work.

8.2.1 Interuser Channel Estimation of QS-CD Systems

In this thesis, the channel state information is assumed to be available at the respective receivers. For implementation, the channel should be estimated using training and pilot symbols. Since the cooperative communication systems are more vulnerable to interuser communication errors, the interuser channel estimation errors degrades the overall system performance. The proposed QS-CD system has an advantage in interuser channel

estimation by utilizing the previously transmitted frame of symbols as training symbols. It gives the practical importance to QS-CD system. In this topic, we would like to study the closeness of the estimated channel to the perfect channel and the performance of the QS-CD system with channel estimation.

8.2.2 Wideband Communication Systems

We consider a narrowband wireless communication system which implies that the channel is assumed as frequency flat fading. But, most of the current communication system are experiencing frequency selective channels due to high data rate (wide band system). Therefore, the proposed QS-CD system should accommodate the techniques such as frequency domain equalization (FDE), orthogonal frequency division multiplexing (OFDM), rake receivers, etc., to mitigate the frequency selectivity. In this context, performance study, power allocation, partner selection and other aspects of CD system could be re-investigated.

8.2.3 Spread Spectrum System

In the proposed QS-CD system, multiple access techniques such as time division multiple access (TDMA) and frequency division multiple access (FDMA) has been taken into account. The QS-CD system has limited direct application to CDMA system due to the half-duplex constraint. This problem can be overcome by allocating two frequency band instead of one for a cell of the CDMA system. So, a user belonging to frequency band 1 can listen to the partner from frequency band 2 while the user is transmitting in the uplink and vice-versa. To implement the proposed cooperative CDMA system the following two aspects need to be addressed: (i) What is the tradeoff between the spreading gain versus cooperative diversity gain? (ii) How to assign users for each sub-band? In addition, well known challenges such as power allocation, multiple access interference cancellation,

multiuser detection, etc. of the CDMA systems need to be explored.

8.2.4 Partner Selection With Partial Side Information

In Chapters 6 and 7, the partner selection algorithms assumed that the global side information (interuser CSIs, user-to-BS CSIs, requested power, etc.) of users is available at the BS. In reality, for example, estimating all interuser channels is not feasible. It would be of practical importance to investigate the partner selection with partial side information. We found that our proposed WLF algorithm is a potential candidate for this scenario and it could be integrated with the channel estimation techniques. This is a rich area for future research.

8.3 Final Remarks

In this dissertation, our main objective is to propose a cooperative diversity system with minimal modification over existing point-point communication system. The proposed QS-CD and WLF matching consider practical implementation problems and provide near optimal performance such that the QS-CD system achieves full diversity order available and the WLF yields performance close to the optimal MW algorithm. The approaches and frameworks proposed in this thesis such as power allocation framework, optimization approach, non-bipartite matching problem formulation and Markov modeling of cooperative channels, are not restricted to QS-CD systems and can be utilized to analyze other CD systems as well.

Appendix A

List of Abbreviations

2I1O	Two-input and one-output
ACK	Acknowledgement
ARQ	Automatic repeat request
BEP	Bit error probability
BFSK	Binary frequency shift keying
BPSK	Binary phase shift keying
BS	Base station
CD	Cooperative diversity
CDMA	Code division multiple access
CDF	Cumulative distribution function
CRC	Cyclic redundancy checksum
CSI	Channel state information
dB	Decibel
dMRC	Differential maximum ratio combining
dSNR	Differential signal-to-noise-ratio
DSTBC	Distributed space-time block coding
DSTC	Distributed space-time coding

EGC	Equal gain combining
EPA	Equal power allocation
FDE	Frequency domain equalization
FDMA	Frequency division multiple access
FEP	Frame error probability
GSM	Global system for mobile communications
I-PAM	I-ary pulse amplitude modulation
ISNR	Interuser signal-to-noise-ratio
LLR	Log-likelihood ratio
M-QAM	M-ary quadrature amplitude modulation
MAP	Maximum a posteriori
MaxGain	Maximizing gain
MIMO	Multiple input and multiple output
MinMaxEnergy	Minimizing maximum energy
MISO	Multiple input and single output
ML	Maximum likelihood
MMS	Multimedia message services
MRC	Maximum ratio combining
MW	Maximum weighted
NAK	Negative acknowledgement
NCD	Non-cooperative diversity
OFDM	Orthogonal frequency division multiplexing
OFDMA	Orthogonal frequency division multiple access
OPA	Optimal power allocation
PDF	Probability density function
PEP	Pairwise error probability
PLR	Packet loss rate
PSK	Phase shift keying

PSA	Partner selection algorithm
QoS	Quality of service
QPSK	Quadrature phase shift keying
QS	Quadrature signaling
RCPC	Rate compatible punctured code
RCPT	Rate compatible turbo code
SC	Selection Combining
SEP	Symbol error probability
SINR	Signal-to-interference-plus-noise-ratio
SNR	Signal-to-noise-ratio
STBC	Space-time block code
STC	Space-time code
TDMA	Time division multiple access
UWB	Ultra wideband
WLAN	Wireless local area network
WLF	Worst link first

Appendix B

List of Symbols

$\lfloor . \rfloor$	Integer which is greater than or equal to its argument
$[.]^*$	Complex conjugate transpose operator
$[.]^T$	Transpose operator
$\|.\|$	Amplitude operator
${}_2F_1(.,.;.;.)$	Gauss hypergeometric function
$a_i(.)$	I-PAM symbols of user i
$\bar{a}_i(.)$	I-PAM symbols of user i which is reproduced at the partner
$\tilde{a}_i(.)$	I-PAM symbols of user i which is detected at the BS
$\arg\min$	Argument which gives minimum
$b_i(.)$	BPSK symbol transmitted by user i
$\hat{b}_i(.)$	Detected BPSK symbol at BS of user i
$\check{b}_i(.)$	Soft decision of the BPSK symbol transmitted by user i at the partner
$\tilde{b}_i(.)$	Soft decision of the BPSK symbol transmitted by user i at the BS
$\bar{b}_i(.)$	Regenerated BPSK symbol at the partner which is transmitted by user i

c	Velocity of light
d_0	Reference distance
$d_{i,B}$	Distance between user i and BS
$d_{i,j}$	Distance between user i and user j
$dSNR_i$	Differential SNR
$E\{\}$	Expectation operator
E_b	Bit energy spent by each user in NCD
E_{bi}	Bit energy spent by user i in NCD
E_{ci}	Bit energy spent by user i when source and relaying bits have equal energy
E_{bi}^R	Bit energy spent for relaying bit at user i when cooperating
E_{bi}^S	Bit energy spent for source's bit at user i when cooperating
$e_{i,j}$	Edge between user i and user j
exp	exponential function
f_c	Carrier frequency
f_d	Doppler frequency
$f_{i,B}$	Doppler frequency shift of user i at the BS
$f_{i,j}$	Doppler frequency shift of user i at user j
$\mathcal{G} = \{\mathcal{V}, \mathcal{E}\}$	A graph, where $\mathcal{V}$ is a set of vertices and $\mathcal{E} \subseteq \mathcal{V} \times \mathcal{V}$ is a set of edges between vertices
G_c	Coding gain
G_d	Diversity gain
G_{cd}	Cooperative diversity energy gain
G_E	Energy gain of the network with cooperative over that without cooperation (in dB)
$G_{i,j}$	Energy gain of cooperation between users i and j
$\mathbf{H}$	Channel matrix
h_0	Fading coefficient of the channel from sender to reference point

$h_{i,B}(.)$	Fading coefficient of the channel from user i to BS
$h_{i,j}(.)$	Fading coefficient of the channel from user i to user j
$\Im\{Z\}$	Imaginary part of complex number Z
I_ν	ν^{th} order modified Bessel function
$J_0(.)$	Zeroth order Bessel function first kind
m_C	Nakagami fading figure of the combined channel
$m_{i,B}$	Nakagami fading figure of the channel between user i and BS
$m_{i,j}$	Nakagami fading figure of the channel between user i and user j
n	Discrete time index
N_0	Noise power spectral density
$N_{e\|m}$	Number of symbol errors in a frame due to error in the m^{th} bit of the symbol
N_f	Number of frames in a packet
N_r^{max}	Maximum number of re-try
N_P	Total number of users paired in a cell
N_S	Number of symbols in a frame
N_U	Total number of active users in a cell
$P(.)$	Probability operator
$p(.)$	Probability density function
$p(.,.)$	Joint probability density function
P_{bi}	BEP of user i
$P_{dMRC}^c(.)$	Average BEP of dMRC
P_{dMRC}^L	Lower bound of average BEP of dMRC
P_e	Average BEP of the CD system
P_e^c	Instantaneous or conditional BEP of the CD system
P_e^L	Lower bound of BEP of the CD system
P_{FEP}	Interuser frame error probability
$P_{i,j}$	BEP at user j for the transmission from user i

P_{MRC}	Average BEP of MRC
$P^{c}_{MRC}(.)$	Instantaneous BEP of MRC
P_{NC}	BEP of the con-cooperative system
P_{NH}	BEP of the system when no help from partner
$Q(.)$	Complementary error function
q_{GG}, q_{GB}, q_{BG} and q_{BB}	State transition probabilities of two state (BAD and GOOD) Markov chain
$\Re\{Z\}$	Real part of complex number Z
R	Radius of the cell centered at the BS
$\mathbf{r}$	Received signal vector
$r_{C,k}(.)$	k^{th} multipath branch of the combined signal
$R_{i,B}$	Normalized distance between user i and BS
$r_{i,B}(.)$	Received signal at the BS from user i
$R_{i,j}$	Normalized distance between user i and user j
$r_{i,j}(.)$	Received signal at user j from user i
$r_{i,B,k}(.)$	k^{th} multipath branch of the signal received at BS from user i
$\mathcal{S}$	A *matching* subset of $\mathcal{E}$ if no two edges in $\mathcal{S}$ share the same vertices
$S(.)$	State of a Markov chain
$sign$	Sign function
$S_C(.)$	State of the Markov model of the combined channel
S_I	Set of I-PAM information symbols
$s_i(.)$	Signal transmitted by user i
$S_{i,j}(.)$	State of the Markov model of the channel from user i to user j
$S_{i,B}(.)$	State of the Markov model of the channel from user i to BS
SNR_T	SNR threshold
T	The period of matching algorithm being executed
$\mathbf{T}$ and $\bar{\mathbf{T}}$	Transition probability matrix of the Markov chain
t	Time instant

T_f	Frame duration
T_S	Symbol duration
v	Velocity of the user
$V_{\max}$	The max velocity of mobile users
V_{norm}	The normalized max velocity of mobile users
$w(e_{i,j})$	The energy gain by cooperation between the two users i and j over no cooperation
X	Transmitted frame
$\hat{X}$	Received frame
α	Path loss coefficient
β_i	Maximum tolerable BEP of user i
$\Gamma(.)$	Gamma function
γ	Effective SNR at the receiver
$\gamma(.,.)$	Incomplete Gamma function
γ_0	SNR at reference point for sender's transmission
γ_i	SNR at BS for user i's transmission
$\gamma_{i,j}$	SNR at user j for user i's transmission
$\bar{\gamma}_i$	Average SNR at BS for user i's transmission
$\bar{\gamma}_i^{nc}$	SNR at BS for user i's non-cooperative transmission
$\bar{\gamma}_{i,j}$	Average SNR at user j for user i's transmission
Δ	Signal threshold
$\eta_{i,B}(.)$	Noise picked at the BS while receiving signal from user i
$\eta_{i,j(.)}$	Noise picked at user j while receiving signal from user i
Θ	Indicator of decoding error
ξ	Channel efficiency
ζ	Throughput
π_G	Steady state probability of being in GOOD state
π_B	Steady state probability of being in BAD state

ρ	Correlation coefficient
$\rho_{i,B}$	Correlation coefficient of the channel from user i to BS channel
$\rho_{i,j}$	Correlation coefficient of the channel from user i to user j
ρ_C	Correlation coefficient of the combined channel
$\sigma^2_{i,B}$	Variance of the fading channel coefficient for the channel from user i to BS
$\sigma^2_{i,j}$	Variance of the fading channel coefficient for the channel from user i to user j
$\phi_\gamma(j\omega)$	Characteristics function of γ
Ω	Nakagami fading signal power
$\Omega_{i,B}$	Nakagami fading signal power of the channel from user i to BS
$\Omega_{i,j}$	Nakagami fading signal power of the channel from user i to user j
Ω_C	Nakagami fading signal power of the combined channel

Bibliography

[1] L. Zhao and J. W. Mark, “Multistep closed-Loop Power control Using Linear receivers for DS-CDMA systems," *IEEE Transaction on Wireless Communications*, vol. 3, no. 6, pp. 2141 - 2155, Nov. 2004.

[2] I. E. Teletar, “Capacity of Multi-Antenna Gaussian Channels,” *Techical Report, Bell Labs, Lucent Technologies*, 1995. Available online at: http://mars.bell-labs.com/papers/proof/proof.pdf.

[3] G. J. Foschini and M. J. Gans, “On limits of Wireless Communications in a Fading Environment when Using Multiple Antennas,” *Wireless Personal Communications*, vol. 6, no. 3, pp. 311 - 355, Mar. 1998.

[4] T. L. Marzetta and B.M. Hochwald, “Capacity of a Mobile Multiple Antenna Communication Link in Rayleigh Flat Fading,” *IEEE Transaction on Information Theory*, vol. 45, no. 1, pp. 139 - 157, Jan. 1999.

[5] J. H. Winters, J. Salz, and R. D. Gitlin, “The Impact of Antenna Ddiversity on the Capacity of Wireless Communications Systems,” *IEEE Transaction on Communications*, vol. 42, no. 2/3/4, pp. 1740 - 1750, Feb./Mar./Apr. 1994.

[6] A. J. Paulraj and C.B.Papadis, “Space-Time Processing for Wireless Communications,” *IEEE Signal Processing Magazine*, vol. 46, no. 6. pp. 49 - 83, 1997.

[7] J. N. Laneman, D. N. C. Tse, and G. W. Wornell, "Cooperative Diversity in Wireless Networks: Efficient Protocols and Outage Behavior," *IEEE Transaction on Information Theory*, vol. 50, no. 12, pp. 3062 - 3080, Dec. 2004.

[8] J. N. Laneman, G. W. Wornell, and D. N. C. Tse, "An Efficient Protocol for Realizing Cooperative Diversity in Wireless Networks," *in Proceedings IEEE International Symposium on Information Theory (ISIT)*, Washington, USA, Jun. 2001.

[9] J. N. Laneman, "Limiting analysis of outage probabilities for diversity schemes in fading channels," *in Proceedings IEEE Global Communications Conference*, San Francisco, USA, Nov. 2003.

[10] J. N. Laneman and G. W. Wornell, "Distributed Space- Time Coded Protocols for Exploiting Cooperative Diversity in Wireless Networks," *IEEE Transaction on Information Theory*, vol. 59, no. 10, pp. 2415 - 2525, Oct. 2003.

[11] E. Zimmermann, P. Herhold, and G. Fettweis, "A Novel Protocol for Cooperative Diversity in Wireless Netwroks," *in Proceedings of The Fifth European Wireless Conference - Mobile and Wireless System Beyond 3G*, Barcelona, Spain, Feb. 2004.

[12] E. Zimmermann, P. Herhold, and G. Fettweis, "On the Performance of Cooperative Diversity Protocols in Practical Wireless Systems," *in Proceedings 58th IEEE Vehicular Technology Conference*, Oct. 2003.

[13] P. Herhold, E. Zimmermann, and G. Fettweis, "A Simple Cooperative Extension to Wireless Relaying" *in Proceedings International Zurich Seminar on Communications*, Feb. 2004.

[14] E. G. Larsson and B. R. Vojcic, "Cooperative transmit diversity based on superposition modulation," *IEEE Communications Letters*, vol. 9, no. 9, pp. 778 - 780, Sep. 2005.

[15] P. Tarasak, H. Minn and V. K. Bhargava, “Differential modulation for two-user cooperative diversity systems,” *IEEE. Journal Selected Areas Communications* vol. 23, no. 9, pp.1891 - 1900, Sep. 2005.

[16] Q. Zhao and H. Li, “Performance of differential modulation with wireless relays in Rayleigh fading channels,” *IEEE Communications Letters*, vol. 9, no. 4, pp. 343 - 345, Apr. 2005.

[17] D. Chen and J. N. Laneman, “Modulation and Demodulation for Cooperative Diversity in Wireless Systems,” *IEEE Transaction Wireless Communications* vol. 5, no.7, pp. 1785 - 1794, Jul. 2006.

[18] J. N. Laneman and G. W. Wornell, “Distributed Space-Time Coded Protocols for Exploiting Cooperative Diversity in Wireless Networks,” *in Proceedings IEEE Global Telecommunications Conference*, (Taipei, Taiwan), Nov. 2002.

[19] P. A. Anghel and M. Kaveh, “Exact symbol error probability of a cooperative network in a Rayleigh-fading environment,” *IEEE Transaction on Wireless Communications*, vol. 3, no.5, pp. 1416 - 1421, Sep. 2004.

[20] M. Uysal, O. Canpolat and M.M. Fareed, “Asymptotic performance analysis of distributed space-time codes,” *IEEE Communications Letters* vol. 10, no. 11, pp. 775 - 777, Nov. 2006.

[21] O. Canpolat and M. Uysal, “Super-orthogonal space-time trellis coded cooperative diversity systems,” *in Proceedings IEEE Vehicular Technology Conference* vol.4, pp. 2429 - 2433, Sep. 2004.

[22] Y. Zhang, “Differential Modulation Schemes for Decode-and-forward cooperative diversity,” *in Proceedings IEEE International Conference on Acoustics, Speech, and Signal Processing*, vol. IV, pp. 917 - 920, 2005.

[23] G. Wang, Y. Zhang and M. Amin, "Cooperative diversity using differential distributed space-time codes," *in Proceedings* 10^{th} *IEEE Asia-Pacific Conference on Communications*, pp. 287 - 291, 2004.

[24] Y. Li and X. G. Xia, "A family of distributed space-time trellis codes with asynchronous cooperative diversity," *IEEE Transaction on Communications*, vol. 55, no. 4, pp. 790 - 800, Oct. 2007.

[25] F. Ng, J. Hwu, M. Chen and X. Li, "Asynchronous space-time cooperative communications in sensor and robotic networks," *in Proceedings IEEE International Conference on Mechatronics and Automation*, pp. 1624 - 1629, Jul. 2005.

[26] Jr. A. R. Hammons, "Algebraic space-time codes for quasi-synchronous cooperative diversity," *in Proceedings IEEE International Conference on Wireless Networks, Communications and Mobile Computing 2005,* vol. 1, pp. 11 - 15, Jun. 2005.

[27] H. Mheidat, M. Uysal and N. Al-Dhahir, "Equalization techniques for distributed space-time block codes with amplify-and-forward relaying signal processing," *IEEE Transaction on Signal Processing*, vol. 55, no. 5, pp.1839 - 1852, May 2007.

[28] H. Wang, "Cooperative Transmission in Wireless Netwroks with Delay Constraints," *in Proceedings IEEE Wireless Communications and Networking Conference*, pp. 1933 - 1938, Mar. 2004.

[29] L. Dai and K. B. Lataief, "Cross-Layer Design for Combining Cooperative Diversity with Truncated ARQ in Ad-hoc Wireless Networks," *in Proceedings IEEE Global Telecommunications Conference*, pp. 3175 - 3179, Nov.-Dec. 2005.

[30] M. Dianati, X. Ling, K. Naik, and X. Shen, "A Node Cooperative ARQ Scheme for Wireless Ad-Hoc Networks," *IEEE Transaction Vehicular Technology,* vol. 55, no. 3, pp. 1032 - 1044, May. 2006.

[31] A. Sendonaris, E. Erkip, and B. Aazhang, "User Cooperation Diversity - Part I: System Description," *IEEE Transaction on Communications,* vol. 51, no. 11, pp. 1927 - 1938, Nov. 2003.

[32] A.Sendonaris, E. Erkip, and B. Aazhang, "User Cooperation Diversity - Part II: Implementation aspects and Performance Analysis," *IEEE Transaction on Communications*, vol. 51, no. 11, pp. 1939 - 1948, Nov. 2003.

[33] A. Sendonaris, E. Erkip, and B. Aazhang, "Increasing Uplink Capacity via User Cooperation Diversity," *in Proceedings IEEE International Symposium on Information Theory (ISIT)*, Cambridge, MA, USA, Aug. 1998.

[34] T. E. Hunter and A. Nosratinia, "Coded cooperation under slow fading, fast fading, and power control," *in Proceedings Asilomar Conferenceon Signals, Systems and Computing*, Pacific Grove, CA, Nov. 2002.

[35] T. E. Hunter and A. Nosratinia, "Cooperative diversity through coding," *in Proceedings IEEE International Symposuim Information Theory (ISIT)*, Laussane, Switzerland, p. 220, Jul. 2002.

[36] T. E. Hunter and A. Nosratinia, "Performance Analysis of Coded Cooperation Diversity,"*in Proceedings IEEE Internation Conference on Communications,* Vol. 4, pp. 2688 - 2692, May 2003.

[37] M. Janani, A. Hedayat, T. E. Hunter, and A. Nosratinia, "Coded Cooperation in Wireless Communications: Space-Time Transmission and Iterative Decoding," *IEEE Transaction on Signal Processings*, vol. 52, no. 2, pp. 362 - 371, Feb. 2004.

[38] A. Stefanov and E. Erkip, "Cooperative coding for wireless networks." *IEEE Transaction on Communications*, vol. 52, no. 9, pp. 1470 - 1476, Sep. 2004.

[39] B. Zhao and M. C. Valenti, "Cooperative Diversity using Distributed Turbo Codes," *in Proceedings Virginia Tech Symposium on Wireless Personal Communications*, Blacksburg, VA, USA, Jun. 2003.

[40] B. Zhao and M.C. Valenti, "Distributed turbo coded diversity for the relay channel," *IEE Electronics Letters*, vol. 39, no. 10, pp. 786 - 787, May 2003.

[41] N. Prasad and M. K. Varanasi, "Diversity and Multiplexing Tradeoff Bounds for Cooperative Diversity Protocols," *in Proceedings IEEE Internation Symposium Information Theory (ISIT)*, Chicago, IL, USA, Jun. 2004.

[42] K. Azarian, H. El Gamal and P. Schniter, "On the Acheivable Diversity-vs-Multiplexing Tradeoff in Half-Duplex Cooperative Channels," *IEEE Transaction on Information Theory*, vol. 51, no. 12, pp. 4152 - 4172, Dec. 2005.

[43] K. Azarian, H. El Gamal and P. Schniter, "On the Acheivable Diversity-vs-Multiplexing Tradeoff in Cooperative Channels," *in Proceedings conference on Information Sciences and Systems*, Princeton, NJ, USA, Mar. 2004.

[44] A. Ribeiro, X. Cai and G. B. Giannakis, "Symbol Error Probabilities for General Cooperative Diveristy in Wireless Networks," *IEEE Transaction on Wireless Communications*, vol. 4, no. 3, pp. 1264 - 1273, May 2005.

[45] W. Mo and Z. Wang, "Average symbol Error Probability and Outage Probability Analysis for General Cooperative Diversity System at High Signal to Noise Ratio," *Proceedings 38th Conference on Information Sciences and Systems*, Princeton, NJ, USA, pp. 1443 - 1448, Mar. 2004.

[46] R. U. Nabar, H. Bölcskei and F. W. Kneubühler, “Fading relay channels: performance limits and spaceŰtime signal design,” *IEEE. Journal Selected Areas on Communications,* vol. 22, no. 6, pp.1099 - 1109, Aug. 2004.

[47] J. Luo, R. S. Blum., L. J. Cimini, L. J. Greenstein and A. M. Haimovich, “Decode-and-Forward Cooperative Diversity with Power Allocation in Wireless Networks”, *in Proceedings IEEE Global Telecommunication Conference,* St Louis, MO, USA, Nov. - Dec. 2005.

[48] Y. Zhao, R. Adve and T. J. Lim, “Improving Amplify-and-Forward Relay Networks: Optimal Power Allocation versus Selection,” *in Proceedings IEEE International Symposium on Inform. Theory,* Seattle, USA, Jul. 2006.

[49] J. Adeane, M. R. D. Rodrigues and I. J. Wassell, “Optimum Power Allocation in Cooperative Networks,” *in Proceedings 12th International Conference on Telecommunications,* Cape Town, South Africa, May 2005.

[50] W. Su, A. K. Sadek, and K. J. R. Liu, “SER Performance Analysis and Optimum Power Allocation for Decode-and-Forward Cooperation Protocol in Wireless Networks”, *in Proceedings IEEE Wireless Communication and Networking Conference,* New Orleans, LA, USA, Mar. 2005.

[51] P. Herhold, E. Zimmermann, and G. Fettweis, “Cooperative multi-hop transmission in wireless networks,” *Elsevier Journal on Computer Networks,* vol. 49, Jun. 2005.

[52] H.F. Lu and P.V. Kumar,“A Unified Construction of Space- Time Codes with Optimal Rate-Diversity Tradeoff,” *IEEE Transaction on Information Theory,* vol. 51, no. 5, pp. 1709 - 1730, May 2005.

[53] S. M. Alamouti, “A Simple Transmit Diversity Technique for Wireless Communications,” *IEEE Journal Select Areas in Communications,* vol. 16, no. 8, pp.1451 - 1458, Oct. 1998.

[54] L. Zheng and D. N. C. Tse, “Diversity and Multiplexing: A Fundamental Tradeoff in Multiple-Antenna Channels,” *IEEE Transaction on Information Theory*, vol. 49, no. 5, pp. 1073 - 1096, May 2003.

[55] D. N. C. Tse, P. Viswanath and L. Zheng, “Diversity-Multiplexing Tradeoff in Multiple Access Channels,” *IEEE Transaction on Information Theory,* vol. 50, no. 9, pp. 1859 - 1874, Sep. 2004.

[56] Z. Wang and G. B. Giannakis, “A Simple and General Parameterization Quantifying Perfromance in Fading Channels,” *IEEE Transaction on Communications*, vol. 51, pp. 1389 - 1398, Aug. 2003.

[57] K. Cho and D. Yoon, “On the general BER expression of one- and two- dimensional modulations”, *IEEE Transaction on Communications*, vol. 50, no. 7, pp. 1074 - 1080, Jul. 2002.

[58] J. W. Mark and W. Zhuang, *Wireless Communications and Networking,* Prentice Hall, 2003.

[59] D.G. Brennan, “Linear diversity combining techniques,” *Proceedings IRE,* vol.47, no. 1, pp. 1075 Ű 1102, Jun. 1959.

[60] J. F. Kurose and K. W. Ross, *Computer Networking: A Top-Down Approach Featuring the Internet*, Addison-Wesley, 2000.

[61] H. N. Gabow, “An efficient implementation of Edmonds’ algorithm for maximum matching on graphs”, *Journal of the Association for Computing Machinery,* vol. 23, no. 2, pp. 221 - 234, Apr. 1976.

[62] D. Avis. “A survey of heuristics for the weighted matching problem,” *Networks*, vol. 13, pp. 475 - 493, 1983.

[63] J. G. Proakis, *Digital Communications*, McGraw-Hill International Editions, 4th Edition, 2001.

[64] V. Tarokh, N. Seshadri, and A. R. Calderbank, “Space-time codes for high data rate wireless communications: perfromance criterion and code construction,” *IEEE Transaction on Information Theory*, vol. 44, pp. 744 - 765, Mar. 1998.

[65] M. K. Simon , “Evaluation of average bit error probability for space-time coding based on a simpler exact evaluation of pairwise error probability”, *Journal of Communications and Networks*, vol. 3, no. 3, pp. 257 - 264, Sep. 2001.

[66] M. S. Raju, A. Ramesh and A. Chockalingam , “BER analysis of QAM with transmit diversity in Rayleigh fading channels”, *in Proceedings IEEE Global Telecommunication Conference 2003*, Nov. 2003.

[67] M. Nakagami, “The m-distribution – A general formula of intensity distribution of rapid fading,” in Statistical Methods in Radio Wave Propagation, W. C. Hoffman, Ed. New York: Pregamon, pp. 3 - 36, 1960.

[68] M. F. Pop and N. C. Beaulieu, “Limitations of sum-of-sinusoids fading channel simulators,” *IEEE Transaction on Communications*, vol. 49, pp. 699 - 708, Apr. 2001.

[69] N. C. Beaulieu and C. Cheng, “Efficient Nakagami-m fading channel simulation,” *IEEE Transaction on Vehicular Technology*, vol. 54, no.2, pp. 413 - 424, Mar. 2005.

[70] C. Tellambura, A. Annamalai and V. K. Bhargava, “Contour intergral representation for generalized Marcum-Q function and its application to unified analy-

sis of dual-branch selection diversity over correleted Nakagami-m fading channels,"*Proceedings IEEE Vehicular Technology conference,* pp. 1031 - 1034, 2000.

[71] A. Ramesh, A. Chockalingam and L. B. Milstein, "A First-order Markov model for correleted Nakagami-m fading channels,"*in Proceedings IEEE International Conference on Communications,* vol. 5, pp. 3413 - 3417, Apr. - May 2002.

[72] R. K. Ahuja, T. L. Magnanti, and J. B. Orlin, *Network Flows: Theory, Algorithms, and Applications,* Prentice-Hall, Englewood Cliffs, NJ, 1993.

[73] J. N. Laneman, *Cooperative Diversity in Wireless Networks: Algorithms and Architectures*, Ph.D. thesis, MIT, 2002.

(The following is a list of the author's publications pertaining to this thesis.)

[74] V. Mahinthan and J.W. Mark, "A simple cooperative diversity scheme based on orthogonal signaling," *in Proceedings IEEE Wireless Communications and Networking Conference,* vol. 2, pp. 1012 - 1017, New Orleans, USA, Mar. 2005.

[75] V. Mahinthan, J. W. Mark and X. Shen, "A cooperative diversity scheme based on quadrature signaling", *IEEE Transaction on Wireless Communications,* vol. 6, no. 1, pp. 41 - 45, Jan. 2007.

[76] V. Mahinthan, J. W. Mark and X. Shen, "Adaptive Regenerate and Forward Cooperative Diversity System based on Quadrature Signaling," *in Proceedings IEEE Global Telecommunication Conference*, San Francisco, CA, USA, Nov. - Dec. 2006.

[77] V. Mahinthan, J. W. Mark and X. Shen, "Performance Analysis and Power Allocation in M-QAM Cooperative Diversity Systems ", *IEEE Transaction on Wireless Comunications*, submitted in Jan. 2007 and revised in Sep. 2007.

[78] V. Mahinthan, H. Rutagemwa, J. W. Mark and X. Shen, "Performance of Adaptive Relaying Schemes in Cooperative Diversity Systems with ARQ," *in Proceedings IEEE Global Telecommunication Conference*, Washington, D.C., USA, Nov. - Dec. 2007.

[79] V. Mahinthan, H. Rutagemwa, J. W. Mark and X. Shen, "Cross-Layer Performance Study of Cooperative Diversity System with ARQ," *IEEE Transaction Vehicular Technology*, under preparation and expected submission in Sep. 2007.

[80] V. Mahinthan, L. Cai, J. W. Mark and X. Shen, "Matching Algorithms for Infrastructure-based Wireless Networks Employing Cooperative Diversity System," *in Proceedings IEEE WCNC'06*, vol. 3, pp. 1669 - 1674. Las Vegas, NV, USA, Apr. 2006.

[81] V. Mahinthan, L. Cai, J. W. Mark and X. Shen, "Maximizing Cooperative Diversity Energy Gain for Wireless Networks," *IEEE Transaction of Wireless Communications*, vol. 6, no. 7, pp. 2530 - 2539, Jul. 2007.

[82] V. Mahinthan, L. Cai, J. W. Mark and X. Shen, "Optimizing Power Allocation and Matching of Cooperative Diversity Systems," *in Proceedings IEEE ICC'07* Glasgow, UK, Jun. 2007.

[83] V. Mahinthan, L. Cai, J. W. Mark and X. Shen, "Partner Selection Based on Optimal Power Allocation in Cooperative Diversity Systems," *IEEE Transaction Vehicular Technology*, accepted in May 2007 and expected to publish in Jan. 2008.